

**ION EXCHANGE CHROMATOGRAPHY COUPLED TO INDUCTIVELY
COUPLED PLASMA MASS SPECTROMETRY: A POWERFUL TECHNIQUE
FOR STABILITY CONSTANT DETERMINATION, SPECIATION ANALYSIS
AND KINETIC STUDIES**

by

Liyan Xing

A thesis submitted to the Department of Chemistry

In conformity with the requirements for

the degree of Doctor of Philosophy

Queen's University

Kingston, Ontario, Canada

(September, 2010)

Copyright ©Liyan Xing, 2010

Abstract

Facile procedures based on hyphenated ion-exchange chromatography (IEC) and inductively coupled plasma mass spectrometry (ICP-MS) were developed to determine conditional stability constants, speciate chromium species and investigate the reduction of Cr(VI).

1. Improvements were made to a method previously developed to determine the conditional stability constant, K_f' , and chelation number, n , using IEC-ICP-MS. This method allowed the accurate determination of the conditional stability constant of a simple system. However, the corresponding chelation number was significantly different to the expected value because the principal assumption, i.e. that the ligand was in excess, was not realized in the experimentation. Furthermore, it neglected complexes other than that formed with EDTA⁴⁻. By taking into account these factors, accurate K_f' and n were obtained for Co-EDTA and Zn-EDTA systems.

2. A simple method was developed for chromium speciation analysis at sub- $\mu\text{g L}^{-1}$ level in potable water by IEC-ICP-MS. Cr(VI) and Cr(III) were separated on IonPac® AG-7 guard column within 7.5 minutes using gradient elution with 0.1 M ammonium nitrate and 0.8 M nitric acid. H₂ collision/reaction interface gas eliminated chlorine-based and carbon-based polyatomic interferences on Cr detection. Water samples were analyzed directly, without any pretreatment. The accuracy of the method was verified through accurate analysis of riverine water certified reference material. Limits of detection of 0.02 and 0.04 $\mu\text{g L}^{-1}$ for Cr(VI) and Cr(III), respectively, were obtained.

3. This speciation analysis method was then used for kinetics studies of Cr(VI) reduction in acidified riverine water. Water was spiked with Cr(VI), with or without Cr(III), and evolution of each Cr species with time was monitored by speciation analysis, showing that the reduction of Cr(VI) was a pseudo first order reaction. By plotting the logarithm of the peak area ratio of the instant Cr(VI) concentration over that of the original spiking versus time, the reaction rate constant was obtained as the slope. The reduction rate increased with decreasing pH and increasing temperature. The activation energy of the reaction at pH 1.3 was calculated using an Arrhenius plot. This method offers the advantages of small sample consumption, minimal sample manipulation, and easy data interpretation.

Co-Authorship

All work contained in this thesis was carried out by the author in the Department of Chemistry at Queen's University under the guidance of Dr. Diane Beauchemin. Parts of this thesis were previously published as two refereed journal articles and one section of an encyclopedia:

Liyan Xing and Diane Beauchemin. Chromium speciation at trace level in potable water using hyphenated ion exchange chromatography and inductively coupled plasma mass spectrometry with collision/reaction interface. *Journal of analytical atomic spectrometry*. 2010, (25), 1046-1055.

Liyan Xing and Diane Beauchemin. Determination of stability constants of metal complexes with IC-ICP-MS. *Journal of analytical atomic spectrometry*. 2009, (24), 336-339.

Liyan Xing and Diane Beauchemin. Liquid chromatography for sample introduction in inductively coupled plasma mass spectrometry in Volume 5 *Elemental, Isotopic and Inorganic Analysis by Mass Spectrometry*, Eds. D. Beauchemin and D. Matthews, of *The Encyclopedia of Mass Spectrometry*, Editors-in-chief M. L. Gross and R. M. Caprioli, Elsevier, London, July 2010.

Acknowledgements

I would like to express my sincere gratitude to my supervisor, Dr. Diane Beauchemin, for her unrelenting inspiration, encouragement and support, which lead to an enjoyable and fulfilling graduate study experience for me.

I am also grateful to Dr. Richard Oleschuk and Dr. Stephen Brown for serving on my supervisory committee. Sincere thanks are also extended to Dr. Anne Petitjean for her consistent support; and Dr. Igor Kozin and Lindsay Hull for helping me to execute TA duties. I would also like to thank the technicians and staff in the Department of Chemistry for their support and help.

The financial support from Queen's School of Graduate Studies is gratefully acknowledged.

I also acknowledge the assistance from my fellow graduate students, particularly in Dr. Beauchemin's group, for their scientific contributions and friendship.

The most special thanks are given to my family for their understanding and patience.

Statement of Originality

I hereby certify that all of the work described within this thesis is the original work of the author. Any published (or unpublished) ideas and/or techniques from the work of others are fully acknowledged in accordance with the standard referencing practices.

Concerning the method development for chromium speciation, it is the first known report to address the effect of purity of the mobile phase on elemental speciation analysis at trace level. Also, it is the first report on applying hyphenated IEC-ICP-MS to investigate the reduction kinetics of Cr(VI) in riverine water.

Table of Contents

Abstract.....	ii
Co-Authorship.....	iv
Acknowledgements.....	v
Statement of Originality.....	vi
Table of Contents.....	vii
List of Tables.....	xii
List of Figures.....	xviii
List of Abbreviations and Acronyms.....	xviii
Chapter 1 General Introduction.....	1
1.1 Introduction.....	1
1.2 Hyphenated techniques.....	2
1.3 Hyphenated HPLC-ICP-MS.....	4
1.3.1 HPLC as a separation technique.....	4
1.3.2 ICP-MS as HPLC detector.....	7
1.3.2.1 Sample introduction system.....	8
1.3.2.2 Plasma generation system.....	9
1.3.2.3 Sampling interface and ion optics.....	11

1.3.2.4 Mass analyzer.....	12
1.3.3 Hyphenation of HPL and ICP-MS.....	14
1.3.3.1 Organic solvents.....	17
1.3.3.1.1 Mitigating the effect of organic solvents on the ICP.....	18
1.3.3.1.2 Minimizing the amount of organic solvents introduced into the ICP.....	20
1.3.3.2 Inorganic salts.....	22
1.3.4 Applications of HPLC-ICP-MS.....	22
1.4 Objectives of this thesis.....	29
References.....	31

Chapter 2 Determination of stability constants of metal complexes with IEC-ICP-

MS.....	42
2.1. Introduction.....	42
2.1.1 General background on metal complexes.....	42
2.1.2 Determination of stability constant.....	44
2.1.3 Hyphenated IEC-ICP-MS to determine stability constant.....	46
2.1.4 Derivation of stability constant expressions.....	47
2.2 Experimental.....	53
2.2.1 Instrumentation.....	53
2.2.1.1 IEC.....	53
2.2.1.2 ICP-MS.....	54
2.2.2 Reagents and solution preparation.....	56
2.2.2.1 Reagents.....	56
2.2.2.2 Sample solution preparation.....	56

2.2.3 Data acquisition and analysis.....	58
2.3 Results and discussion.....	60
2.3.1 Validity of different equations for Co-EDTA and Zn-EDTA complexes on IonPac®AG7.....	60
2.3.1.1 Co-EDTA complex.....	61
2.3.1.2 Zn-EDTA complex.....	66
2.3.2 Determination of stability constant of Co-EDTA with IonPac® CG-5A.....	69
2.3.3 Multi-elemental determination of the conditional stability constants of Co-EDTA and Zn-EDTA by gradient elution with IonPac® CG-5A.....	73
2.4 Summary.....	77
References.....	78

**Chapter 3 Chromium speciation analysis at trace level in potable water using
hyphenated ion exchange chromatography and inductively coupled
plasma mass spectrometry with collision/reaction interface.....82**

3.1 Introduction.....	82
3.1.1 IEC as separation technique for chromium speciation analysis.....	83
3.1.2 ICP-MS as IEC detector.....	84
3.2 Experimental.....	87
3.2.1 Instrumentation.....	87
3.2.1.1 IEC.....	87
3.2.1.2 ICP-MS.....	88
3.2.1.2.1 Varian 820-MS ICP-MS.....	88

3.2.1.2.2 Optimization for chromium speciation analysis.....	92
3.2.2 Reagents and solution preparation.....	94
2.2.1.1 Reagents.....	94
3.2.2.2 Sample solution preparation.....	95
3.2.3 Recovery test.....	96
3.2.4 Data processing.....	96
3.3 Results and discussion.....	97
3.3.1 Optimization of CRI conditions to reduce ArC ⁺ interference.....	97
3.3.2 Optimization of Cr speciation analysis method.....	98
3.3.2.1 Chromatographic separation.....	98
3.3.2.2 Elimination of chlorine-based spectroscopic interferences.....	98
3.3.2.3 Elimination of carbon-based spectroscopic interferences.....	100
3.3.3 Background correction.....	104
3.3.4 Determination of limit of detection (LOD).....	105
3.3.5 Determination of the Cr content of the mobile phase.....	108
3.3.6 Speciation analysis of chromium in certified riverine water SLRS-2.....	108
3.3.7 Speciation analysis of chromium in tap water.....	113
3.4 Summary.....	115
References.....	117

Chapter 4 Kinetics study of the reduction of Cr(VI) in natural water with IEC-ICP-MS.....123

4.1 Introduction.....	123
-----------------------	-----

4.2 Experimental.....	126
4.2.1 Instrumentation and procedure.....	126
4.2.2 Data analysis.....	127
4.4 Results and discussion.....	128
4.4.1 Evolution of Cr(VI) spike in SLRS-2.....	128
4.4.2 Reduction of Cr(VI) in presence of Cr(III).....	134
4.4.2.1 Evolution of Cr(VI) spike in presence of a similar Cr(III) concentration.....	134
4.4.2.2 Effect of pH and temperature.....	136
4.5 Summary.....	138
References.....	139
Chapter 5 General discussion.....	142
5.1 Selection of mobile phases.....	143
5.2 Selection of columns.....	144
5.3 Alleviating spectroscopic interferences.....	146
References.....	146
Chapter 6 Summary and Conclusions.....	150
References.....	154

List of Tables

Table 1.1 Selected examples of application of HPLC-ICP-MS in speciation analysis.....	25
Table 2.1. IEC separation conditions.....	55
Table 2.2. Typical operating conditions for UltraMass 700 ICP-MS instrument.....	57
Table 2.3. Sample compositions for Co-EDTA and Zn-EDTA complexes in 0.1 M NH ₄ NO ₃ (pH 3.8) for testing different equations.....	58
Table 2.4. Sample compositions for Co-EDTA complex in 0.1 M NH ₄ NO ₃ (pH 3.8) with varied total cobalt concentration.....	59
Table 2.5. Sample compositions for Co-EDTA/Zn-EDTA complexes in 0.1 M NH ₄ NO ₃ (pH 3.8) to test the applicability of the method to the simultaneous determination of stability constants of a multi-elemental complex system.....	59
Table 2.6. Conditional stability constant ($\log K_f'$) and chelation number (n) of Co-EDTA calculated using different equations.....	66
Table 2.7. Conditional stability constant ($\log K_f'$) and chelation number (n) of Zn-EDTA calculated using different equations.....	68
Table 2.8. Conditional stability constant ($\log K_f'$) and chelation number (n) of Co-EDTA complex determined with Equation 2.13 at different cobalt concentrations...	70
Table 3.1. IEC separation conditions.....	88
Table 3.2. ICP-MS operating conditions.....	93
Table 3.3. Signal intensity at m/z 52 and m/z 55 for DDW spiked with 10 µg/L Mn using different CRI modes.....	97
Table 3.4. Tentative assignment of the peaks on the mass spectrum in Figure 3.13.....	111

Table 3.5. Concentrations ($\mu\text{g/L}$) of chromium species in SLRS-2 ($n = 3$).....	112
Table 3.6. Measured concentrations ($\mu\text{g/L}$) of chromium species in tap water ($n = 3$)...	115
Table 4.1. Comparison of rate constants obtained for the reduction of Cr(VI).....	132
Table 4.2. Parameters extracted from the fitting curve expressions for Cr species.....	134
Table 4.3. Rate constants under different reaction conditions for the reduction of Cr(VI) in riverine water SLRS-2. The initial spiking concentration of Cr(VI)/Cr(III) is 20 $\mu\text{g/L}$ (or 0.385 μM) each.....	137

List of Figures

Figure 1.1. Hyphenated techniques for speciation analysis.....	3
Figure 1.2. Schematic of an ICP torch and load coil showing how the inductively coupled plasma is formed.	10
Figure 1.3. Schematic diagram of ICP and ion extraction device	12
Figure 1.4. Typical setup used when hyphenating HPLC to ICP-MS.....	15
Figure 2.1. IEC-ICP-MS chromatogram for Co with isocratic.....	61
Figure 2.2. Stacked IEC-ICP-MS chromatograms for Co-EDTA solutions (1.70 μM or 100 $\mu\text{g/L}$ Co^{2+} and 0.339-3.39 μM EDTA) at pH 3.8.....	62
Figure 2.3. IEC-ICP-MS chromatograms of EDTA-free 10-120 $\mu\text{g/L}$ Co solutions.....	63
Figure 2.4. Linear regression to determine $\log K_f'$ (intercept) and n (slope) of Co-EDTA complex with Equation 2.13.....	64
Figure 2.5. Linear regression to determine $\log K_f'$ (intercept) and n (slope) of Co-EDTA complex with Equation 2.12.....	65
Figure 2.6. Linear regression to determine $\log K_f'$ (intercept) and n (slope) of Co-EDTA complex with Equation H-1.....	65
Figure 2.7. IEC-ICP-MS chromatogram for Zn-EDTA solution (100 $\mu\text{g/L}$ or 1.53 μM Zn and 0.76 μM EDTA).....	67
Figure 2.8. Linear regression to determine $\log K_f'$ (intercept) and n (slope) of Zn-EDTA complex with Equation 2.13.....	68
Figure 2.9. IEC-ICP-MS chromatograms for 100 $\mu\text{g/L}$ Co with isocratic and gradient elution using IonPac®CG-5A	69

Figure 2.10. IEC-ICP-MS chromatogram for Co-EDTA solution (100 $\mu\text{g/L}$ or 1.69 μM Co and 0.848 μM EDTA) on CG-5A with gradient elution.....	71
Figure 2.11. Linear regression to determine $\log K_f'$ (intercept) and n (slope) of Co-EDTA complex with 50 $\mu\text{g/L}$ or 0.854 μM Co using Equation 2.13.....	71
Figure 2.12. Linear regression to determine $\log K_f'$ (intercept) and n (slope) of Co-EDTA complex with 25 ppb or 0.427 μM Co using Equation 2.13.....	72
Figure 2.13. Linear regression to determine $\log K_f'$ (intercept) and n (slope) of Co-EDTA complex with 12 $\mu\text{g/L}$ or 0.205 μM Co using Equation 2.13.....	72
Figure 2.14. Stacked IEC-ICP-MS chromatograms of Co-EDTA and Zn-EDTA in a di-elemental complex system.	74
Figure 2.15. Linear regression to determine $\log K_f'$ (intercept) and n (slope) of Co-EDTA and Zn-EDTA with a di-elemental complex system containing 1.70 μM of Co, 4.13 μM of Zn and an EDTA concentration ranging from 1.17 μM to 4.66 μM	75
Figure 3.1. Diagram of Varian 820-MS sample introduction system.....	89
Figure 3.2. Spatial arrangement of the interlaced coils, the CRI system, the 90-degree reflection mirror and the off-axis quadrupole.....	90
Figure 3.3 Diagrammatic illustration of the CRI system.	91
Figure 3.4. Chromatograms obtained for 1000 mg/L of Cl and 20 $\mu\text{g/L}$ each of Cr(VI) and Cr(III) under three different modes: without CRI gas, with 50 mL/min He and with 70 mL/min H_2	100

Figure 3.5. Stacked chromatograms observed without CRI gas for a series of sodium bicarbonate solutions with concentrations ranging from 10 to 500 mg/L.....	101
Figure 3.6. Chromatograms obtained without CRI gas, with 70 mL/min H ₂ CRI gas for solutions containing 500 mg/L sodium bicarbonate, with and without 20 µg/L each of Cr(VI) and Cr(III), and with 70 mL/min H ₂ CRI gas for 250 mg/L sodium bicarbonate solution without Cr, spiked with 10 µg/L of Cr(VI) and spiked with 10 µg/L of Cr(III)	103
Figure 3.7. Blank chromatogram obtained by injection of DDW with CRI gas on.....	104
Figure 3.8. Blank-subtracted chromatograms of 0.1-100 µg/L Cr standard solutions...	106
Figure 3.9. Calibration curve for Cr(VI) using standards ranging from 0.1 to 100 µg/L.....	107
Figure 3.10. Calibration curve for Cr(III) using standards ranging from 0.1 to 100 µg/L.....	107
Figure 3.11. Stacked chromatograms of riverine water SLRS-2 and DDW.....	110
Figure 3.12. Typical blank-subtracted chromatogram for chromium speciation of riverine water SLRS-2.....	110
Figure 3.13. Electrospray mass spectrum of the fraction eluted at void time.....	111
Figure 3.14. Typical blank-subtracted chromatogram for chromium speciation in tap water.....	115
Figure 4.1. IEC-ICP-MS chromatograms showing the time-dependent reduction of Cr(VI) in riverine water sample SLRS-2 (pH = 1.3; ambient temperature= 20 °C).	128

Figure 4.2. Plot of peak area vs. time illustrating the time-dependent evolution of chromium species in riverine water.....	129
Figure 4.3. Plots of $\ln(x/c_0)$ versus time to determine reaction rate constant k in s^{-1} with linear regression.....	131
Figure 4.4. The best fitting curves showing the time-dependent behaviour of each Cr species during the process of Cr(VI) reduction in riverine water.....	133
Figure 4.5. IEC-ICP-MS chromatograms showing the time dependent reduction of Cr(VI) in riverine water SLRS-2 (pH = 1.3; ambient temperature= 20 °C) in presence of Cr(III).....	135
Figure 4.6. Plots of $\ln(x/c_0)$ vs. time in minute and linear regression curves under pH 1.3 and pH 2.3 as labeled.....	136
Figure 4.7. Plot of $\ln k$ vs $1/T$ (in Kelvin) and linear regression treatment to calculate the activation energy (E_a).....	138

List of Abbreviations and Acronyms

AAS:	Atomic absorption spectrometry
AEC:	Anion exchange chromatography
AES:	Atomic emission spectrometry
AsB:	Arsenobetaine
AsC:	Arsenocholine
p-ASA:	p-Arsanilic acid
CE:	Capillary electrophoresis
CEC:	Cation exchange chromatography
CRI:	Collision/reaction interface
CRM:	Certified reference material
DC:	Direct current
DDW:	Doubly deionized water
DIN:	Direct injection nebulizer
DIHEN:	Direct injection high efficiency nebulizer
DMA:	Dimethylarsenic acid
DMF:	Dimethylformamide
DMPAO:	Dimethylphenylarsine oxide
DNA:	Deoxyribonucleic acid
DPAA:	Diphenylarsonic acid
DPC:	Diphenylcarbazide
DRC:	Dynamic reaction cell
EDTA:	Ethylenediaminetetraacetic acid

EPR: Electron magnetic resonance

EPA: Environmental Protection Agency

ESI-MS: Electrospray ionization mass spectrometry

EtHg⁺: Ethylmercury

FIP: First ionization potential

GC: Gas chromatography

HDPE: High-density polyethylene

HFBA: Heptafluorobutanoic acid

HILIC: Hydrophilic interaction liquid chromatography

HPLC: High performance liquid chromatography

ICP-MS: Inductively coupled plasma mass spectrometry

IEC: Ion exchange chromatography

IP-RP-HPLC: Ion Pairing reverse phase high performance liquid chromatography

LOD: Limit-of-detection

MALDI-MS: Matrix-assisted laser desorption ionization mass spectrometry

MCN: Micro-concentric nebulizer

MeHg⁺: Methylmercury

MMA: Monomethylarsonate

MPA: Mobile phase A

MPAO: Methylphenylarsine oxide

MPB: Mobile phase B

MS: Mass spectrometry

SSDSID: Species specific double spike isotope dilution

Chapter 1

General Introduction

1.1 Introduction

In recent years, there has been increasing interest in elemental (metal, metalloid, and heteroatom) speciation analysis, which involves the determination of the nature and quantities of one or more individual chemical species of an element in a sample [1]. These species may differ in isotopic composition, electronic or oxidation state, or complex molecular structure of the element of interest [1]. Numerous evidences have shown that the total concentration of an element in a sample does not provide enough information on its mobility, toxicity, essentiality, etc., which depends on chemical forms of the element.

For example, arsenic is notorious for its acute toxicity; however, this notion started to change with the discovery that the toxicity of arsenic compounds is closely related to their chemical forms. Organic As species are much less toxic than the inorganic ones, and toxicity generally decreases as the degree of methylation increases, where arsenobetaine (AsB), the prevalent arsenic compound in seafood products is found to be metabolically inert and non-toxic [2, 3]. So, it is important to take into consideration the proportion of the different types of As compounds when doing risk assessment [4, 5].

Another example is chromium, which exists in two major oxidation states, hexavalent and trivalent, possessing very different physical and chemical properties and affecting biological processes differently [6, 7]. Cr(III) is an essential trace element in glucose me-

tabolism, and is usually included in dietary supplements [8-10]. However, it has a low solubility under most physiological pH conditions and is thus poorly absorbed. On the other hand, Cr(VI) is regarded as genotoxic and carcinogenic [11-14]. It is highly soluble under almost any pH conditions and can penetrate the cell membrane via a general non-selective anion transport channel [15].

A final example is that of platinum-containing compounds, such as cisplatin, carboplatin, iproplatin and tetraplatin, which are widely used for cancer chemotherapy [16, 17]. To understand their effect, speciation analysis is required to determine their purity and stability, as well as to monitor their metabolites to assess their cytotoxicity and pharmacokinetics [18-20].

In summary, the chemical nature and quantity of an element in a sample matrix is highly responsible for its essentiality, mobility, bioavailability and toxicity in biological organisms and in ecosystems. Therefore, speciation analysis is required to assess whether or not it is toxic, which depends on the concentration level of each species, for example, Se is an essential trace element up to a certain level but toxic at higher levels [21]. Speciation information can also be exploited in studying the equilibration process, such as the determination of stability constant and reaction kinetics [18, 22-27].

1.2 Hyphenated techniques

Hyphenation of techniques in elemental speciation analysis refers to the online combination of a chromatographic separation technique and a sensitive element-specific detection

technique [28]. Separation techniques include high performance liquid chromatography (HPLC), gas chromatography (GC), capillary electrophoresis (CE), etc.; and detection techniques include inductively coupled plasma (ICP) atomic emission spectroscopy (AES), flame atomic absorption spectrometry (AAS), ICP mass spectrometry (MS), etc. Various possibilities of hyphenated techniques are schematically shown in Figure 1.1 [28]. The hyphenation of HPLC with ICP-MS constitutes the most popular tool for elemental speciation.

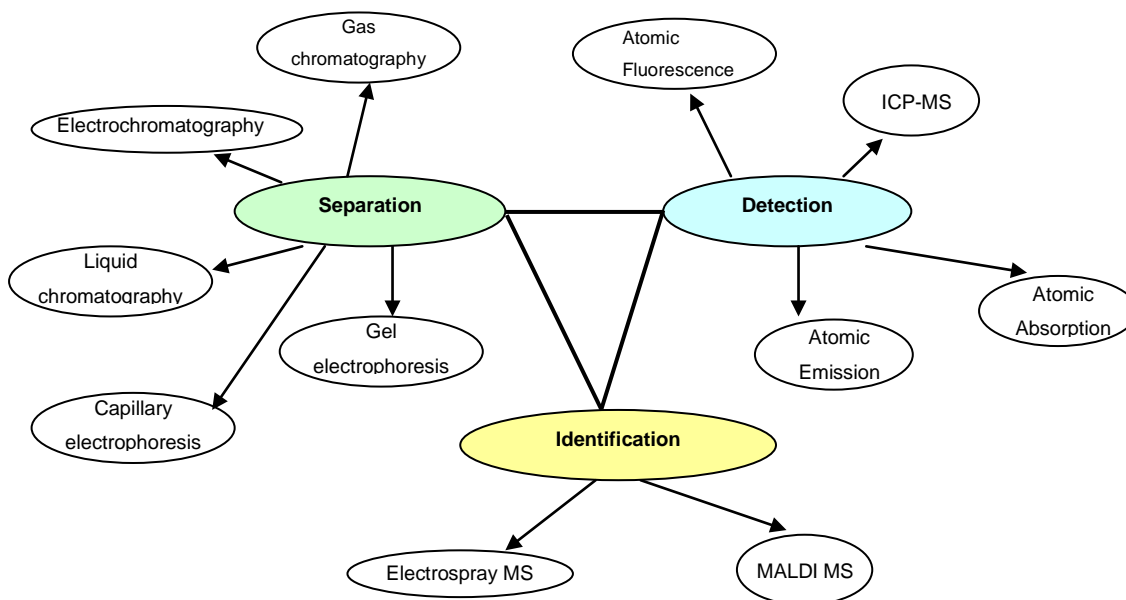


Figure 1.1. Hyphenated techniques for speciation analysis (adapted from [28]).

In liquid chromatography, species separation occurs according to their different distributions between a stationary phase and a liquid mobile phase, which arise from differences in their polarity, electrostatic properties, size and van der Waals forces, depending on the separation mode, i.e., the type of stationary and mobile phases. It is more broadly appli-

cable than GC, which is restricted to volatile and thermally stable compounds, but does not, in general, provide as high a chromatographic resolution as GC. Furthermore, it is not applicable to labile species, unlike CE, which, however, is not as straightforward to couple to ICP-MS.

As an element specific detector, ICP-MS offers the advantages of multi-element and isotope measurement capabilities, high sensitivity, low detection limits and large linear dynamic range. As a result, it is practically the default detector for speciation analysis due to its versatility and outstanding detection power. Although it is possible to do off-line separation before submitting the collected fractions to ICP-MS analysis, on-line separation ensures the highest sensitivity while eliminating contamination, loss or species transformation that could occur during collection and storage of the fractions.

1.3 Hyphenated HPLC-ICP-MS

1.3.1 HPLC as a separation technique

HPLC is a very versatile, well-established analytical and preparative tool that can practically separate any chemical mixture through careful selection of stationary and mobile phases, temperature and pH [29]. A basic HPLC system consists of a solvent pumping system, a sample injection device, a guard column, an analytical column and a detector. The column is the heart of the system, and determines the dominant separation mechanism. The columns that are commonly used in elemental speciation analysis include ion exchange, reversed phase and size exclusion.

Ion-exchange columns are packed with silica or cross-linked polymer beads with diameter in the range of 3-10 μm , which are grafted with organic phases containing functional groups that either have permanent or induced ionic charges. There are two types of charged functional groups: anionic and cationic, each of which can be subdivided into strong or weak types. The functional groups in strong column packing materials are, usually, quaternary amines for anion exchange or sulfonic acid for cation exchange, while, in weak column packing material, they often are organic acids and primary amines [29]. The separation is mainly based on coulombic (ionic) interactions, ‘opposite attracts’, where analytes with opposite-sign charge interact more strongly with the stationary phase and, thus, elute later than neutral ones or those with same-sign charge. Neutral species can also be separated after being transformed into charged species with a complexing agent. The mobile phase for ion exchange separation usually contains some inorganic electrolyte of high concentration. A low percentage of miscible organic solvent such as methanol or acetonitrile can be added in some cases to facilitate elution of the analytes [30].

A reversed phase column is usually packed with silica-bonded organic moieties, such as C18 and C8 (18-carbon and 8-carbon aliphatic chains, respectively) and use the ‘likes attracts likes’ principle, where less polar analytes have a stronger interaction with the non-polar stationary phase and elute later than more polar analytes, as a result of van der Waals interactions and solubility differentiation of the analytes between the polar eluent and the hydrocarbon moieties of the stationary phase. It is normally used for the separation of polar, uncharged compounds with molecular weight less than 3000. The mobile

phase is usually composed of aqueous buffer with some organic modifier like methanol and acetonitrile. In order to apply it to the determination of ionic species, an ionic reagent is usually added to the mobile phase to pair with sample ions of opposite charge. In this case, separations are based on differences in retention of the various ion pairs on the stationary phase. Common ion pairing reagents include lipophilic cations, such as tetrapropylammonium or tetrabutylammonium, for sample anions; and alkyl sulfonated C6-C10, and some inorganic anions such as perchlorate or PF_6^- for sample cations [30].

Size exclusion chromatography (SEC) is the simplest type of chromatography that theoretically involves a pure mechanical separation based on hydrodynamic-radius size. The surface of the column packing materials, usually made of silica or polymeric resin, can be visualized as beads containing pits and pores. Analytes of smaller size will penetrate deeper into the pore and require a larger volume of mobile phase to be washed out than larger analytes. A buffered solution of an inorganic salt is usually used as the mobile phase. This type of column is normally used for the separation of large biomolecules and polymers [29].

However, although a column is classified by its major separation mechanism, the actual separation process usually involves the combination of several mechanisms.

Further development in HPLC is driven by the needs of trace and ultra-trace analyses, such as the high-throughput speciation analysis of many biological and environmental samples that have a complex composition and are available in very limited quantity. Because of these demands for high speed and, hence, chromatographic resolution, as well as

reduced sample size, microbore columns were developed. They are miniature versions of conventional columns, with smaller internal diameter (0.5-2.1 mm vs. 3.9-5 mm for a conventional column), and containing smaller-size particles, which operate with the same mechanisms. Thus, microbore columns can be used to separate all kinds of species that are accessible to standard HPLC separations. The advantages of microbore columns include increased mass sensitivity, higher chromatographic resolution, shortened separation time, and reduced sample and solvent consumptions [31, 32].

Capillary HPLC, where the column has an internal diameter smaller than 0.5 mm, is a natural product of this scaling down trend. The reduced column volume requires a corresponding lowered mobile phase flow rate, usually in the range of 0.4-100 $\mu\text{L}/\text{min}$, which subsequently requires a more precise solvent pumping system. A micro-flow splitting device is often adopted to achieve the desired flow rate [33].

1.3.2 ICP-MS as HPLC detector

ICP-MS was first introduced in the early 1980s by coupling ICP and a mass spectrometer [34]. Although a late bloomer in the stellar team of atomic spectroscopy, it, however, stands out with the merits of multi-element and isotope measurement capabilities, high sensitivity, low detection limits and large linear dynamic range, and is the primary choice in elemental analysis nowadays. An ICP-MS instrument consists of the following basic components: the sample introduction system, the plasma generation system, the sampling interface and ion optics, and the mass analyzer.

1.3.2.1 Sample introduction system. Liquid is the most common sample state in ICP-MS analysis. There are a variety of designs of liquid sample introduction systems, which usually consist of a peristaltic pump, a nebulizer and a spray chamber. A liquid sample is pumped into the liquid channel of a nebulizer and shattered into an aerosol at the tip of the nebulizer by the pneumatic action of flowing gas. The aerosol then travels through a spray chamber where finer droplets are selected and carried away by the nebulizer gas into the plasma, while larger droplets settle down under gravity or condense on the side wall of the spray chamber and eventually are removed as waste by continuous pumping [35].

Ideally, an aerosol containing small droplets with a narrow droplets size distribution is desired to minimize the noise induced by desolvation/vaporisation in the ICP. Pneumatic nebulizers like glass concentric nebulizers are commonly used as ICP-MS sample introduction devices due to their robustness, simplicity and low cost. Micro-uptake nebulizers were designed for low flow rate sampling by improving the gas-liquid interaction and reducing the droplets size distribution [36, 37], and are suitable when sample size is limited, such as with biological and forensic samples, or when minimal sample consumption is desired. These nebulizers include the micro-concentric nebulizer (MCN), ultrasonic nebulizer (USN) and direct injection nebulizer (DIN). The advantages of a MCN lie in its good compatibility with a conventional spray chamber, wide commercial availability and rugged performance at normal or elevated nebulizer gas pressures [37]. A DIN is a micro-concentric nebulizer that replaces the torch injector (i.e., central tube). It thus introduces the liquid sample directly into the plasma where the aerosol is desolvated *in situ*,

thereby improving transport efficiency up to 100% theoretically. A spray chamber is not used with a DIN, affording the benefits of faster response time, reduced dead volume and memory effect. However, this *in situ* desolvation nature also makes a DIN less tolerant to samples with a high content of dissolved salts or volatile organic solvents, which cause plasma instability and tip clogging [38].

The spray chambers are responsible for the loss of transport efficiency in sample introduction. Cyclonic designs can reduce interaction between the aerosol and the walls of the spray chamber, thereby improving transport efficiency and reducing memory effects. Double-pass spray chambers provide a lower transport efficiency, making them useful for samples containing a high concentration of dissolved salts. Cylindrical type spray chambers are designed for use with micro-uptake nebulizers at low flow rate, which is useful for the eluent from chromatographic and electrophoretic separations [39].

1.3.2.2 Plasma generation system. A plasma is a partially ionized gas that conducts electricity and is affected by a magnetic field. The ICP is generated by inductively coupling of a gas flowing through a specially designed torch to a Tesla coil, as illustrated in Figure 1.2 [40]. The plasma ignition starts with a high voltage spark passing through the main plasma gas stream. The seed electrons are then accelerated in the radio frequency (RF) magnetic field induced by a water-cooled coil wound around the end the torch. A high frequency (27 or 40 MHz) current flows through the coil, producing a rapidly changing direction magnetic field. The highly mobile light electrons are forced to change directions quickly by the alternating current, resulting in collision between electrons and the argon atoms, which in turn produces more electrons, ions and heat. As this self-

perpetual process goes on, a stable plasma is produced and sustained as long as the RF current is supplied continuously.

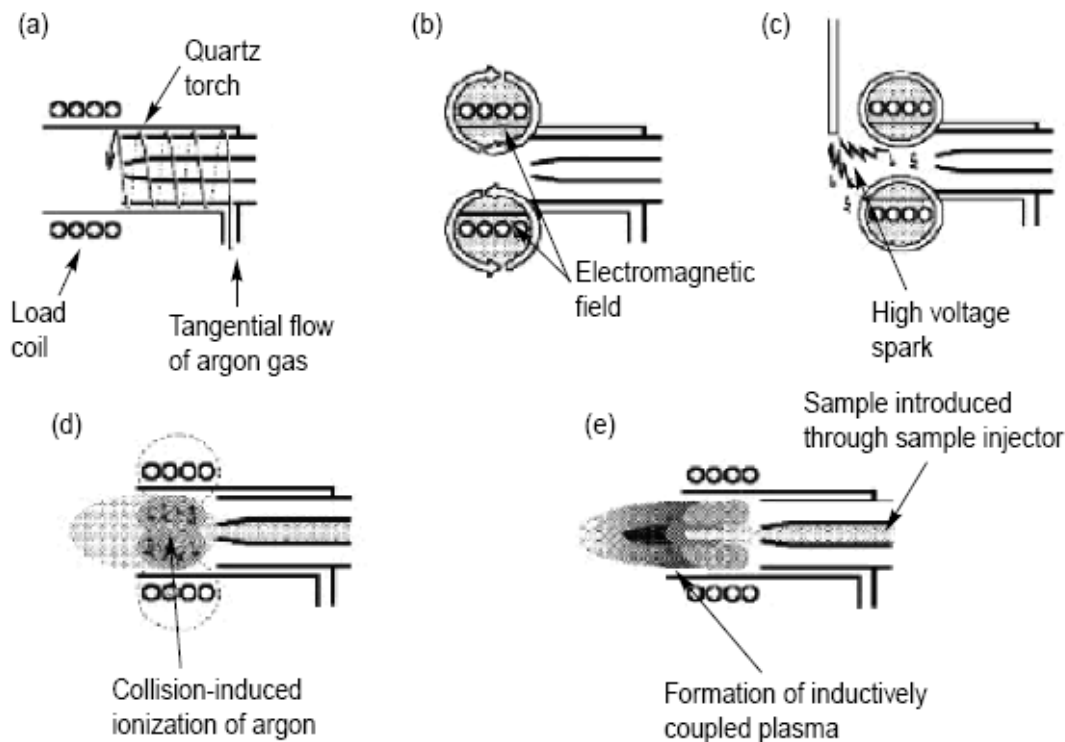


Figure 1.2. Schematic of an ICP torch and load coil showing how the inductively coupled plasma is formed. (a) A tangential flow of argon gas is passed between the outer and middle tube of the quartz torch. (b) RF power is applied to the load coil, producing an intense electromagnetic field. (c) A high-voltage spark produces free electrons. (d) Free electrons are accelerated by the RF field, causing collisions and ionization of the argon gas. (e) The ICP is formed at the open end of the quartz torch. The sample is introduced into the plasma via the sample injector (taken from reference [40]).

As there is no electrode involved in this energy transfer mode, it is called inductive coupling [41]. Energy is transferred into the plasma most efficiently in the induction region, i.e., within and slightly above the load coil, where the temperature can reach as high as 10,000 K. The central region of the plasma has a lower temperature, i.e., 6000-7000 K,

as it is cooled by the carrier gas and the sample aerosol; however, this is where ionization of the analytes ultimately takes place [41].

Once the sample aerosol is swept axially into the plasma by the carrier gas, it will undergo a series of processes sequentially, i.e., (1) desolvation; (2) vaporisation; (3) atomisation and (4) ionization. The high temperature of the plasma makes it an efficient elemental ion source for MS. The majority of elements in the periodic table with first ionization potential (FIP) ≤ 10 eV are singly ionized, while a few doubly-charged ions are formed, resulting in a simple, easy to interpret mass spectrum [41].

1.3.2.3 Sampling interface and ion optics. After the ICP is formed, a portion of the plasma is extracted from the central channel into the mass analyzer where ions are separated and analyzed according to their mass-to-charge ratios (m/z). The sampling interface assembly is used to sample the high temperature, atmospheric pressure plasma into a vacuum chamber, which consists of two coaxially positioned water-cooled metal cones, i.e., the sampler and the skimmer, and is maintained at a pressure of 1-5 torr using a mechanical roughing pump (Figure 1.3). The nozzle of the sampler is immersed in the plasma along the central axis. The portion of plasma passing through the sampler orifice undergoes rapid expansion because pressure within the interface is much smaller than in the atmospheric plasma. Both the temperature and pressure of the plasma fall drastically in this region and most of the plasma gas is removed through pumping [42].

Ions emerging from the skimmer cone are isolated by ion optics prior to entering the mass analyzer. The ion optics consists of a series of electrically controlled plates, barrels

or cylinders [44]. The electric potentials are set to negative so as to guide the positively charged ions and repel the negatively charged electrons. Most photons and neutral species are also filtered out by appropriately designed ion optics.

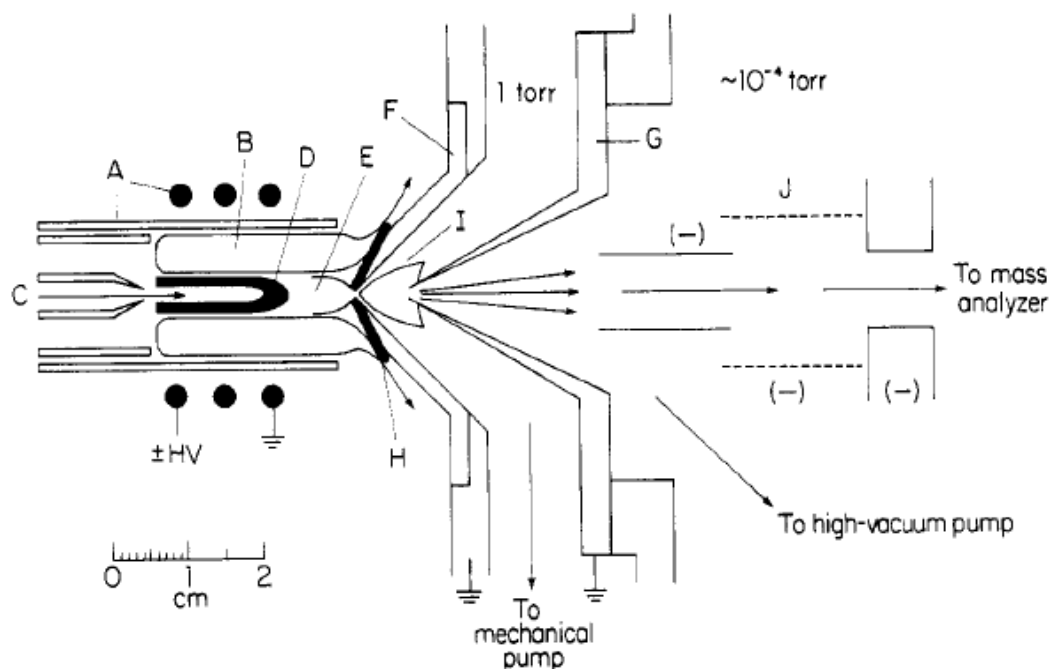


Figure 1.3. Schematic diagram of ICP and ion extraction device: A, load coil around the torch; B, hot outer torus of ICP; C, sample flowing into central channel of ICP; D, emission from oxides and neutral atoms; E, emission from ions; F, sampling nozzle with 1-mm hole in tip; G, skimmer; H, boundary layer of cold gas outside of sampler; I, supersonic jet between sampler and skimmer; J, ion lens. The negative sign represents negative voltage applied onto the ion optics (taken from reference [43]).

1.3.2.4 Mass analyzer. Ions emerging from the ion optics are separated in a mass analyzer. Different types of mass analyzers have been coupled with ICP, including quadrupole, time-of-flight (TOF), and electrostatic/magnetic devices. As quadrupole analyzer is used in both ICP-MS instruments for this thesis work, its working principle will be intro-

duced briefly.

A quadrupole analyzer consists of a set of four conductive rods mounted parallel into a square shape. The opposite pairs of rods are electrically connected. RF and DC potentials are applied to each pair of rod with opposite signs so that each pair has the potential $P = U + V\cos(2\pi ft)$, where U is a DC potential and $V\cos(2\pi ft)$ is a RF potential of constant f and a maximum amplitude V . The electrical fields of the rods influence the ions by inducing a transverse potential causing the ions to oscillate perpendicularly to the direction of the travelling path of the ions. With a specified U and V , only ions with a specific m/z ratio can survive the oscillation to emerge from the end, while others will eventually collide with the rods and be evacuated. If U and V are varied with time to maintain a constant U/V ratio while increasing the absolute value of the potential, ions of increasing m/z will pass through the quadrupole in rapid succession, which is how a mass spectrum is obtained [45]. In a sense, a quadrupole is an ion filter that separates ions with a defined m/z at a time, which makes it a sequential mass analyzer. The time during which a specific m/z is isolated is called dwell time, which is usually a few to hundreds of milliseconds. A longer dwell time can increase the signal-to-noise (S/N) ratio and thus lower the limit of detection (LOD), but at the expense of extended acquisition time. The dwell time must be selected carefully during the measurement of time-dependent transient signals, e.g. those resulting from a chromatographic separation, to avoid the spectral skew that would result from an insufficient number of measurement points across a chromatographic peak. Furthermore, the number of isotopes that can be monitored has to be limited for a quasi-simultaneous measurement of each isotope [28].

After ions emerge from the mass analyzer, they are detected by an electron multiplier. Each ion arriving at the detector impinges on an electrode that is maintained at a high negative potential, causing it to emit a pulse of electrons. These electrons are then accelerated toward a nearby dynode with a less negative potential. The collision of the electrons with the dynode cause more electrons to emit and the electrical pulse is thus magnified. As this process repeats a sufficient number of times, one ion striking the detector generates a measurable electrical pulse of current.

1.3.3 Hyphenation of HPLC and ICP-MS

The compatibility of HPLC and ICP-MS, two top players in their own fields, is exceptionally good. The physical hyphenation is straightforward and simply involves connecting the outlet of the HPLC system to the liquid inlet of the ICP-MS nebulizer (Figure 1.4) with narrow-bore tubing, which is kept as short as possible to minimize dispersion, as this would degrade the chromatographic resolution. The two parts can be controlled separately or integrated, which greatly facilitates automation [46]. In any case, all tubing, fittings and other detection cells, such as spectrophotometry, which is often used prior to ICP-MS detection, should preferably be made of metal-free material like PEEK (polyetheretherketone) and Teflon®.

A bypass valve is usually inserted between the HPLC system and the nebulizer so as to allow the continuous introduction of standard solution to optimize the ICP-MS operating conditions. This so-called tuning solution should be prepared in the mobile phase so that the conditions selected will be optimal when the chromatographic system is put on-line,

especially if isocratic elution is carried out. The matrix can indeed affect the optimal voltage applied to the ion optics. The latter should thus be adjusted so as to reach a satisfactory compromise between signal stability and sensitivity.

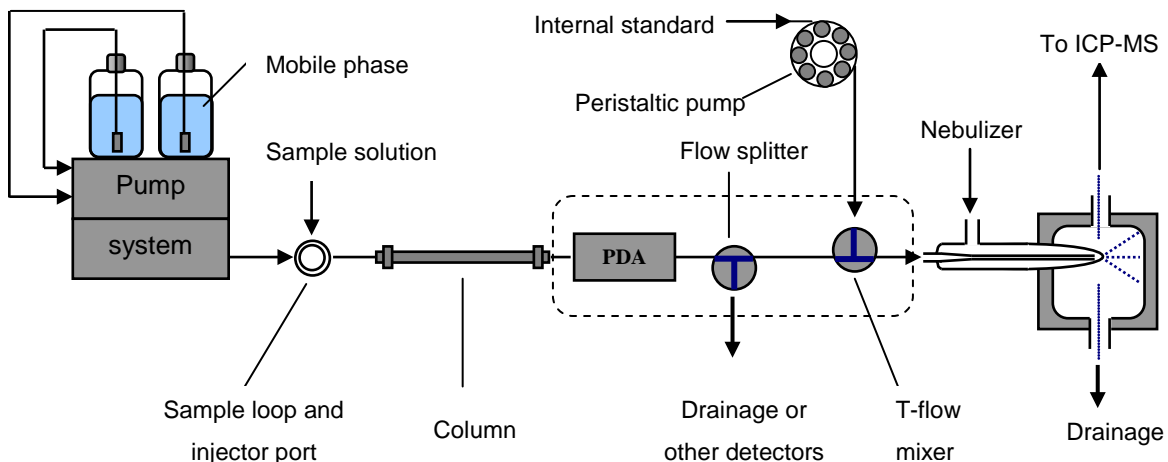


Figure 1.4. Typical setup used when hyphenating HPLC to ICP-MS. The components in the dashed region are optional (PDA = photodiode array detector.)

An internal standard may also be added on-line to compensate for non-spectroscopic interferences or drift induced by the mobile phase, even more so if gradient elution is carried out. However, such addition should be done carefully so as to minimize dilution of the column effluent, which would translate to reduced sensitivity, and so as to avoid degrading the chromatographic resolution.

Alternatively, an enriched isotope spike solution of the element being determined can be used, as the ideal internal standard, to perform species-unspecific isotope dilution analysis on-line [47], if the analyte has at least two isotopes that are free of spectroscopic inter-

ference. For example, to do the speciation analysis of the metabolites of a drug molecule containing Br, the effluent from the HPLC column would be continuously mixed with ^{81}Br -enriched spiked solution and $^{81}\text{Br}^+ / ^{79}\text{Br}^+$ monitored by ICP-MS. Because the different isotopes of an element are affected similarly, monitoring an isotope ratio instead of individual isotope intensities effectively counteracts any change in Br sensitivity caused by the HPLC gradient [48].

For an adequate hyphenation, care should be taken to: (1) match up the eluent flow rate with the sample uptake rate of the nebulizer, and (2) select an eluent that ICP-MS can handle (i.e., that does not contain too high a concentration of dissolved salts or volatile organic solvents). These two factors are not independent: a high flow rate leads to a larger amount of matrix uptake during a given time, which can lead to faster clogging of the cones of the interface by gradual salt or soot deposition. To minimize the total quantity of salt or organic solvent entering the ICP-MS system, the bypass valve can be switched so that the mobile phase drains to waste while the HPLC system is equilibrating. Only when the analysis is started, is the mobile phase directed to the ICP-MS instrument. This can be done automatically if the bypass valve is automated [46].

The mobile phase flow rate for typical HPLC separations is in the range of 0.2-1.5 mL/min, which matches the sample uptake rate of the conventional sample introduction system of ICP-MS. Microbore and capillary HPLC require the use of a micro-nebulizer with small-volume spray chamber or of some direct injection nebulizer (DIN), which operate at much smaller flow rates, as it is important to minimize the dead volume. A DIN is advantageous in this regard, as it does not require a spray chamber, hence totally elimi-

nating the dead volume of the latter.

The mobile phase for HPLC separations often contains a relatively high concentration of dissolved salts or volatile organic solvents. Thus, for a typical HPLC separation that takes 5-20 minutes, a great amount of matrix substance will be aspirated into the ICP-MS instrument. The matrix from the sample is usually negligible compared to that from the mobile phase, as only a minute amount of sample is injected whereas the mobile phase is pumped continuously [46]. The matrix may affect the ICP-MS performance in three ways: (1) it can result in spectroscopic interference on the analyte signal; (2) it can cause analyte signal drift and loss of sensitivity from soot and salt deposition on the interface cones and ion optics; and (3) it can induce non-spectroscopic interference, which may suppress or enhance the analyte signal. This matrix issue is discussed further below, according to the nature of the eluent matrix used for different types of liquid chromatography.

1.3.3.1 Organic solvents. As mentioned in section 1.3.1 (*HPLC as a separation technique*), organic solvent is sometimes added to the mobile phase to facilitate the mass transfer between the two phases, especially in RP-HPLC, where a gradient elution is usually required, with up to 100% organic solvent at a certain stage. The introduction of organic solvents into the plasma can make the plasma less energetic, by requiring energy for their desolvation, vaporisation and atomisation, which is no longer available for the analyte. This, in turn, leads to poor ionization efficiency and thus decreased sensitivity. Overloading the plasma with organic solvents destabilizes or even extinguishes the plasma. Additionally, thermal decomposition of organic solvent results in carbon deposition

on the sampler and skimmer cones as well as on the ion optics, which reduces sensitivity and induces signal drifting. In order to minimize these effects, it is imperative to reduce the amount of organic matrix, or to minimize the impact of the organic solvent on the plasma. Several approaches can be used to tackle this problem:

- (1) use a hot plasma with a high RF power;
- (2) titrate oxygen into the nebulizer carrier gas until the carbon emission (green color) disappears;
- (3) select a different solvent;
- (4) reduce the amount of mobile phase reaching the plasma by using a flow splitter;
- (5) cool the spray chamber;
- (6) substitute a surfactant for the organic solvent;
- (7) use a desolvation system;
- (8) use low flow rate liquid chromatography (such as microbore or capillary HPLC);

where (1)-(3) aim to diminish the effect of organic solvents, and (4)-(8) aim at reducing the amount of organic solvent being introduced into the plasma. These methods are detailed in the following sub-sections.

1.3.3.1.1 Mitigating the effect of organic solvents on the ICP. A high RF power (1.4-1.7 kW) will result in a more energetic plasma, which will counteract the weakening ef-

fect of organic solvents. It is also a general practice to titrate oxygen gas into the argon nebulizer gas to transform thermal decomposition into oxidative combustion. Carbon deposits are therefore prevented in favour of the formation of gaseous carbon oxide. Only a few percent (3-7%) of oxygen gas need to be added [49], as an excessive amount of oxygen can cause serious oxidative corrosion of the sampler and skimmer cones. The oxygen must thus be added in proportion with the amount of organic solvent being introduced to minimize damage to the sampling cones. This poses a dilemma when gradient elution is conducted, where the concentration of organic solvent can vary drastically during a chromatographic separation, unless the amount of oxygen can be varied along with the gradient. Sampler and/or skimmer cones made of platinum are more oxygen-resistant and more suitable for this situation than those made of nickel, but at a higher cost [50]. Appropriately selecting the solvent can efficiently reduce the amount of oxygen needed. For example, methanol has a higher oxygen-to-carbon ratio and combusts more thoroughly, making it a preferable organic solvent over ethanol and acetonitrile.

As mentioned earlier, organic solvents in the mobile phase can be problematic during a gradient elution as they may induce changes in ICP-MS sensitivity and background. Indeed, analyte signal enhancement or suppression can result, depending on the experimental conditions used and the element detected. A correction function is thus needed to account for the baseline drift caused by the change of organic solvent concentration during a gradient elution [51]. This can be obtained by continuously spiking elemental standards into the mobile phase as it elutes from the column without sample injection while recording the chromatogram by ICP-MS in time-resolved mode. The signal trace data thus ob-

tained are then used to calculate a fitting function that is subsequently applied as a correction function in real sample analysis [51]. However, this approach is scarcely used because it is only effective if the baseline shift is very reproducible from one chromatographic separation to the next and unaffected by sample injection.

1.3.3.1.2 Minimizing the amount of organic solvents introduced into the ICP. A flow splitter can be used to reduce the flow rate reaching the nebulizer by diverting part of the mainstream eluent flow into drainage or towards other detectors like UV-spectrophotometry, conductivity, etc. These are commercially available, from simple T-piece to more complicated multi-channels valves. Flow rates down to a few microliters per minutes can be accurately realized. Properly designed flow splitters streamline the flow to avoid clogging by dissolved salts, and reduce dead volume efficiently. However, this diversion also reduces the amount of analyte reaching the plasma, so a balance must be reached between reducing the solvent load and keeping the necessary analyte mass flow.

Most transport efficiency loss occurs in the spray chamber [41]. Although this is usually the Achille's heel of ICP-MS, it can be taken advantage of when coupling ICP-MS with HPLC in order to reduce solvent uptake. Cooling the spray chamber down to $-10\text{ }^{\circ}\text{C}$ reduces solvent evaporation and promotes solvent condensation, thus reducing the amount of solvent reaching the plasma [48, 52]. Reducing the internal diameter of the torch injector from the common 2 mm to 1 mm also decreases the solvent vapour loading in the plasma [48, 53].

Another approach is to substitute surfactants for organic solvent, which form micelles in aqueous solution above their critical micelle concentration. Indeed, the presence of micelles improves the interaction between the mobile phase and solutes, allowing a better and faster separation, with a concurrent reduction in the amount of organic solvent in the mobile phase [31].

Microbore HPLC offers higher chromatographic resolution and separation efficiency than conventional HPLC, making it an ideal candidate for hyphenation to ICP-MS. The flow rate of microbore HPLC is in the range of a hundred to a few microliters per minute. As a result, the amount of organic solvent being introduced into ICP-MS during a typical chromatographic separation over 5-20 minutes is often not problematic. However, the interface of microbore HPLC with ICP-MS is crucial for a successful hyphenation. It is imperative to use a micro-uptake nebulizer with or without compatible spray chamber so as to minimize extra column dead volume and ensure enough sample introduction efficiency for adequate analyte detection (see section *1.3.2.1 Sample introduction system*).

All of the above methods that aim to reduce the amount of solvent introduced in the plasma concurrently reduce the absolute amount of analyte being introduced. An alternative approach is to remove the solvent before the eluent penetrates the plasma. This can be accomplished with a desolvation device, which usually consists of a heater/condenser system that is sometimes coupled to a membrane desolvator when an ultrasonic nebulizer (USN) is used [54]. This approach increases the sample introduction efficiency, compared to that with a conventional sample introduction system, while drastically reducing the solvent load. It is especially useful when gradient elution involving solely a change

in organic solvent concentration is carried out.

1.3.3.2 Inorganic salts. The presence of highly concentrated inorganic salts, either as part of buffers or electrolytes, may lead to deposits on the interface cones and ion optics, in turn resulting in signal drift, suppression and, eventually, clogged cones. This problem is especially eminent in IEC. The methods described earlier that reduce the amount of sample reaching the plasma, such as a flow splitter and low flow rate chromatography, are also applicable to salts reduction. Additionally, electrolytes that form or decompose into gaseous components in the plasma can preferentially be selected as the mobile phase. Ammonium salts, such as ammonium nitrate, ammonium acetate and ammonium formate are popular components of mobile phases in IEC-ICP-MS analysis [32, 55-57], among which ammonium nitrate is especially attractive as there is then no carbon-containing components generated during the ionization process. An addition of complexing agent to the mobile phase can also result in faster separation while reducing the amount of salts that is required in the mobile phase [58, 59].

1.3.4 Applications of HPLC-ICP-MS

The hyphenation of HPLC and ICP-MS has been widely applied in speciation analysis for element-containing species that are non-volatile and cannot be converted to volatile species, such as organometallic species (with metal-carbon covalent bond), metal-complexes (with metal coordination bond) and inorganic species of different oxidation states. The most significant elements in term of speciation analysis include As, Sb, Hg, Cr, Se, Pt, Br, I, etc. Selected reports on HPLC-ICP-MS speciation analyses, which have

been published recently, are summarized in Table 1.1. Although different types of chromatographic techniques have been used in elemental speciation analysis, IEC is most common due to the naturally ionic character of most elemental species as well as the better compatibility of column eluents with ICP-MS detection. The general practice and focus in speciation analysis are to identify and quantify the target element species in a sample to assess their toxicity and/or essentiality.

However, reports on the application of IEC-ICP-MS to the study of solution equilibria are relatively rare, such as the determination of stability constant [22-24] and reaction kinetics [18, 25-27]. Huang and Beauchemin [22-24] developed a novel method to determine stability constants by utilizing the speciation information measured by hyphenated IEC-ICP-MS. The distinct advantage of this method was that it could determine the stability constant at concentration ranges as low as μM , which was not attainable with conventional electrochemical techniques, making it a promising method for evaluating the metal-ligand binding strength under biological conditions. Another feature of the method was the simultaneous determination of the stability constants of two metal complexes in one solution, which was also beyond the reach of those conventional methods.

Hann et al.[18] used RP-HPLC–ICP-MS to study the degradation process of cisplatin in water with varied chloride concentrations. This study was based on the fact that the decomposition of cisplatin in water is slow enough to fit with the time scale of an HPLC separation. In this process, samples were taken from the reaction solution intermittently and were submitted to speciation analysis over a period of 48 hours. The instant concentrations measured of each species were then plotted against time, which vividly showed

the reaction and transformation of the starting material and the products. The reaction rate constants of each species were then obtained.

Hence, in addition to its application to the speciation analysis of a variety of samples, HPLC-ICP-MS can be used to study the equilibration process as well as reactions. It may thus be not only useful and complementary to traditional methods but may also open new avenues of research by enabling ultra-trace measurements on a relatively short time scale. Further exploration of this powerful analytical technique is thus warranted.

Table 1.1 Selected examples of the application of HPLC-ICP-MS in speciation analysis*

Species and matrix	Instrumentation method	Elution mode, column brand and mobile phase compositions	LOD	Other details	Ref
As(III), As(V), MMA, DMA, four oxo-arsenosugars and four thio-arsenosugars Oyster tissue	IEC-ICP-MS (AEC)	Hamilton PRP-X100; gradient; MPA: 20 mM phosphate buffer; MPB: phosphate buffer containing 50% methanol	0.3-0.8 µg/L	25% aqueous acetone was introduced into the spray chamber to compensate for carbon content change during elution; External calibration	[60]
As(III), As(V), AsB, MMA and DMA Aqueous standard	IEC- (HR)-ICP-MS (AEC)	Dionex AS11/AG11; gradient: MPA: 0.5 mM ammonium nitrate MPB: 100 mM ammonium nitrate	5-10 ng/L	Column i.d.: 2.0mm; External calibration	[61]
As(III), As(V), MMA, DMA, AsB, AsC and TMAO Frozen human urine	IEC-ICP-MS (AEC)	Dionex AS7/AG7; gradient: MPA: 0.25mM Acetic acid/Sodium acetate MPB: 25mM nitric acid	0.2-0.8 µg/L	Calibration by standard addition	[62]
As(III), As(V), MMA, DMA and p-ASA Aqueous standards	Nano-IP-RP-HPLC-ICP-MS	NanoEase; Isocratic; 0.5 mM TBAP, pH 5.9	0.4-5.4 pg	Column i.d.: 0.3mm; HIHEN used as the nebulizer; External calibration	[63]
DPAA, PAA, DMPAO, MPAO Rice and soil	RP-HPLC-(DRC)-ICP-MS Cell gas: H ₂ ;	SunFire-C18; gradient; MPA: 0.1 formic acid in DDW; MPB: 0.1 formic acid in methanol	0.1-0.48 µg/L	USN with membrane desolvator used to remove organic solvent; External calibration	[64]
As(III), As(V), MMA, DMA, AsB, AsC, TMAO and TeMA ;Sb(III) and Sb(V) Hot spring water and fish tissue	IP-RP-HPLC-(DRC)-ICP-MS Cell gas: He	DevelosilC30-UG-5; isocratic: 10 mM sodium butanesulfonate/4 mM malonic acid/4 mM TMAOH/0.1 (v/v)% methanol/20 mM ammonium tartrate; pH 2.0	~0.2 µg/L for As ~0.5 µg/L for Sb	External calibration	[65]

Species and matrix	Instrumentation method	Elution mode, column brand and mobile phase compositions	LOD	Other details	Ref
Sb(III) and Sb(V) Soil extract	IEC- ICP-MS (AEC)	Hamilton PRP-X100; isocratic: 10 mM EDTA/1 mM phthalic acid	20-65 ng/L	Calibration by isotope dilution	[66]
Sb(III) and Sb(V) Tap water	IEC-ICP-MS (AEC)	Dionex AS 14; isocratic; 1.25 mM EDTA pH 4.7	12-14 ng/L	USN with membrane desolvator was used as the nebulizer; External calibration	[67]
Hg(II) and MeHg ⁺ Mussel, fish tissue and embryos	RP-ICP-MS	Symmetry Shield RP18; isocratic; 0.1% (v/v) formic acid/0.1%(v/v) HFBA/2%(v/v) methanol/0.02% (w/v) L-cysteine, pH 2.1	n/a	Calibration by standard addition	[68]
Hg(II), MeHg ⁺ and EtHg ⁺ hair	RP-ICP-MS	C18; isocratic: 0.05% v/v mercaptoethanol/ 0.4% (m/v) L-cysteine/ 0.06 mM ammonium acetate/5% (v/v) methanol	10-38 ng/g	External calibration	[69]
Pb(II), trimethyl-Pb, triethyl-Pb; Hg(II), MeHg ⁺ , EtHg ⁺ Fish muscle and tissue	RP-ICP-MS	Alletch-C18; isocratic: 0.2% (v/v) 2-mercaptoethanol/1 mg/L EDTA/ 174.2 mg/L sodium 1-pentanesulfonate/12% (v/v) methanol, pH 2.8	0.1-0.3 µg/L for Pb; 0.2-0.3 µg/L for Hg	Column i.d.: 1.0 mm; DIHEN used as nebulizer. External calibration	[70]
SeMet, SeCys, SeUr and TMSe; Hg(II) and MeHg ⁺ Human urine	RP-(DRC)-ICP-MS Cell gas: He/H ₂ (92.72/ 7.29)	SymmetryShield RP18; gradient: MPA: 0.3% aqueous methanol; MPB: 3% (v/v) aqueous methanol / 0.06 M ammonium acetate/ 0.1% (v/v)/2-mercaptoethanol	0.05-0.3 µg/L for Se; 2.5-2.0 µg/L for Hg	External calibration	[71]
Cr(VI) and Cr(III) Synthetic biomedium	IEC-(DRC)-ICP-MS (AEC) Cell gas: H ₂	Dionex AS11; gradient: Nitric acid/6mM 2,6-pyridinedicarboxylic acid with varied flow rate	0.3 µg/L for Cr(III); 0.8 µg/L for Cr(VI)	External calibration	[59]

Species and matrix	Instrumentation method	Elution mode, column brand and mobile phase compositions	LOD	Other details	Ref
Cr(VI) and Cr(III) Synthetic biofluid	RP-HPLC-(DRC)-ICP-MS Cell gas: ammonia	Brownlee-C8; isocratic: 2.0 mM TBAOH/ 0.5 mM EDTA/ 5% (v/v) methanol, pH 7.6	0.06-0.09 µg/L	Cr(III) is complexed with EDTA prior to separation. External calibration	[72]
Se(IV) and Se(VI); Cr(III) and Cr(VI) Surface water, ground water and tap water	IEC-(DRC)-ICP-MS (AEC) Cell gas: methane	Dionex AS11/AG11; isocratic; 20 mM sodium hydroxide	<1 µg/L	Cr(III) is complexed with EDTA prior to separation. External calibration	[73]
Cr(VI) and Cr(III) Mineral water	IEC-(CRI)-ICP-MS (AEC) CRI gas: H ₂	Hamilton PRP-X100; isocratic: 60 mM ammonium nitrate, pH 9.3	<0.1 µg/L	Cr(III) is complexed with EDTA prior to separation. External calibration	[74]
Cr(VI) and Cr(III) Natural water	IEC-ICP-MS (CEC)	Dionex CS5A/CG5A; gradient; MPA: 0.3 M nitric acid; MPB: 1 M nitric acid	0.19-0.32 µg/L	External calibration	[75]
cisplatin and its mono-hydrolyzed metabolite Cell incubating medium	HILIC-ICP-MS	ZIC-HILIC; isocratic: (70/30) DMF/20 mM acetate	0.2 ng/mL	External calibration	[76]
Cisplatin adducts with DNA Oligonucleotide and DNA	RP-HPLC-ICP-MS	Alltech C8; isocratic: 60 mM ammonium acetate, 7.5% MeOH, pH 5.8	n/a	External calibration	[77]

Species and matrix	Instrumentation method	Elution mode, column brand and mobile phase compositions	LOD	Other details	Ref
Cisplatin, monoaquaa- and/diaquacisplatin Cancer patient urine	RP-HPLC-ICP-MS	Thermo Hypersil-Keystone Hypercar; Gradient; MPA: 1 mM NaOH MPB: H ₂ O	0.65-0.74 µg/L	Column i.d.: 2.1 mm; A make-up flow was added to the main chromatographic flow with a T piece. Calibration by isotope dilution	[18]
I ⁻ and IO ₃ ⁻ Br ⁻ and BrO ₃ ⁻ Whole milk powder and seaweed	IEC-DRC-ICP-MS (AEC) Cell gas: O ₂	Hamilton PRP-X100; gradient: A: 15 mM NH ₄ NO ₃ , pH 10 B: 100 mM NH ₄ NO ₃ , pH 10	0.001-0.002 ng/mL for I; 0.03-0.04 ng/mL for Br	External calibration	[78]
I ⁻ and IO ₃ ⁻ Seawater	IEC-ICP-MS (AEC)	Agilent G3154A/101; isocratic: 20 mM ammonium nitrate, pH 5.6	1.5-2.0 µg/L	External calibration	[79]

**Abbreviations* AEC: Anion exchange chromatography; AsB: Arsenobetaine; AsC: Arsenocholine; DIHEN: Direct injection high efficiency nebulizer; DMA: Dimethylarsenic acid; DMF: Dimethylformamide; DMPAO: Dimethylphenylarsine oxide; DNA: Deoxyribonucleic acid; DPAA: Diphenylarsonic acid; DRC: Dynamic reaction cell; EDTA: Ethylenediaminetetraacetic acid; EtHg⁺, Ethylmercury; HFBA: Heptafluorobutanoic acid; HILIC: Hydrophilic interaction liquid chromatography; i.d.: internal diameter; IEC: Ion exchange chromatography; IP-RP-HPLC: Ion Pairing reversed phase high performance liquid chromatography; LOD: Limit of detection; MeHg⁺: Methylmercury; MMA: Monomethylarsonate; MPA: Mobile phase A; MPAO: Methylphenylarsine oxide; MPB: Mobile phase B; p-ASA: p-Arsanilic acid; SeCys: Selenocystine; SeMet: Selenomethionine; SeUr: Selenourea; TBAOH: Tetrabutylammonium hydroxide; TBAP: tetra-n-butylammonium phosphate; TeMA: Tetramethylarsenium; TMAO: Trimethylarsine oxide; TMAOH: Tetramethylammonium hydroxide; TMSb: Trimethylantimony; USN: Ultrasonic nebulizer

1.4 Objectives of this thesis

This thesis aims to explore the versatility and powerfulness of IEC-ICP-MS in elemental speciation analysis and equilibration process. To be specific, the main body of the thesis will address the following three objectives, in individual chapters.

- a) To improve a method for the determination of conditional stability constant

A method to determine conditional stability constants was previously developed in this laboratory, using IEC coupled to ICP-MS. When it was applied to the complexation of cobalt and zinc with ethylenediaminetetraacetic acid (EDTA) separately, the value determined for the conditional stability constant agreed with the literature but the chelation number deviated from an integer. Chapter 2 will look into the cause of this deviation and propose a remedy.

- b) To develop a simple method for chromium speciation analysis at ultra-trace level

For risk assessment purposes, a rapid speciation analysis method is required for chromium because Cr(III) is an essential micro-nutrient for biological activities whereas Cr(VI) is believed to be toxic and carcinogenic. The commonly used chromatographic separation methods usually involve the application of a complexing agent to facilitate the elution of Cr(III), which is not desired in order to preserve the original speciation. Indeed, several factors need to be considered when performing chromium speciation analysis: the oppositely charged states and the interconversion of the redox couple, and spectroscopic interferences with ICP-MS detection. For analysis at ultra-trace level, contami-

nation control also constitutes a key factor for reliable measurement. Chapter 3 will describe a simple IEC-ICP-MS method that addresses these issues. It involves a column with dual ion exchange capability to separate the oppositely charged species directly, without using charge-switching reagent, thus preserving the originality of the sample. A gradient elution is also used to elute the two chromium at different pH and ionic strength to ensure separation while avoiding the reduction of Cr(VI). And a new collision-reaction interface is employed to eliminate spectroscopic interferences during ICP-MS detection.

- c) To develop a simple method to study the kinetics of the reduction of Cr(VI) in riverine water

Chapter 4 will demonstrate that the speciation analysis developed in Chapter 3 provides a simple yet powerful tool for studying the reduction of Cr(VI) in real samples. Indeed, Cr(VI) can be reduced to Cr(III) in the natural environment in the presence of inorganic/organic substances, with humic substances being an important type of reducing agent in soil and natural water. The proposed approach is in contrast to conventional methods, which involve off-line processes, where chromium species are selectively precipitated or modified with chromophore(s) before spectrometric or spectrophotometric detection, and usually involve tedious sample treatment and relatively large sample consumption. The simplicity of the proposed chromium speciation analysis method will be demonstrated while studying the effect of pH and temperature during a kinetics study of Cr(VI) in acidified riverine water sample.

References

1. D.M. Templeton, F. Ariese, R. Cornelis, L.G. Danielsson, H. Muntau, H.P. Van Leeuwen, and R. Lobinski, *Guidelines for terms related to chemical speciation and fractionation of elements. Definitions, structural aspects, and methodological approaches (IUPAC Recommendations 2000)*. Pure and Applied Chemistry, 72 (2000) 1453-1470.
2. P. Vandael, *The importance of chromium in occupational health*, in *Trace element speciation for environment, food and health*, L. Ebdon, L. Pitts, R. Cornelis, H. Crews, O.F.X. Donard, and P. Quevauviller, Editors. 2001, The Royal Society of Chemistry: Cambridge.
3. D. Caussy, *Case studies of the impact of understanding bioavailability: arsenic*. Ecotoxicology and Environmental Safety, 56 (2003) 164-173.
4. S. Baker, M. Herrchen, K. Hund-Rinke, W. Klein, W. Kordel, W. Peijnenburg, and C. Rensing, *Underlying issues including approaches and information needs in risk assessment*. Ecotoxicology and Environmental Safety, 56 (2003) 6-19.
5. J.A. Caruso, B. Klaue, B. Michalke, and D.M. Rocke, *Group assessment: elemental speciation*. Ecotoxicology and Environmental Safety, 56 (2003) 32-44.
6. G. Darrie, *The importance of chromium in occupational health*, in *Trace element speciation for environment, food and health*, L. Ebdon, L. Pitts, R. Cornelis, H. Crews, O.F.X. Donard, and P. Quevauviller, Editors. 2001, The Royal Society of Chemistry: Cambridge.
7. E.J. Underwood, *Trace elements in human and animal nutrition*. 3rd edition ed.

- 1971, New York: Academic press.
8. R.A. Anderson, *Chromium, glucose intolerance and diabetes*. Journal of the American College of Nutrition, 17 (1998) 548-555.
 9. R.A. Anderson, *Effects of chromium on body composition and weight loss*. Nutrition Reviews, 56 (1998) 266-270.
 10. F. Dong, M.R. Kandadi, J. Ren, and N. Sreejayan, *Chromium(D-phenylalanine)(3) supplementation alters glucose disposal, insulin signaling, and glucose transporter-4 membrane translocation in insulin-resistant mice*. Journal of Nutrition, 138 (2008) 1846-1851.
 11. K.W. Jennette, *Microsomal reduction of the carcinogen chromate produces chromium(V)*. Journal of the American Chemical Society, 104 (1982) 874-875.
 12. M.J. Tsapakos, T.H. Hampton and K.W. Jennette, *The carcinogen chromate induces DNA cross-links in rat liver and kidney*. Journal of Biological Chemistry, 256 (1981) 3623-3626.
 13. A.L. Holmes, S.S. Wise and J.P. Wise, *Carcinogenicity of hexavalent chromium*. Indian Journal of Medical Research, 128 (2008) 353-372.
 14. S.S. Wise, A.L. Holmes, Q. Qin, H. Xie, S.P. Katsifis, W.D. Thompson, and J.P. Wise, *Comparative Genotoxicity and Cytotoxicity of Four Hexavalent Chromium Compounds in Human Bronchial Cells*. Chemical Research in Toxicology, 23 (2010) 365-372.
 15. M.D. Cohen, B. Kargacin, C.B. Klein, and M. Costa, *Mechanisms of chromium carcinogenicity and toxicity*. Critical Reviews in Toxicology, 23 (1993) 255-281.
 16. B. Rosenberg, *Fundamental studies with cisplatin*. Cancer, 55 (1985) 2303-2316.

17. S.E. Sherman and S.J. Lippard, *Structural aspects of platinum anticancer drug interactions with DNA*. Chemical Reviews, 87 (1987) 1153-1181.
18. S. Hann, G. Koellensperger, Z. Stefanka, G. Stingeder, M. Fuerhacker, W. Buchberger, and R.M. Mader, *Application of HPLC-ICP-MS to speciation of cisplatin and its degradation products in water containing different chloride concentrations and in human urine*. Journal of analytical atomic spectrometry, 18 (2003) 1391-1395.
19. E. Jerremalm, I. Wallin and H. Ehrsson, *New Insights Into the Biotransformation and Pharmacokinetics of Oxaliplatin*. Journal of Pharmaceutical Sciences, 98 (2009) 3879-3885.
20. R. Munoz-olivass and C. Camara, *The importance of chromium in occupational health*, in *Trace element speciation for environment, food and health*, L. Ebdon, L. Pitts, R. Cornelis, H. Crews, O.F.X. Donard, and P. Quevauviller, Editors. 2001, The Royal Society of Chemistry: Cambridge.
21. B. Michalke, *Perspective on element speciation*. Journal of Environmental Monitoring, 11 (2009) 1754-1756.
22. C. Huang, *Determination of conditional stability constants using ion chromatography coupled with inductively coupled plasma mass spectrometry*, in *Chemistry*. 2006, Queen's university: Kingston.
23. C. Huang and D. Beauchemin, *Simultaneous determination of two conditional stability constants by IC-ICP-MS*. Journal of analytical atomic spectrometry, 21 (2006) 1419-1422.
24. C. Huang and D. Beauchemin, *A simple method based on IC-ICP-MS to deter-*

- mine conditional stability constants*. Journal of analytical atomic spectrometry, 21 (2006) 317-320.
25. O. Heudi, A. Cailleux and P. Allain, *Kinetic studies of the reactivity between cis-platin and its monoquo species with L-methionine*. Journal of Inorganic Biochemistry, 71 (1998) 61-69.
 26. Q. Tu, T. Wang, C.J. Welch, P. Wang, X. Jia, C. Raab, X. Bu, D. Bykowski, B. Hohenstaufen, and M.P. Doyle, *Identification and Characterization of Isomeric Intermediates in a Catalyst Formation Reaction by Means of Speciation Analysis Using HPLC-ICPMS and HPLC-ESI-MS*. Analytical Chemistry, 78 (2006) 1282-1289.
 27. J. Wang, F.-J. Zhao, A.A. Meharg, A. Raab, J. Feldmann, and S.P. McGrath, *Mechanisms of arsenic hyperaccumulation in Pteris vittata. Uptake kinetics, interactions with phosphate, and arsenic speciation*. Plant Physiology, 130 (2002) 1552-1561.
 28. J. Szpunar and R. Lobinski, *Hyphenated techniques in speciation analysis*. RSC Chromatography monographs, ed. R.M. Smith. 2003, Cambridge: The Royal Society of Chemistry.
 29. M.C. McMaster, *HPLC, a practical user's guide*. 2nd ed. 2007, Hoboken, N.J: Wiley-Interscience.
 30. J.S. Fritz and D.T. Gjerde, *Ion Chromatography*. 4th ed. 2009, Weinheim: Wiley-VCH.
 31. H. Garraud, A. Woller, P. Fodor, and O.F.X. Donard, *Trace elemental speciation by HPLC using microbore columns hyphenated to atomic spectrometry: A review*.

- Analisis, 25 (1997) 25-31.
32. A. Castillo, A.F. Roig-Navarro and O.J. Pozo, *Capabilities of microbore columns coupled to inductively coupled plasma mass spectrometry in speciation of arsenic and selenium*. Journal of Chromatography A, 1202 (2008) 132-137.
 33. Z. Stefanka, G. Koellensperger, G. Stingeder, and S. Hann, *Down-scaling narrowbore LC-ICP-MS to capillary LC-ICP-MS: a comparative study of different introduction systems*. Journal of analytical atomic spectrometry, 21 (2006) 86-89.
 34. R.S. Houk, *Mass spectrometry of inductively coupled plasma*. Analytical Chemistry, 58 (1986) 97A-105A.
 35. R. Thomas, *Spectroscopy tutorial - A beginner's guide to ICP-MS - Part II: The sample-introduction system*. Spectroscopy, 16 (2001) 56-60.
 36. D. Iwahata, K. Hirayama and H. Miyano, *A highly sensitive analytical method for metal-labelled amino acids by HPLC/ICP-MS*. Journal of analytical atomic spectrometry, 23 (2008) 1063-1067.
 37. K.L. Ackley, K.L. Sutton and J.A. Caruso, *A comparison of nebulizers for microbore LC-ICP-MS with mobile phases containing methanol*. Journal of analytical atomic spectrometry, 15 (2000) 1069-1073.
 38. J.A. McLean, H. Zhang and A. Montaser, *A direct injection high-efficiency nebulizer for inductively coupled plasma mass spectrometry*. Analytical Chemistry, 70 (1998) 1012-1020.
 39. M. Mahar, J.F. Tyson, K. Neubauer, and Z. Grosser, *High throughput sample introduction system for the analysis of drinking waters and wastewaters by ICP-MS*. Journal of analytical atomic spectrometry, 23 (2008) 1204-1213.

40. R. Thomas, *A beginner's guide to ICP-MS - Part III: The plasma source*. Spectroscopy, 16 (2001) 26-30.
41. D. Beauchemin, D.C. Gregoire, D. Gunther, V. Karanassios, J.M. Mermet, and T.J. Wood, *Discrete Sample Introduction Techniques for Inductively Coupled Plasma Mass Spectrometry*. 2000
42. H. Niu and R.S. Houk, *Fundamental aspects of ion extraction in inductively coupled plasma mass spectrometry*. Spectrochimica Acta Part B-Atomic Spectroscopy, 51B (1996) 779-815.
43. R.S. Houk, *Elemental and isotopic analysis by inductively-coupled plasma mass spectrometry*. Accounts of Chemical Research, 27 (1994) 333-339.
44. R. Thomas, *A beginner's guide to ICP-MS - Part V: The ion focusing system*. Spectroscopy, 16 (2001) 38-44.
45. Varian, *Varian 810/820MS customer training manual*. 2009.
46. K. Neubauer, *Innovations in speciation analysis using HPLC with ICP-MS detection*. Spectroscopy, 22 (2008) 24-31.
47. K.G. Heumann, *Isotope-dilution ICP-MS for trace element determination and speciation: from a reference method to a routine method?* Analytical and Bioanalytical Chemistry, 378 (2004) 318-329.
48. F. Cuyckens, L.I.L. Balcaen, K. De Wolf, B. De Samber, C. Van Looveren, R. Hurkmans, and F. Vanhaecke, *Use of the bromine isotope ratio in HPLC-ICP-MS and HPLC-ESI-MS analysis of a new drug in development*. Analytical and Bioanalytical Chemistry, 390 (2008) 1717-1729.
49. B. Gammelgaard and B. Packert Jensen, *Application of inductively coupled plas-*

- ma mass spectrometry in drug metabolism studies*. Journal of analytical atomic spectrometry, 22 (2007) 235-249.
50. S.M. Nelms, *ICP Mass Spectrometry Handbook*. 2005, Oxford: Blackwell Publishing Ltd.
 51. C. Siethoff, I. Feldmann, N. Jakubowski, and M. Linscheid, *Quantitative determination of DNA adducts using liquid chromatography electrospray ionization mass spectrometry and liquid chromatography high-resolution inductively coupled plasma mass spectrometry*. Journal of Mass Spectrometry, 34 (1999) 421-426.
 52. B.P. Jensen, C.J. Smith, C.J. Bailey, C. Rodgers, I.D. Wilson, and J.K. Nicholson, *Investigation of the metabolic fate of 2-, 3- and 4-bromobenzoic acids in bile-duct-cannulated rats by inductively coupled plasma mass spectrometry and high-performance liquid chromatography/inductively coupled plasma mass spectrometry/electrospray mass spectrometry*. Rapid Communications in Mass Spectrometry, 19 (2005) 519-524.
 53. L.I.L. Balcaen, B. De Samber, K. De Wolf, F. Cuyckens, and F. Vanhaecke, *Hyphenation of reverse-phase HPLC and ICP-MS for metabolite profiling-application to a novel antituberculosis compound as a case study*. Analytical and Bioanalytical Chemistry, 389 (2007) 777-786.
 54. http://www.cetac.com/pdfs/U-6000AT_brochure.pdf
 55. Y.C. Sun, Y.S. Lee, T.L. Shiah, P.L. Lee, W.C. Tseng, and M.H. Yang, *Comparative study on conventional and low-flow nebulizers for arsenic speciation by means of microbore liquid chromatography with inductively coupled plasma mass spectrometry*. Journal of Chromatography A, 1005 (2003) 207-213.

56. Y. Ogra, K. Ishiwata, Y. Iwashita, and K.T. Suzuki, *Simultaneous speciation of selenium and sulfur species in selenized odorless garlic (*Allium sativum* L. Shiro) and shallot (*Allium ascalonicum*) by HPLC-inductively coupled plasma-(octopole reaction system)-mass spectrometry and electrospray ionization-tandem mass spectrometry*. Journal of Chromatography A, 1093 (2005) 118-125.
57. E. Bakkaus, N. Collins Richard, J.-L. Morel, and B. Gouget, *Anion exchange liquid chromatography-inductively coupled plasma-mass spectrometry detection of the Co^{2+} , Cu^{2+} , Fe^{3+} and Ni^{2+} complexes of mugineic and deoxymugineic acid*. Journal of Chromatography A, 1129 (2006) 208-215.
58. G. Fernandez Ruben and J.I. Garcia Alonso, *Separation of rare earth elements by anion-exchange chromatography using ethylenediaminetetraacetic acid as mobile phase*. Journal of Chromatography A, 1180 (2008) 59-65.
59. A.P. Vonderheide, J. Meija, K. Tepperman, A. Puga, A.R. Pinhas, J.C. States, and J.A. Caruso, *Retention of Cr(III) by high-performance chelation ion chromatography interfaced to inductively-coupled plasma mass spectrometric detection with collision cell*. Journal of Chromatography A, 1024 (2004) 129-137.
60. G. Raber, R. Raml, W. Goessler, and K.A. Francesconi, *Quantitative speciation of arsenic compounds when using organic solvent gradients in HPLC-ICPMS*. Journal of analytical atomic spectrometry, 25 (2010) 570-576.
61. A.A. Ammann, *Arsenic speciation by gradient anion exchange narrow bore ion chromatography and high resolution inductively coupled plasma mass spectrometry detection*. Journal of Chromatography A, 1217 (2010) 2111-2116.
62. W.C. Davis, R. Zeisler, J.R. Sieber, and L.L. Yu, *Methods for the separation and*

- quantification of arsenic species in SRM 2669: arsenic species in frozen human urine*. Analytical and Bioanalytical Chemistry, 396 (2010) 3041-3050.
63. R.G. Brennan, S.-A.E. O'Brien Murdock, M. Farmand, K. Kahen, S. Samii, J.M. Gray, and A. Montaser, *Nano-HPLC-inductively coupled plasma mass spectrometry for arsenic speciation*. Journal of analytical atomic spectrometry, 22 (2007) 1199-1205.
64. K. Baba, T. Arao, Y. Maejima, E. Watanabe, H. Eun, and M. Ishizaka, *Arsenic Speciation in Rice and Soil Containing Related Compounds of Chemical Warfare Agents*. Analytical Chemistry, 80 (2008) 5768-5775.
65. Y. Morita, T. Kobayashi, T. Kuroiwa, and T. Narukawa, *Study on simultaneous speciation of arsenic and antimony by HPLC-ICP-MS*. Talanta, 73 (2007) 81-86.
66. S. Amereih, T. Meisel, E. Kahr, and W. Wegscheider, *Speciation analysis of inorganic antimony in soil using HPLC-ID-ICP-MS*. Analytical and Bioanalytical Chemistry, 383 (2005) 1052-1059.
67. M. Krachler and H. Emons, *Speciation analysis of antimony by high-performance liquid chromatography inductively coupled plasma mass spectrometry using ultrasonic nebulization*. Analytica Chimica Acta, 429 (2001) 125-133.
68. I. Lopez, S. Cuello, C. Camara, and Y. Madrid, *Approach for rapid extraction and speciation of mercury using a microtip ultrasonic probe followed by LC-ICP-MS*. Talanta, 82 (2010) 594-599.
69. S.S. de Souza, J.L. Rodrigues, V.C. de Oliveira Souza, and F. Barbosa, Jr., *A fast sample preparation procedure for mercury speciation in hair samples by high-performance liquid chromatography coupled to ICP-MS*. Journal of analytical

- atomic spectrometry, 25 (2010) 79-83.
70. L.-F. Chang, S.-J. Jiang and A.C. Sahayam, *Speciation analysis of mercury and lead in fish samples using liquid chromatography-inductively coupled plasma mass spectrometry*. Journal of Chromatography A, 1176 (2007) 143-148.
 71. Y.-F. Li, C. Chen, B. Li, Q. Wang, J. Wang, Y. Gao, Y. Zhao, and Z. Chai, *Simultaneous speciation of selenium and mercury in human urine samples from long-term mercury-exposed populations with supplementation of selenium-enriched yeast by HPLC-ICP-MS*. Journal of analytical atomic spectrometry, 22 (2007) 925-930.
 72. R.E. Wolf, J.M. Morrison and M.B. Goldhaber, *Simultaneous determination of Cr(iii) and Cr(vi) using reversed-phased ion-pairing liquid chromatography with dynamic reaction cell inductively coupled plasma mass spectrometry*. Journal of analytical atomic spectrometry, 22 (2007) 1051-1060.
 73. A.J. Bednar, R.A. Kirgan and W.T. Jones, *Comparison of standard and reaction cell inductively coupled plasma mass spectrometry in the determination of chromium and selenium species by HPLC-ICP-MS*. Analytica Chimica Acta, 632 (2009) 27-34.
 74. M. Leist, R. Leiser and A. Toms, *Low-level speciation of chromium in drinking waters using LC-ICP-MS*. Spectroscopy, (2006) 29-31.
 75. F. Seby, S. Charles, M. Gagean, H. Garraud, and O.F.X. Donard, *Chromium speciation by hyphenation of high-performance liquid chromatography to inductively coupled plasma-mass spectrometry - study of the influence of interfering ions*. Journal of analytical atomic spectrometry, 18 (2003) 1386-1390.

76. Y. Nygren, P. Hemstroem, C. Astot, P. Naredi, and E. Bjoern, *Hydrophilic interaction liquid chromatography (HILIC) coupled to inductively coupled plasma mass spectrometry (ICPMS) utilizing a mobile phase with a low-volatile organic modifier for the determination of cisplatin, and its monohydrolyzed metabolite*. Journal of analytical atomic spectrometry, 23 (2008) 948-954.
77. D. Garcia Sar, M. Montes-Bayon, E. Blanco Gonzalez, and A. Sanz-Medel, *Speciation studies of cis-platin adducts with DNA nucleotides via elemental specific detection (P and Pt) using liquid chromatography-inductively coupled plasma-mass spectrometry and structural characterization by electrospray mass spectrometry*. Journal of analytical atomic spectrometry, 21 (2006) 861-868.
78. K.-E. Wang and S.-J. Jiang, *Determination of iodine and bromine compounds by ion chromatography/dynamic reaction cell inductively coupled plasma mass spectrometry*. Analytical Sciences, 24 (2008) 509-514.
79. Z. Chen, M. Megharaj and R. Naidu, *Speciation of iodate and iodide in seawater by non-suppressed ion chromatography with inductively coupled plasma mass spectrometry*. Talanta, 72 (2007) 1842-1846.

Chapter 2

Determination of stability constants of metal complexes

with IEC-ICP-MS

2.1. Introduction

2.1.1 General background on metal complexes

Metal complexes are prevalent in nature and the artificial world. The research on metal complexes is interdisciplinary, involving chemistry, biology, geology, physics, pharmacology, etc. Generally, this research falls into two categories: one to study the structural peculiarities - configuration and/or conformation - of the complexes at the atomic level mostly in solid state; and the other to study the interaction of the complexes with solvent molecules or other metal ions and ligands in solution. It must be emphasized that research in these two fields is interdependent and has evolved to rely on each other [1].

Many researchers active in analytical chemistry are interested in speciation of metal complexes in solution. Metal speciation analysis is to identify and quantify specific forms of a metal in a sample. It has been generally accepted that it is the particular species and/or forms present instead of the total concentration of metals in a sample that dictate toxicity, bioavailability, bioactivity, transport in the organism, bio-geological distribution, transportation of metals, etc.[2] Except for rare kinetically inert systems, metal complexes coexist with metal ions, ligands and protons for protic labile ligands under

forces exerted by solvent molecules. The distribution of each species relies on the binding strength of the metal-ligand complexes, which is quantitatively expressed as the stability constant of the specific metal complex.

Stability constants, or equilibrium constants, of metal complexes have long been employed as an effective measurement of the affinity of a ligand for a metal ion in solution [3]. They play a key role to 1) assess metal-ligand binding strength in solution; 2) understand the solution equilibrating process; 3) screen appropriate complexing agents; and 4) provide practical guidance for ligand design [3].

Biologically active organic molecules (proteins, nucleotides, carbohydrates, etc.) and their derivatives or decomposition products all contain electron pair donor motifs (amino, carbonyl, sulphhydryl, etc.), which make them potential ligands to coordinate with the ubiquitously present metal ions [1, 4]. The coordination of biomolecules with metal ions is indispensable for some of the most important physiological processes, like protein catalytic processes. Besides the innate biomolecules, extraneous drug molecules often bear electron donor groups. They will inevitably interfere with the metal ions, free or bonded, inside the biological environment. Chelation therapy has been used successfully to treat genetic diseases caused by excessive accumulation of certain metal ions. It is based on the premise that the chelator selected has a better binding strength than the biomolecule(s) for the target metals ions to carry out an efficient removal. For example, β -Thalassemia major is a genetic disease in which β subunits of hemoglobin could not be synthesized in adequate quantities. The treatment is frequent transfusion of normal blood

cells, which leads to iron poisoning over the long term, as the body does not have a mechanism to excrete large quantities of iron. To tackle this lethal side effect, *desferrioxamine B*, a powerful iron chelator with a conditional formation constant of 10^{13} is used to remove the excess iron by forming *desferrioxamine* complex that can be excreted in the bile and subsequently urine [5, 6].

2.1.2 Determination of stability constant

A stability constant, K_f , by definition is the equilibrium constant for the reaction of a metal with a ligand:



where ML_n^{m-nl} represents the complex, M^{m+} the free metal ion, L^{l-} the ligand, n is the chelation number and $[]$ indicates molar concentration. When $n > 1$, K_f represents the cumulative stability constant, β_n .

In Equation 2.2, molar concentrations are adopted instead of activities of the reactants and products for the convenience of measurement [3]. This treatment is based on the assumption that concentrations parallel activities of ionic solutes when the ionic strength is kept constant by a non-reacting electrolyte present at a concentration far in excess of that of the reacting ionic species under investigation [7]. In fact, it has become a general prac-

tice to measure equilibrium constants involving coordination compounds at a constant ionic strength maintained by a supporting electrolyte [3].

At equilibrium, the concentrations of the complex, the ligand and the free metal ions are interrelated and their variation relies on the total composition of the experimental solution and the stability constant. Theoretically, if the concentration of one of the species is known, the concentration of the remaining species can be calculated and thus the stability constant to be determined. To be specific, a series of such measurements are made to cover a sufficient range of conditions, and then a suitable mathematical treatment like linear square regression is applied to determine the unknown parameters. Practically, any technique that can determine the concentration of at least one of the species at equilibrium of a complexation reaction can be applied to determine the stability constant. A complexation reaction is usually accompanied by changes in the properties of a solution as a whole and the individual species as well, before and after complex formation, such as potential, absorbance, conductivity, structural and conformational alteration, etc., which are measured by different techniques to perform the equilibrium analysis [3].

Conventional methods to determine stability constants fall into two categories, *in situ* and *ex situ*, according to whether a separation step is involved or not. Direct determination methods, such as potentiometry [3, 8-10], polarography [11-13], spectrophotometry [14-17] etc., are regarded as standard methods, as no or little external interference is involved. As an example, potentiometry is the most widely used method to determine stability constants. It makes use of the competition of the metal ions and protons for a ligand. In this procedure, a base is added incrementally into an acid ligand solution in both the presence

and absence of the investigated metal ions. The pH changes in these processes are then rationalized to get the formation constant [3]. On the other hand, two-step methods are usually more sensitive and selective, as they involve the combination of a separation technique, such as ultrafiltration, capillary isotachopheresis, ion-exchange chromatography (IEC), etc., [3, 7, 18] to a powerful detector. Techniques that can be used to detect either the metal or the metal complex can be mass spectrometry, ultraviolet spectroscopy (UV), atomic emission spectroscopy, inductively coupled plasma mass spectrometry (ICP-MS), etc., which usually have the advantage of a relatively higher sensitivity to the complexes and/or the free metal ions.

2.1.3 Hyphenated IEC-ICP-MS to determine stability constant

Recently, one such two-step method was developed by coupling IEC with ICP-MS to determine conditional stability constants [19-21]. In this procedure, the metal complex and the free metal ion of a homogeneous complex solution are separated by an ion exchange column prior to their detection by ICP-MS. This method takes advantage of the multi-elemental detection capability and high sensitivity of ICP-MS and the separation efficiency of IEC. Because the peak area response of ICP-MS was independent of the metal species, a plot of the logarithm of the peak area ratio of the complex over the free metal as a function of the logarithm of the analytical concentration of the ligand gave $\log K_f'$ as the intercept and the chelation number, n , following Equation H-1:

$$\log \frac{[ML_n^{m-nl}]}{[M^{m+}]} = \log K_f' + n \log C_L \quad (\text{H-1})$$

where ML_n^{m-nl} represents the complex, M^{m+} the free metal ion, C_L the ligand analytical concentration, n is the chelation number, K_f' is the conditional stability constant and [] indicates molar concentration.

The stability constants thus obtained matched the literature values, but the chelation number n deviated from integers. The discrepancy was interpreted to be caused by the presence of other partially protonated EDTA species other than the target EDTA⁴⁻ and random errors. To take advantage of the multi-elemental detection capability of ICP-MS, the method was then applied to simultaneous determination of the conditional stability constants of Co-EDTA and Zn-EDTA in one solution. Initial results were also obtained in the application of this method to a Co (Gly-Phe)₂ complex as a model biological system, demonstrating the potential of this method in the biological field [19].

In fact, one assumption for Equation (H-1) to be valid is that the concentration of the ligand must be in large excess compared to that of the metal, which was actually not the case. Furthermore, it neglected complexes other than EDTA⁴⁻, such as those with HEDTA³⁻ and H₂EDTA²⁻. Revision was thus made on the stability constant expressions.

2.1.4 Derivation of stability constant expressions

The fundamental mass-balanced Equations 2.1 and 2.2 were used to derive equations to calculate the conditional stability constant K_f' in terms of concentrations of complex and free metal, i.e., parameters that can be detected by ICP-MS.

The concentration of the ligand species, L^{l-} can be expressed as the product of the fractional composition $\alpha_{L^{l-}}$ and the total concentration of *uncomplexed* or free ligand, C_f , as shown in Equation 2.3.

$$[L^{l-}] = \alpha_{L^{l-}} C_f \quad (2.3)$$

By substituting $\alpha_{L^{l-}}$ into Equation 2.2, the conditional stability constant, K'_f , is obtained as Equation 2.4.

$$K'_f = K_f (\alpha_{L^{l-}})^n = \frac{[ML_n^{m-nl}]}{[M^{m+}] C_f^n} \quad (2.4)$$

By taking the logarithm on both sides of Equation 2.4 and rearranging, Equation 2.5 is obtained.

$$\log \frac{[ML_n^{m-nl}]}{[M^{m+}]} = \log K'_f + n \log C_f \quad (2.5)$$

In view of mass balance, C_f can be expressed as the difference between C_L , the total ligand concentration or the analytical concentration of the ligand and the concentration of the formed complex multiplied by the chelation number of binding sites, as shown in Equation 2.6.

$$C_f = C_L - n[ML_n^{m-nl}] \quad (2.6)$$

Substitution of Equation 2.6 into Equation 2.5 yields Equation 2.7.

$$\log \frac{[ML_n^{m-nl}]}{[M^{m+}]} = \log K_f' + n \log(C_L - n[ML_n^{m-nl}]) \quad (2.7)$$

When the concentration of the ligand is larger than that of the metal, the metal can be regarded as being reacted ‘completely’ to form the complex. So, if the concentration of the ligand is *much larger* than that of the metal, the $-n[ML_n^{m-nl}]$ part becomes negligible, and Equation 2.7 can be reduced to Equation H-1.

However, for metal complexes with a large stability constant, it is practically impossible to use a large excess of ligand to measure the stability constant with this two-step method. For example, for a complex formed by mixing cobalt and EDTA in a 1:1 molar ratio at pH 3.8, the free metal comes entirely from the dissociation at equilibrium that accounts for $\frac{1}{\sqrt{K_f' C_M}}$ of the concentration of the complex, where C_M is the analytical concentration of the cobalt or EDTA. If C_M is in the range 1×10^{-6} M as in Huang’s thesis [19], the concentration of the free metal is calculated to be about 15% of the concentration of the metal complex. As the concentration of the ligand becomes larger, the concentration of the free metal from dissociation will become drastically smaller due to mass-action effect. Roughly, for complex systems with $n = 1$ of ligand : metal ratio, the free metal from dissociation accounts for $\frac{1}{(n-1)K_f'}$ regardless of C_M . The error introduced by the calculation based on the area ratio obtained from integration of the chromatograms will become very large. So, when applying the simplified Equation H-1 to systems

with a large formation constant, extreme care must be taken to control the measurement and data analysis on the basis of *large excess* of ligand(s). Equation 2.7 is universally applicable to systems with one complex species since it is simply the metamorphosis of equilibrium constant Equation 2.2. In the case of systems with multiple complex species, Equation 2.7 needs to be further adjusted. For example, while EDTA⁴⁻ is the major species complexing with metal ions in EDTA solution, other protonated species like HEDTA³⁻, H₂EDTA²⁻ can also complex metal ions in certain pH ranges. The sum of these complexed species can be expressed as the difference between the total amounts of metal ions minus that of the free metal ions as shown in Equation 2.8.

$$\log \frac{[ML_n^{m-nl}]}{[M^{m+}]} = \log K_f' + n \log(C_L - n(C_M - [M^{m+}])) \quad (2.8)$$

In Equations 2.7 and 2.8, $[M^{m+}]$ and $[ML_n^{m-nl}]$ are not directly measured by ICP-MS. We assume a linear relationship between the concentration of an element and its response, which is the basis for most ICP-MS quantitative analysis, to do the rationalization. Here, A_{ML} , A_M and A_t are used to denote the ICP-MS response to $[ML_n^{m-nl}]$, $[M^{m+}]$ and C_M respectively, and the following relationships can be obtained straightforwardly [22, 23].

$$\frac{[ML_n^{m-nl}]}{[M^{m+}]} = \frac{A_{ML}}{A_M} \quad (2.9)$$

$$[M^{m+}] = \frac{A_M}{A_t} \times C_M \quad (2.10)$$

$$[ML_n^{m-nl}] = \frac{A_{ML}}{A_t} \times C_M \quad (2.11)$$

$$\log \frac{[A_{ML}]}{[A_M]} = \log K_f' + n \log(C_L - n(\frac{A_{ML}}{A_t} \times C_M)) \quad (2.12)$$

$$\log \frac{[A_{ML}]}{[A_M]} = \log K_f' + n \log(C_L - n(C_M - \frac{A_M}{A_t} \times C_M)) \quad (2.13)$$

A plot of $\log \frac{A_{ML}}{A_M}$ versus $n \log(C_L - n(C_M - \frac{A_M}{A_t} \times C_M))$ or $n \log(C_L - n(\frac{A_{ML}}{A_t} \times C_M))$ will give $\log K_f'$ as the intercept and n as the slope. The problem with n that is included in the concentration variable can be solved by successive approximation; i.e. assuming n to be a certain number to calculate the conditional stability constant and the chelating n ; if the calculated n equals the assumed one, then the assumption is verified; otherwise, another number can be tried until the correct one is found. Fortunately, the chelation numbers are integers in most cases.

For multi-element systems with one common ligand, Equation 2.12 or 2.13 is also applicable if there are no reactions between the elements and the complexes formed. The metals will get their share of the ligand according to their stability constant. For a solution with j different metal species, each species will display distinct $\log \frac{[A_{ML}]}{[A_M]}$ values and a common C_f that can be expressed as Equation 2.14 or 2.15.

$$C_f = C_L - n \sum_{i=1}^j \frac{A_{ML_i}}{A_{M_i}} \times C_{M_i} \quad (2.14)$$

$$C_f = C_L - n \sum_{i=1}^j (C_{M_i} - \frac{A_{M_i}}{A_{M_i}} \times C_{M_i}) \quad (2.15)$$

Therefore, a plot of $\log \frac{A_{ML_i}}{A_{M_i}}$ versus $n \log(C_L - n \sum_{i=1}^j \frac{A_{ML_i}}{A_{M_i}} \times C_{M_i})$ or

$n \log(C_L - n \sum_{i=1}^j (C_{M_i} - \frac{A_{M_i}}{A_{M_i}} \times C_{M_i}))$ will give $\log K'_{f_i}$ as the intercept of each species and

the chelation number as the slope n .

2.2 Experimental

2.2.1 Instrumentation

2.2.1.1 IEC. A Dionex 600/BioLC liquid chromatography system equipped with a GS 50 gradient pump, a Rheodyne 9750E injector and a 50- μ L sample loop was used for the separations. The GS 50 gradient pump is a microprocessor-based pulse-free eluent delivery system, which can deliver mixtures of up to four mobile phase components at precisely controlled flow rates [24]. All the connections, fittings and pump heads are made of PEEK. The PDA100 (UV-Vis) detector was bypassed to reduce the dead volume.

Anionic IonPac®AG-7 column (50 \times 4mm, 10 μ m) and cationic IonPac®CG-5A column (50 \times 4mm, 9 μ m) were used for the separations. Both AG-7 and CG-5A displayed cationic as well as anionic exchange capability due to the unique pellicular structure of the packing particles. The column packing of AG-7 consists of three different regions, including 1) an inert, nonporous, chemically and mechanically stable core; 2) a sulfonated region completely covering the core surface and 3) an outer layer of attached submicron anion-exchange MicroBead™ with alkyl quaternary ammonium as functional group [25]. The column packing of CG5A has a similar character yet with reversed anion and cation exchange regions, so that CG5A has a stronger affinity for metal ions [26].

The IEC system was controlled by a Chromeleon® chromatography management workstation through methods and sequence programming. The sample solution was manually loaded into a 50- μ L sample loop with a syringe and injected automatically when

an elution program was executed. The syringe was rinsed with sample solution thoroughly before injecting a sample for analysis.

The columns were cleaned whenever appreciable peak broadening or deformation was observed. The cleaning procedure includes pumping 200 mM of nitric acid for two hours and subsequently flushing with water for another two hours. The columns were then equilibrated with the mobile phase for one hour at a flow rate of 1.0 mL/min and then stabilized at 1.5 mL/min or 25 μ L/s. The flow rate was calibrated at a backpressure of *ca.* 2000 psi. The mobile phase was pumped continuously while the sample was loaded.

Isocratic elution was used for separation with AG-7. For separation with CG-5A, a gradient elution procedure was adopted to facilitate the removal of metal ions from the stationary phase. The IEC operation conditions are summarized in Table 2.1. The IEC system was hyphenated to ICP-MS using a piece of PEEK tubing between the outlet of the column and the nebulizer liquid inlet, which was 0.25 mm in inner diameter and 50 cm in length.

2.2.1.2 ICP-MS. An UltraMass 700 quadrupole-based ICP-MS instrument from Varian was used for this project. It was equipped with a Meinhard concentric nebulizer, a Sturman-Masters spray chamber, a three channel peristaltic pump and a Fassel-type quartz torch. Two water-cooled interlaced induction coils were used to sustain the ICP, which efficiently couple RF power and prevent any problem of “secondary discharge” caused by the potential difference between the plasma and the interface. The sampler and skimmer cones were made of nickel, with a cone orifice diameter of 1.0 mm and 0.5 mm, re-

spectively.

Table 2.1. IEC separation conditions

Parameter	Setting (anion exchange)	Setting (cation exchange)
Column	IonPac® AG-7	IonPac® CG-5A
	4.0 mm ID × 50 mm, 10 μm	4.0 mm ID × 50 mm, 9 μm
Column temperature	Ambient	Ambient
Mobile phase	MPA: 0.1 M ammonium nitrate, pH = 3.8	
	MPB: 0.1 M ammonium nitrate with 3×10^{-5} M EDTA, pH = 3.8	
Elution program	Isocratic elution with MPA	0-0.9 min: MPA
		0.9-1.5 min: MPB
		1.5-6.0 min: MPA
Flow rate (mL/min)	1.5	1.5
Sample injection volume (μL)	50	50
Backpressure (psi)	500	500

Optimization of plasma position was done daily using a solution containing the target element(s), where analyte signal was maximized by adjusting the horizontal and vertical positions of the torch relative to the sampling interface. Optimization of nebulizer gas flow rate, RF power and sampling depth was also carried out when an obvious signal decrease (compared to that typically observed) was evident during plasma positioning. Mass calibration, and adjustments of quadrupole resolution and ion detector voltage were done less frequently using 100 μg/L multi-elemental solution of Ba, Be, Ce, Co, In, Pb, Mg, Ti and Th in 1% nitric acid prepared from a 10 μg/mL stock solution supplied by

Varian. Data acquisition was carried out in time-resolved, peak hopping mode with three points per peak, one scan per replicate, a dwell time of 100 ms and 0.025 amu spacing. Typical operating conditions are listed in Table 2.2.

2.2.2 Reagents and solution preparation

2.2.2.1 Reagents. Standard metal solutions (1000 $\mu\text{g/ml}$, 4% HNO_3) for ICP-AES & ICP-MS from SCP Science were used as the metal source. $\text{Na}_2\text{H}_2\text{EDTA}\cdot 2\text{H}_2\text{O}$ (IDRAN-AL®III) was dried at 80°C for 1 hour before use. Concentrated nitric acid (70%, J.T.Baker) and ammonia (20-22%, Fischer Scientific) were all ultra-pure reagents. Doublely deionized water (DDW, Milli-Q Plus system, Millipore, Mississauga, Canada) was used throughout for preparing solutions and rinsing the nebulizer. Ammonium nitrate solution was prepared by mixing ultra-pure nitric acid and ammonium hydroxide in DDW.

2.2.2.2 Sample solution preparation. The EDTA stock solution was prepared by dissolving $\text{Na}_2\text{H}_2\text{EDTA}\cdot 2\text{H}_2\text{O}$ in 0.1 M ammonium nitrate solution. The mono-elemental and di-elemental solutions of Co-EDTA, Zn-EDTA and Co-EDTA/Zn-EDTA were prepared by spiking the corresponding stock metal(s) standard solution(s) and EDTA stock solution into 0.1 M ammonium nitrate solution and adjusting the pH to 3.8 with nitric acid or ammonium hydroxide.

One series of solutions with a fixed metal concentration and varied EDTA concentration (Table 2.3) was used to test the validity of different constant stability equations derived in

section 2.14 and Equation H-1.

Table 2.2. Typical operating conditions for UltraMass 700 ICP-MS instrument

	Parameters	Settings
ICP conditions	Ar plasma flow rate (L/min)	15
	Ar auxiliary gas flow rate (L/min)	1.15
	Ar nebulizer flow rate (L/min)	0.93
	RF power (kW)	1.26
	Sampling depth (mm)	5.5
	Isotopes monitored	^{59}Co , ^{66}Zn , ^{68}Zn
Sample introduction	Sample uptake rate (mL/min)	1.5
Ion optics	Extraction lens (V)	-200
	First lens (V)	-260
	Second lens (V)	-11.8
	Third lens (V)	3.0
	Fourth lens (V)	-45
	Photon stop (V)	-11.2

To investigate the applicability of the proposed method in terms of total metal concentration range, a series of Co-EDTA solutions with varied Co concentration was used (Table 2.4). Also, to test its applicability to the simultaneous determination of stability constants, another series of solutions with fixed concentrations of Co and Zn and varied EDTA concentration was used (Table 2.5). The 0.1 M ammonium nitrate solution was also used as the mobile phase (MPA) for IEC isocratic elution. MPB was prepared by spiking MPA

with EDTA stock solution up to a concentration of 3×10^{-5} M. Sample solutions were equilibrated for about one hour at 20 °C in the air-conditioned ICP-MS laboratory before speciation analysis.

Table 2.3. Sample compositions for Co-EDTA and Zn-EDTA complexes in 0.1 M NH_4NO_3 (pH 3.8) for testing different equations.

Co-EDTA		Zn-EDTA	
C_M , M	C_L , M	C_M , M	C_L , M
1.70E-6	3.39E-7	3.08E-6	1.23E-6
1.70E-6	8.48E-7	3.08E-6	1.54E-6
1.70E-6	1.36E-7	3.08E-6	1.85E-6
1.70E-6	2.54E-6	3.08E-6	2.16E-6
1.70E-6	3.39E-6	3.08E-6	2.77E-6

2.2.3 Data acquisition and analysis

The samples were injected in order of increasing EDTA concentration. Normally, three replicates were made and the mean was used in the calculations. The raw data were treated with in-house QBASIC programs. Raw data were smoothed with a 7-point polynomial Savitzky- Golay moving window. Excel® graphs function was used to visualize the chromatograms and to position the peaks. Then, another QBASIC program was used to integrate peak areas. The program corrected for background by assuming a straight line between the start and the end of the peak.

Table 2.4. Sample compositions for Co-EDTA complex in 0.1 M NH_4NO_3 (pH 3.8) with varied total cobalt concentration.

	C_M, M		
	8.54E-07 (50 $\mu\text{g/L}$)	4.27E-07 (25 $\mu\text{g/L}$)	2.05E-07 (12 $\mu\text{g/L}$)
C_L, M	1.71E-07	8.54E-08	6.15E-08
	3.41E-07	1.71E-07	1.23E-07
	5.12E-07	2.56E-07	1.64E-07
	6.83E-07	3.41E-07	2.05E-07
	8.54E-07	4.27E-07	3.07E-07
	1.71E-06	8.54E-07	4.10E-07

Table 2.5. Sample compositions for Co-EDTA/Zn-EDTA complexes in 0.1 M NH_4NO_3 (pH 3.8) to test the applicability of the method to the simultaneous determination of stability constants of a multi-elemental complex system.

$C_M(\text{Co}), \text{M}$	$C_M(\text{Zn}), \text{M}$	C_L, M
1.70E-6	4.13E-6	1.17E-6
1.70E-6	4.13E-6	1.75E-6
1.70E-6	4.13E-6	2.33E-6
1.70E-6	4.13E-6	2.91E-6
1.70E-6	4.13E-6	3.50E-6
1.70E-6	4.13E-6	4.08E-6
1.70E-6	4.13E-6	4.66E-6

2.3 Results and discussion

2.3.1 Validity of different equations for Co-EDTA and Zn-EDTA complexes on IonPac® AG-7

Cobalt and zinc were selected as the metal elements to test equations because of their good compatibility with IonPac® AG-7, as shown in Huang's thesis. The ICP-MS sensitivity for Zn was not as great as for Co because, unlike monoisotopic Co, the response for Zn is spreaded among its isotopes (^{64}Zn : 48.63%; ^{66}Zn : 27.92%; ^{68}Zn : 18.84%, etc.). Divalent elements such as lead, cadmium and copper that have stability constants around 10^{16} - 10^{20} , close to that of zinc and cobalt, were also tested. While the complexes of these metals could elute easily from IonPac® AG-7, the free metals could not elute within a period of 20 minutes under the same conditions as for zinc and cobalt. So, cobalt and zinc are the only two elements that will be discussed in this section.

Huang's work [19] showed that the pH of the sample solution affected the complexation of Co and Zn to EDTA by affecting the distribution of EDTA in different protonation states as well as the concentration of ammonia dissociated from the supporting electrolyte, which can act as auxiliary ligand. At pH 3.81-3.87, EDTA^{4-} was the major species and the competition from ammonia as binding ligand was negligible, so the following work was carried out within this pH range. Because the matrix effect of EDTA on ICP-MS analyte signal was negligible in the concentration range used for the experiments, peak areas of the metal complex and free metal chromatographic peaks were used directly to derive the concentration ratio without correction.

2.3.1.1 Co-EDTA complex. A typical IEC-ICP-MS chromatogram for the speciation analysis of Co is shown in Figure 2.1. The two major peaks in the elution sequence belong to Co-EDTA complex and free Co ions, as seen in Huang's thesis [19]. The first peak eluted 13 s following sample injection and its peak width was about 17 s. Obviously, the complex has a very short stay within the column and can even be regarded as eluting at the void time. This is preferable to avoid a shift in equilibrium. The peak of free cobalt ion is of broader pseudo Gaussian shape.

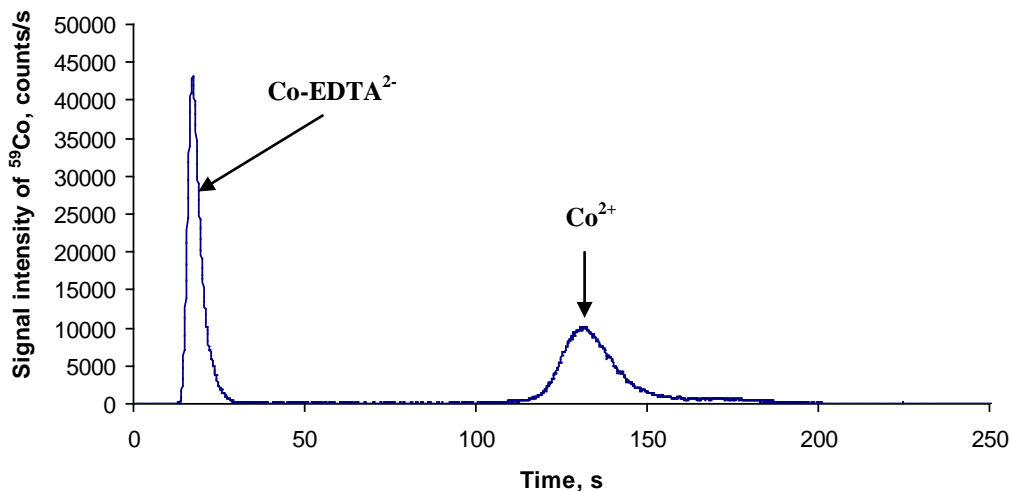
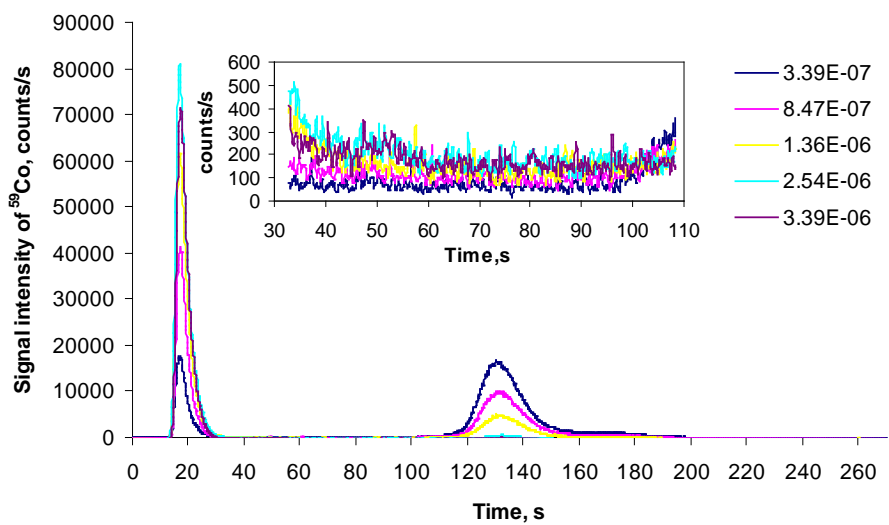
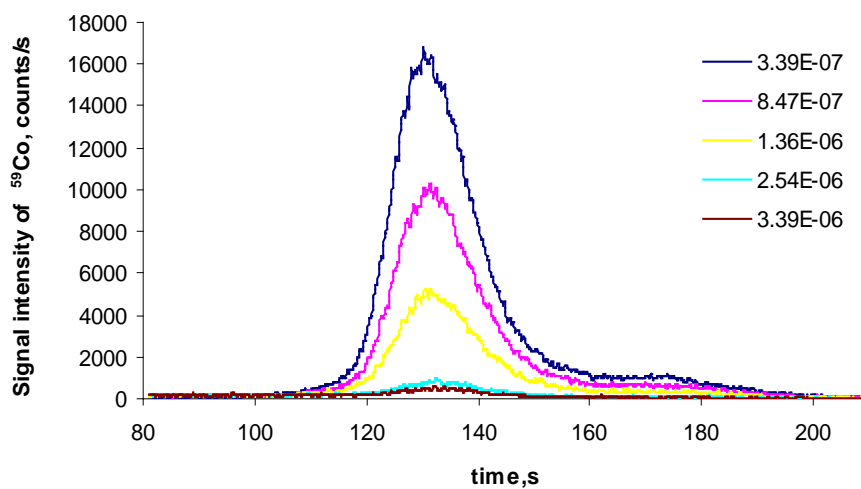


Figure 2.1. IEC-ICP-MS chromatogram for Co (100 $\mu\text{g/L}$ or 1.69 μM of Co and 0.848 μM of EDTA, pH = 3.80) with isocratic elution (mobile phase: 0.1 M ammonium nitrate; flow rate: 1.5 mL/min).

Stacked chromatograms of the solutions used to derive the stability constant are shown in Figure 2.2. The area between the two major peaks is enlarged in the inset, showing that



(a)



(b)

Figure 2.2. Stacked IEC-ICP-MS chromatograms for Co-EDTA solutions ($1.70 \mu\text{M}$ or $100 \mu\text{g/L Co}^{2+}$ and $0.339\text{-}3.39 \mu\text{M EDTA}$) at pH 3.8. (a) The whole chromatogram and its enlargement between 30-110 s; (b) enlargement of free cobalt ions peaks.

certain cobalt species eluted incessantly between Co-EDTA and free cobalt ions. These peaks were tentatively attributed to complexes of partially protonated EDTA species, i.e., Co-HEDTA, Co-H₂EDTA, etc. The presence of these species will cause errors when integrating the major species, especially when the free cobalt ion peak becomes very small as the concentration of EDTA increases.

To minimize this error, the total area for cobalt was obtained by integrating from the start of the first major peak to the end of the second major peak. The free cobalt peak was also expanded to have a better view of its evolution as ligand concentration increased. For a complex system with twice the concentration of EDTA to cobalt, the peak was rather flattened. Conceivably, it will be hard to *read* a chromatogram when EDTA is in much excess. The peak also showed tailing that resembles the tailing pattern in EDTA-free cobalt solutions as shown in Figure 2.3. This tailing pattern might be caused by column degradation.

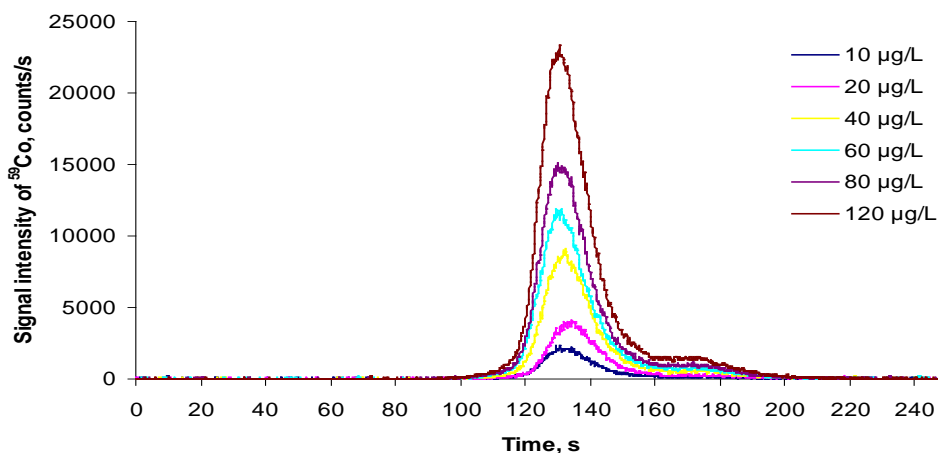


Figure 2.3. IEC-ICP-MS chromatograms of EDTA-free 10-120 µg/L Co solutions.

Figures 2.4-2.6 display the linear regression lines obtained using Equations 2.13, 2.12 and H-1 respectively, with the chelation number set to 1. The $\log K_f'$ and n values thus obtained are summarized in Table 2.6.

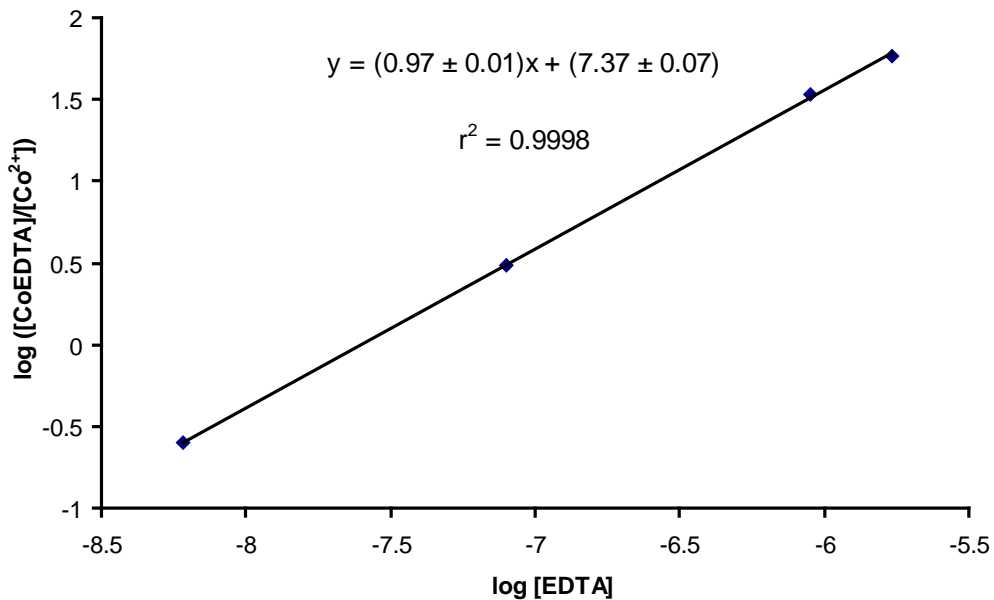


Figure 2.4. Linear regression to determine $\log K_f'$ (intercept) and n (slope) of Co-EDTA complex with Equation 2.13.

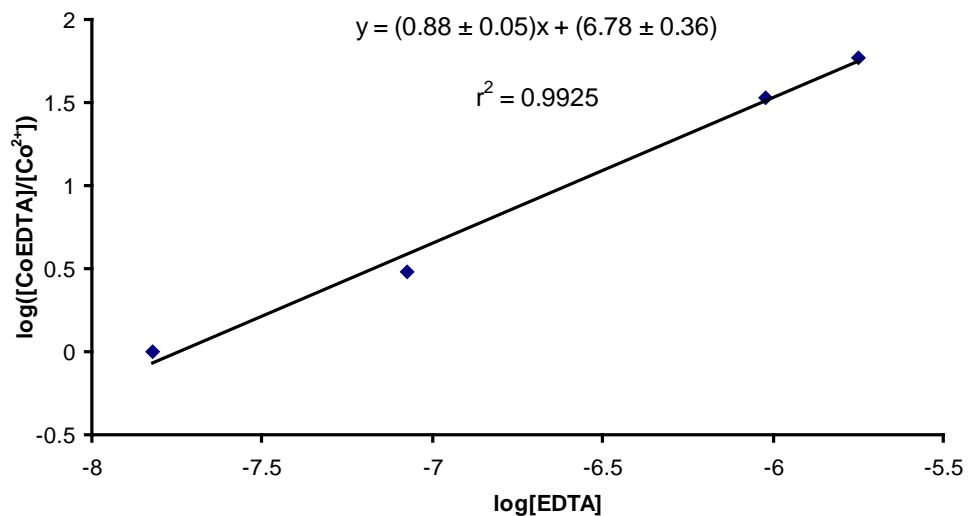


Figure 2.5. Linear regression to determine $\log K_f'$ (intercept) and n (slope) of Co-EDTA complex with Equation 2.12.

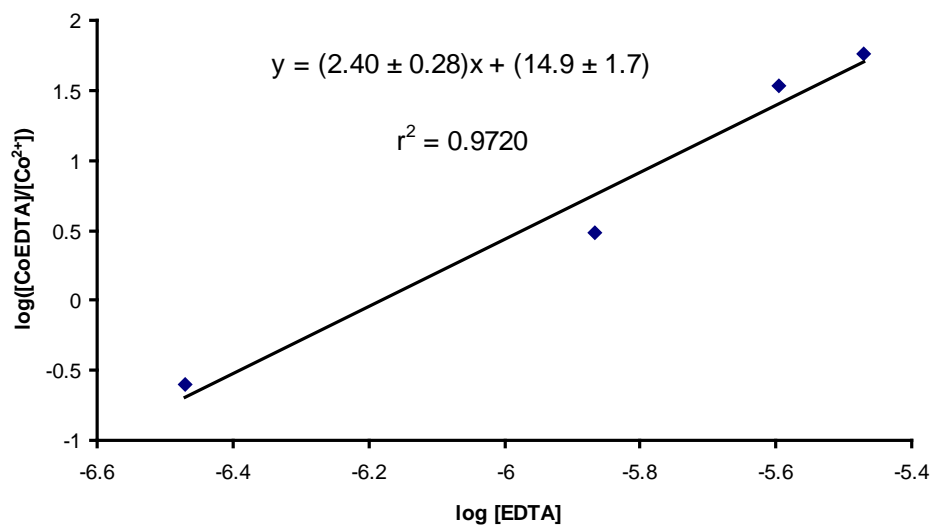


Figure 2.6. Linear regression to determine $\log K_f'$ (intercept) and n (slope) of Co-EDTA complex with Equation H-1.

Table 2.6. Conditional stability constant ($\log K_f'$) and chelation number (n) of Co-EDTA calculated using different equations.

Equations	$\log K_f'$		n	
	Expected	Obtained	Expected	Obtained
Equation 2.13	7.48	7.37 ± 0.07	1	0.97 ± 0.01
Equation 2.12	7.48	6.78 ± 0.36	1	0.88 ± 0.05
Equation H-1	7.48	14.9 ± 1.7	1	2.48 ± 0.28

The chelation number was first set to 1. From Figure 2.4, the conditional stability constant $\log K_f'$ obtained is 7.37, which is close to the literature value. The chelation number is 0.97, so the assumption $n = 1$ is valid. When protonated complex species were not included in the calculation, as shown in Figure 2.5, both the conditional stability constant and the chelation number deviated from the literature values. They deviated from theoretical values substantially using Equation H-1. Theoretically, the results from the calculation with Equations 2.13 and 2.12 should be close if the *minor* species are not in significant proportion, as in this example. However, the chromatograms show that the peaks of the free metal for the last two samples are rather flattened, which can introduce more error during area integration. This example demonstrates the difficulties in using a large excess of ligand to determine the stability constant with this method.

2.3.1.2 Zn-EDTA complex. A typical chromatogram for the Zn system is shown in Figure 2.7. Similar to Co-EDTA, the complex elutes at void time, while the free zinc ion elutes later. However, the retention time for free zinc ion is smaller than that of cobalt

and the peak is narrower, indicating that free zinc ion has a weaker retention on AG-7. Linear regression with Equation 2.13 is shown in Figure 2.8.

The $\log K_f'$ and n values calculated with different equations are listed in Table 2.7, showing that Equation 2.13 is also applicable to the Zn-EDTA complex, except that the linearity is not as good as for cobalt. This may be due to a higher background in the chromatograms and competition from ammonia from the mobile phase, which introduces more error in the area integration. This was also observed by Huang [19].

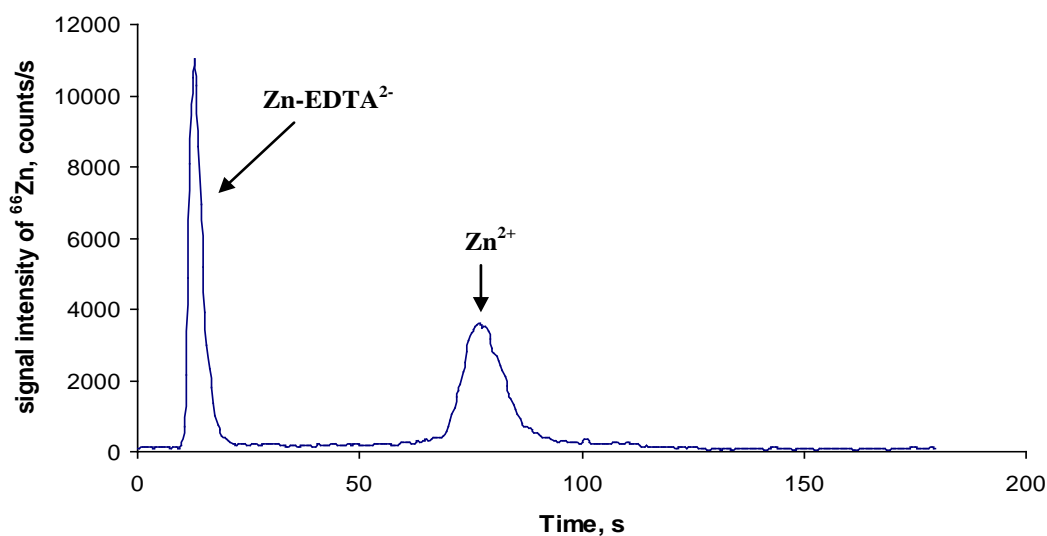


Figure 2.7. IEC-ICP-MS chromatogram for Zn-EDTA solution (100 $\mu\text{g/L}$ or 1.53 μM Zn and 0.76 μM EDTA).

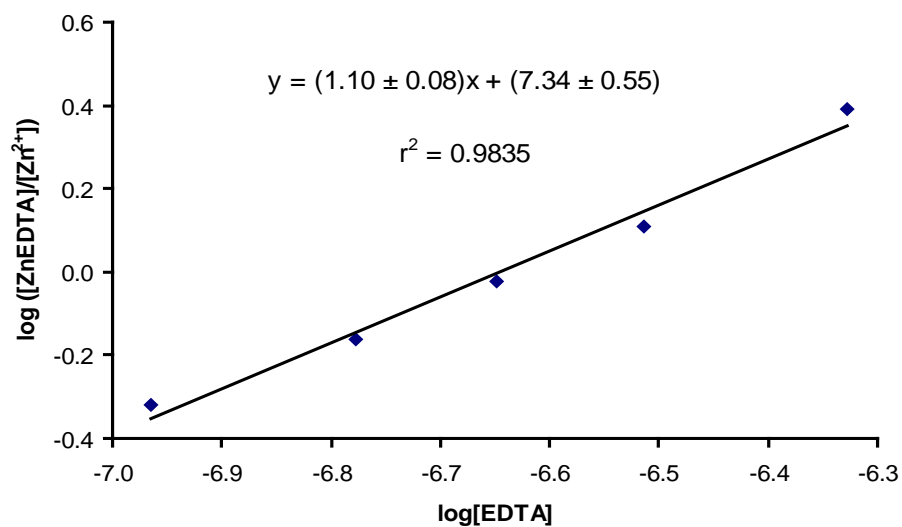


Figure 2.8. Linear regression to determine $\log K_f'$ (intercept) and n (slope) of Zn-EDTA complex with Equation 2.13.

Table 2.7. Conditional stability constant ($\log K_f'$) and chelation number (n) of Zn-EDTA calculated using different equations.

Equations	$\log K_f'$		n	
	Expected	Obtained	Expected	Obtained
Equation 2.13	7.66	7.34 ± 0.55	1	1.10 ± 0.08
Equation 2.12	7.66	9.56 ± 0.32	1	1.52 ± 0.05
Equation H-1	7.66	11.5 ± 0.75	1	2.00 ± 0.13

2.3.2 Determination of stability constant of Co-EDTA with IonPac®CG-5A

Another column, IonPac®CG-5A, was also tested for the separation for a single metal complex. The packing material has a similar layered structure as AG-7, but with reversed sulfonated and quaternary ammonium regions (see section 2.2.1.1 IEC), affording it a more cationic ion exchange character.

Under the same isocratic separation conditions, free metal eluted later with CG-5A compared to AG-7 and its peak was thus broader, whereas elution of the complex was similar. In other words, CG-5A makes the elution of free metals more difficult in isocratic mode. However, EDTA as a complexing agent in gradient elution made free cobalt ion elute earlier, resulting in a sharper symmetrical peak, as shown in Figure 2.9.

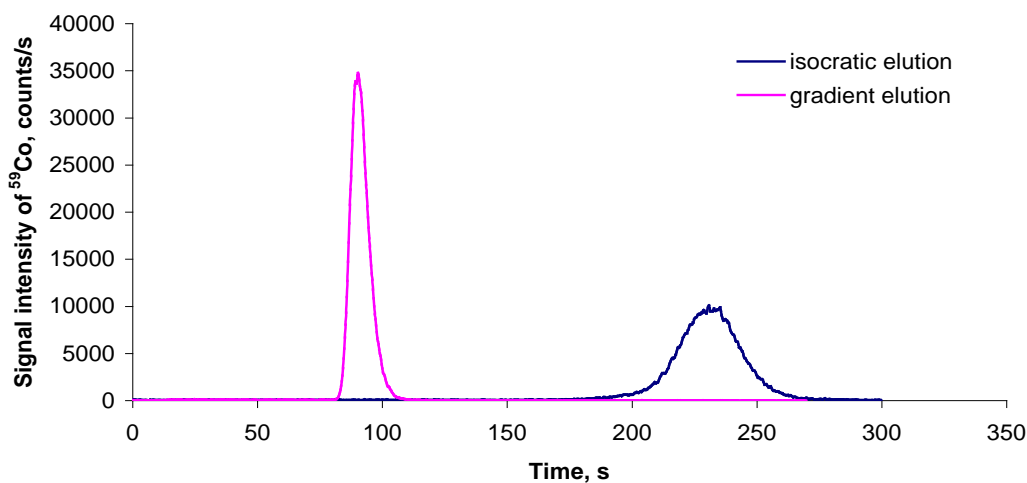


Figure 2.9. IEC-ICP-MS chromatograms for 100 µg/L Co with isocratic (blue) and gradient (pink) elution using IonPac®CG-5A (flow rate: 1.5 mL/min).

Elution profiles for repeated injections of free metal ions showed no extra signals before the free metal peak, confirming that there was no leftover EDTA after one complete elution cycle. Figure 2.10 shows a typical chromatogram of Co-EDTA complex separated on CG-5A with gradient elution, using EDTA to elute the free cobalt ions following elution of the complex. Solutions with varied Co concentrations were used to check the Co concentration range over which stability constant and chelation number can be obtained. Figures 2.11-2.13 show the resulting linear regression plots using Equation 2.13. Table 2.8 summarizes the data thus obtained.

Table 2.8. Conditional stability constant ($\log K_f'$) and chelation number (n) of Co-EDTA complex determined with Equation 2.13 at different cobalt concentrations.

Concentration of total Co, M	$\log K_f'$		n	
	Expected	This work	Expected	This work
8.54×10^{-7}	7.48	7.44 ± 0.41	1	1.06 ± 0.06
4.27×10^{-7}	7.48	7.86 ± 0.12	1	1.09 ± 0.02
2.05×10^{-7}	7.48	7.69 ± 0.42	1	1.08 ± 0.06

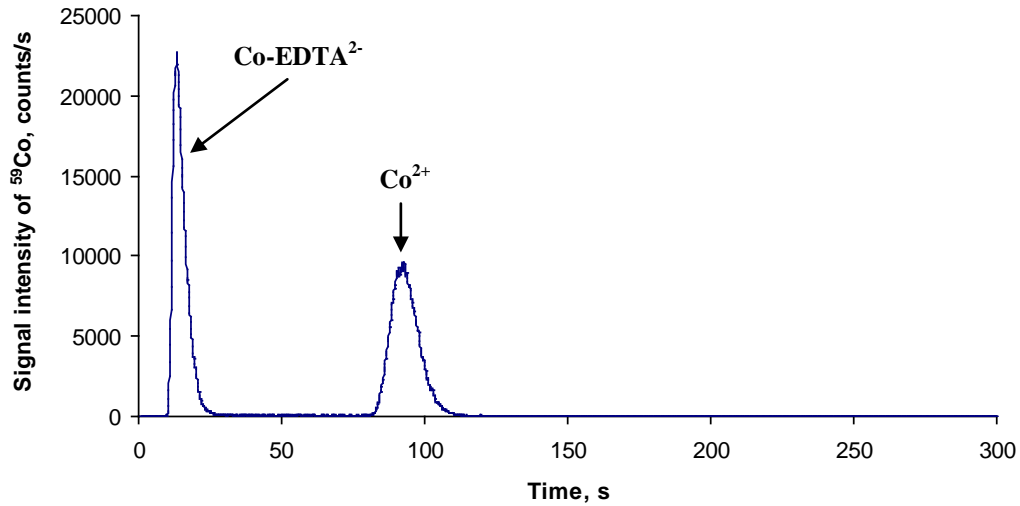


Figure 2.10. IEC-ICP-MS chromatogram for Co-EDTA solution (100 $\mu\text{g/L}$ or 1.69 μM Co and 0.848 μM EDTA) on CG-5A with gradient elution.

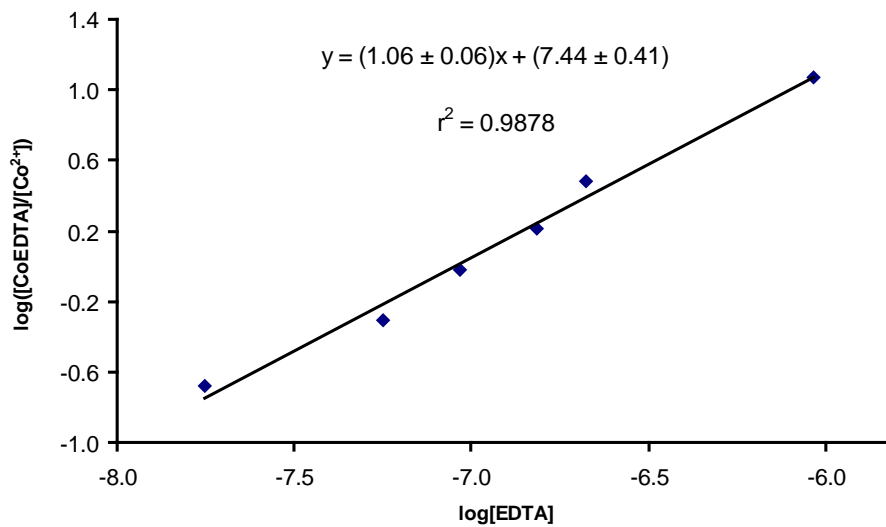


Figure 2.11. Linear regression to determine $\log K_f'$ (intercept) and n (slope) of Co-EDTA complex with 50 $\mu\text{g/L}$ or 0.854 μM Co using Equation 2.13 (pH 3.8, flow rate 1.5 mL/min).

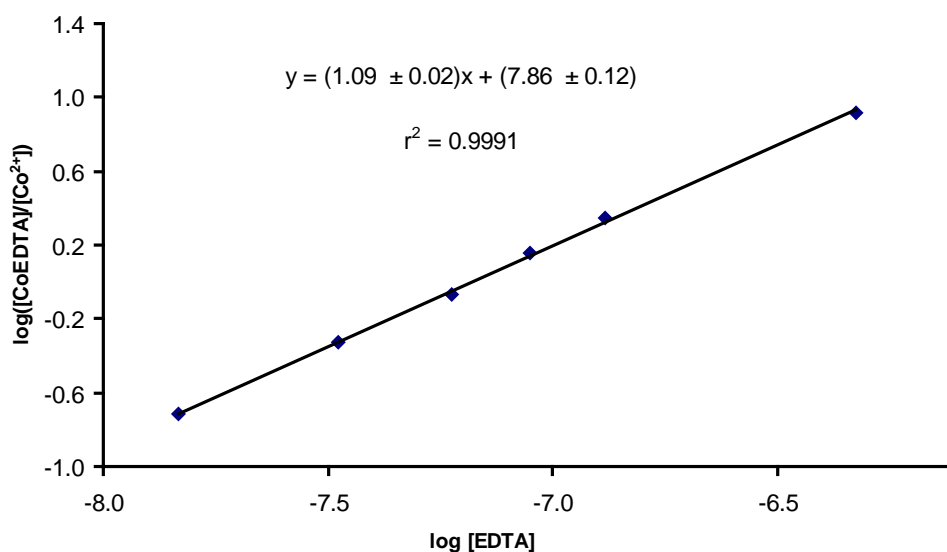


Figure 2.12. Linear regression to determine $\log K_f'$ (intercept) and n (slope) of Co-EDTA complex with 25 ppb or 0.427 μM Co using Equation 2.13 (pH 3.8, flow rate 1.5 mL/min).

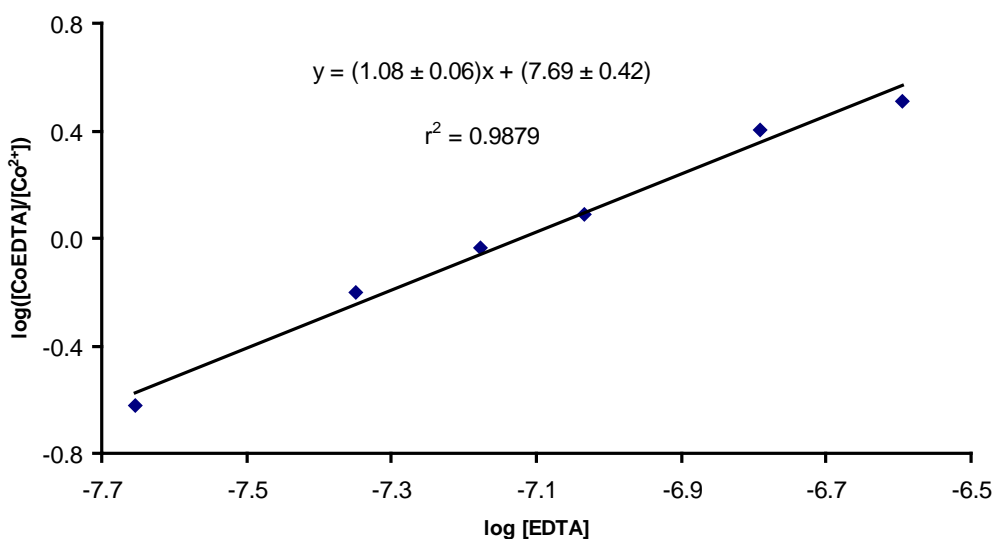


Figure 2.13. Linear regression to determine $\log K_f'$ (intercept) and n (slope) of Co-EDTA complex with 12 $\mu\text{g/L}$ or 0.205 μM Co using Equation 2.13 (pH 3.8, flow rate 1.5 mL/min).

Consistently good results were obtained down to 2.05×10^{-7} M Co. Note that the range of concentration of a specific metal over which this method applies largely depends on the sensitivity of the ICP-MS instrument to this specific element.

2.3.3 Multi-elemental determination of the conditional stability constants of Co-EDTA and Zn-EDTA by gradient elution with IonPac® CG-5A

The multi-elemental detection capability of ICP-MS provides the possibility to simultaneously determine the stability constants of complexes of different metals. The proposed method was thus further applied to the simultaneous determination of the stability constants of complexes of different metals with the same complexing agent. Due to the preliminary success with the single element complex, Co-EDTA and Zn-EDTA, mixtures of Zn^{2+} and Co^{2+} with EDTA, in the same conditions, i.e., 0.1 M NH_4NO_3 at pH 3.80, were used. The separation was performed on IonPac®CG-5A with the same gradient elution program as described in section 2.3.2.

A typical chromatogram is shown in Figure 2.14. Similar to the single elemental complex system in section 2.3.2, both complexes eluted at void time with MPA, while the free metal ion eluted with MPB. Equation 2.14 was used to calculate the concentration of EDTA. Figure 2.15 shows the resulting linear regression plots to calculate the $\log K_f'$ and n values of Co-EDTA and Zn-EDTA, respectively, which deviated more from the expected values than those obtained from the mono-elemental systems. Also, the repeatability was not very good, indicating a poorer robustness of this procedure for multi-elemental complex system. One rationale for this difference (versus a mono-elemental

complex system) is that, the concentration of the uncomplexed EDTA was calculated with more variables in a multi-elemental complex system than in a mono-elemental one, which in turn introduced more errors. One way to increase the accuracy is to increase the concentration of reacting species to reduce relative errors in both sample manipulation and mathematical treatment, which, however, will compromise the benefit of this two-step method.

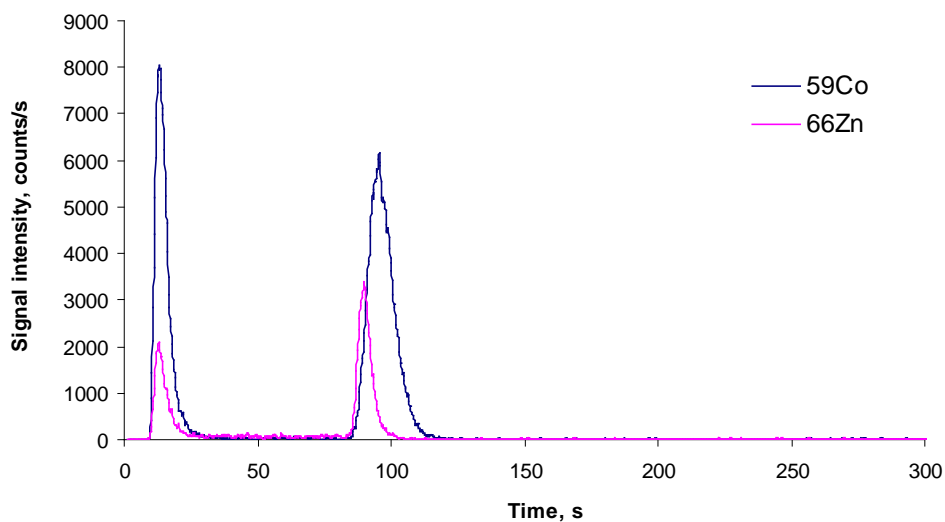


Figure 2.14. Stacked IEC-ICP-MS chromatograms of Co-EDTA and Zn-EDTA in a di-elemental complex system. The total concentrations of Co, Zn and EDTA are 1.70, 4.13 and 2.91 μM , respectively.

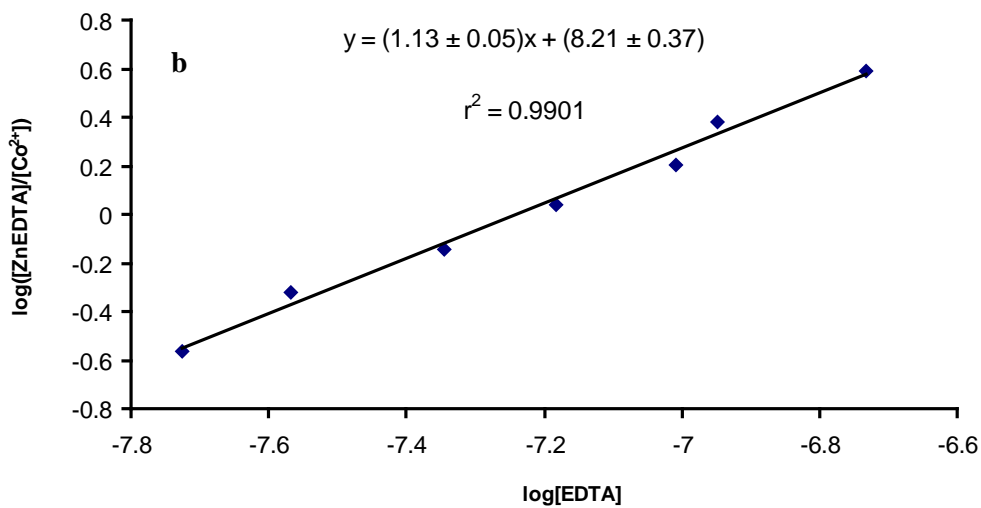
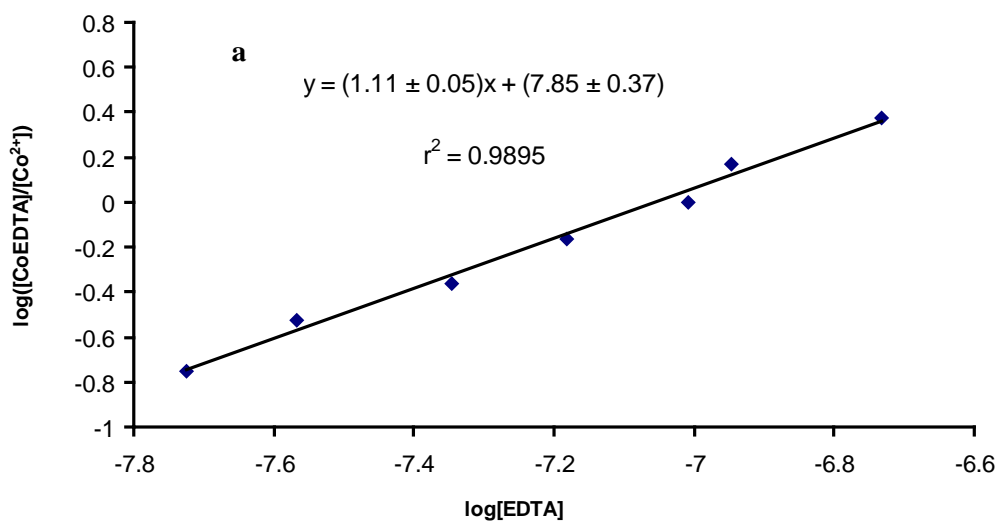


Figure 2.15. Linear regression to determine $\log K_f'$ (intercept) and n (slope) of Co-EDTA (a) and Zn-EDTA (b) with a di-elemental complex system containing 1.70 μM of Co, 4.13 μM of Zn and an EDTA concentration ranging from 1.17 μM to 4.66 μM .

In any case, the scope of applicability in terms of the candidate metal species is also limited. Let us suppose an ideal 2 metals/1 ligand complex, where metals A and B form complexes with ligand L independently, so that the ratio of metal complex concentration to free metal concentration for each element can be expressed by rearrangement of Equation 2.2 as:

$$[M_A L^{m_A-nl}]/[M^{m_A+}] = K_{f_A} \times [L^-]^n \quad (2.16)$$

$$[M_B L^{m_B-nl}]/[M^{m_B+}] = K_{f_B} \times [L^-]^n \quad (2.17)$$

It is apparent that the ratio of metal complex to its free metal counterpart is proportional to the conditional stability constant. So, one prerequisite to the simultaneous determination of stability constants is that these stability constants are close; otherwise the concentration window over which the regression process can be applied will be very narrow (see discussion in *section 2.1.4 Derivation of stability constant expressions*). For example, if the logarithm of the stability constant of A and B with ligand L differs by 2, i.e. $\frac{K_{f_A}}{K_{f_B}} = 100$, the ratio of $[ML^{m-nl}]/[M^{m+}]$ of metal A will be 100 times that of metal B.

This big difference in their requirements of ligand amounts to form complexes makes the area-ratio based analysis practically impossible to execute. In fact, a far more sensitive detector than ICP-MS would be required.

To test the usefulness of applying this IEC-ICP-MS procedure on, for instance, the simplest 2-element system, two metals with stability constants close in value would be re-

quired, according to the above theoretical analysis. In the extreme case, where the two metals have identical stability constants, the multi-elemental test will be meaningless: it is of no difference from determining stability constant using different isotopes like ^{66}Zn or ^{64}Zn in one-elemental complexing system. Therefore, this subject was not further pursued in this thesis work.

2.4 Summary

Hyphenated IEC and ICP-MS is a useful method for the determination of stability constants of metal complexes at very low concentrations (μM level) with appropriate mathematical treatments. The over simplification of the formation constant expression (H-1) caused the deviation of the chelation number in the previously approach. The primary assumption in using ion exchange chromatography to separate metal complexes is that there is no shift of equilibrium during the elution process [18, 22, 27, 28]. It is preferable that the free metal ions bind to the ion exchanger while the complexes elute freely from the column. As the data fit the equations that were deduced without considering the influence of the ion exchanger, the primary assumption appears to be justified.

Both IonPac AG-7 and CG-5A are suitable columns for this purpose. With AG-7, isocratic elution was able to separate both the metal complex and free metal species of Co and Zn within 5 minutes; while with CG-5A, a gradient elution was adopted to elute the free metal species. The multielemental detection capability of ICP-MS provides the possibility of extending the method thus developed to multielemental complexation system; how-

ever, the accuracy of the resultant values for both K_f' and n were not as good as for a mono-elemental system. Besides, fundamental calculations also showed that the ratio of metal complex to free metal is proportional to K_f' , making it difficult to execute the measurement for metals that have a relative large difference in value of K_f' . In view of these limitations, this line of work was not further pursued in this thesis.

References

1. K. Burger, *Biocoordination Chemistry: coordination equilibria in biologically active systems*. Inorganic chemistry, ed. J. Burgess. 1990: Ellis Horwood.
2. R.J. Reeder, M.A.A. Schoonen and A. Lanzirotti, *Metal speciation and its role in bioaccessibility and bioavailability*. Reviews in Mineralogy & Geochemistry, 64 (2006) 59-113.
3. A.E. Martell, *Determination and Use of Stability Constants*. 1988: VCH Publishers Inc.
4. H. Sigel, *Metal ions in Biological Systems*. 1973, New York: Marcel Dekker.
5. R.S. Smith, *Chelating Agents in the Diagnosis and Treatment of Iron Overload in Thalassaemia*. Annals of the New York Academy of Sciences, 119 (1964) 776-788.
6. A.V.C. Simionato, M.D. Cantu and E. Carrilho, *Characterization of metal-deferoxamine complexes by continuous variation method: A new approach using*

- capillary zone electrophoresis*. Microchemical Journal, 82 (2006) 214-219.
7. A.E. Martell, R.D. Hancock and Editors, *Metal Complexes in Aqueous Solutions*. 1996: Plenum Press.
 8. A.E. Martell and R.J. Motekaitis, *Potentiometry revisited: the determination of thermodynamic equilibria in complex multicomponent systems*. Coordination Chemistry Reviews, 100 (1990) 323-361.
 9. A.M. Crouch, L.E. Khotseng, M. Polhuis, and D.R. Williams, *Comparative study of cyclic voltammetry with potentiometric analysis for determining formation constants for polyaminocarboxylate-metal ion complexes*. Analytica Chimica Acta, 448 (2001) 231-237.
 10. F. Sancenon, A. Benito, F.J. Hernandez, J.M. Lloris, R. Martinez-Manez, T. Pardo, and J. Soto, *Difunctionalised chemosensors containing electroactive and fluorescent signalling subunits*. European Journal of Inorganic Chemistry, (2002) 866-875.
 11. P.W. Linder, *Handbook of Metal-Ligand Interactions in Biological Fluids: Bioinorganic Chemistry*. Vol. 1. 1995
 12. A. Sil and A.K. Srivastava, *Studies on the complexation of transition metal ions with macrocyclic compounds in mixed solvents by competitive potentiometry and polarography*. Supramolecular Chemistry, 16 (2004) 343-351.
 13. Z.A. Filmwala and P.S. Fernandes, *Polarographic study of few metal complex with L-hydroxy proline*. Research Journal of Chemistry and Environment, 5 (2001) 59-64.
 14. S. Karaderi, D. Bilgic, E. Dolen, and M. Pekin, *Determination of stability con-*

- stants of mixed ligand complexes of Cu(II) with creatinine and ethylenediamine tetra-acetic acid or L-glutamic acid: potentiometric and spectrophotometric methods.* Reviews in Inorganic Chemistry, 27 (2007) 459-472.
15. S. Karaderi and D. Bilgic, *The determination of the stability constants binary complexes of alizarin with Mg(II) and Al(III) by potentiometric and spectrophotometric methods.* Reviews in Analytical Chemistry, 27 (2008) 251-261.
 16. J.L. Stair and J.A. Holcombe, *Metal Binding Characterization and Conformational Studies Using Raman Microscopy of Resin-Bound Poly(aspartic acid).* Analytical Chemistry, 79 (2007) 1999-2006.
 17. G.T. Castro and S.E. Blanco, *Structural and spectroscopic study of 5,7-dihydroxyflavone and its complex with aluminum.* Spectrochimica Acta, Part A: Molecular and Biomolecular Spectroscopy, 60A (2004) 2235-2241.
 18. P. Janos, *Ion-interaction chromatographic separation of metal cations in the presence of complexing agents.* Fresenius' Journal of Analytical Chemistry, 350 (1994) 646-648.
 19. C. Huang, *Determination of conditional stability constants using ion chromatography coupled with inductively coupled plasma mass spectrometry,* in *Chemistry.* 2006, Queen's university: Kingston.
 20. C. Huang and D. Beauchemin, *Simultaneous determination of two conditional stability constants by IC-ICP-MS.* Journal of analytical atomic spectrometry, 21 (2006) 1419-1422.
 21. C. Huang and D. Beauchemin, *A simple method based on IC-ICP-MS to determine conditional stability constants.* Journal of analytical atomic spectrometry, 21

- (2006) 317-320.
22. M.R. Pitluck, B.D. Pollard and D.T. Haworth, *Determination of stability constants of a copper/citric acid complex by ion-exchange chromatography and atomic absorption spectrometry*. *Analytica Chimica Acta*, 197 (1987) 339-342.
 23. C.Y. Li, J.Z. Gao, G.H. Zhao, J.W. Kang, and H.H. He, *Determination of stability constants of Cu(II), Fe(III), and Pb(II) chelates with N,N,N',N'-ethylenediamine tetrakis(methylenephosphonic acid) by reversed-phase ion-pair chromatography*. *Chromatographia*, 46 (1997) 489-494.
 24. http://www.dionex.com/en-us/webdocs/57753-31612-03_V20.pdf.
 25. http://www.dionex.com/en-us/webdocs/4195-AS7_DataSheet_V30_releasedJC090706.pdf.
 26. http://www.dionex.com/en-us/webdocs/4263-CS5A_V13.pdf.
 27. P.R. Haddad and R.C. Foley, *Modeling of cation retention in ion chromatography using fixed-site and dynamically coated ion-exchange columns*. *Journal of chromatography A*, 500 (1990) 301-312.
 28. P. Hajos, G. Revesz, C. Sarzanini, G. Sacchero, and E. Mentasti, *Retention model for the separation of anionic metal-EDTA complexes in ion chromatography*. *Journal of chromatography A*, 640 (1993) 15-25.

Chapter 3

Chromium speciation analysis at trace level in potable water using hyphenated ion exchange chromatography and inductively coupled plasma mass spectrometry with collision/reaction interface

3.1 Introduction

Chromium is widely used in industrial processes such as metallurgy, metal plating, paint and fertilizer production, and wood preservation. Waste disposal from these industrial activities is a major source of chromium pollution in the environment. Rocks and minerals that have high chromium content can also release chromium into soils and waters through natural weathering processes [1]. Chromium affects humans through direct contact, inhalation of air, drinking and eating.

Hexavalent Cr and trivalent Cr are its two major oxidation states, which have very different physical and chemical properties. While Cr(VI) exists as H_2CrO_4 , HCrO_4^- , $\text{H}_2\text{CrO}_4^{2-}$ or $\text{Cr}_2\text{O}_7^{2-}$, depending on acidity and concentration, and is highly soluble in aqueous solution, Cr(III) exists as Cr(III) in acidic solutions and forms $\text{Cr}(\text{OH})^{2+}$, $\text{Cr}(\text{OH})_2^+$ and $\text{Cr}(\text{OH})_3$ in neutral to slightly basic conditions [2]. The interconversion of this redox pair is pH dependent: acidic conditions increase the reduction potential energy of Cr(VI), facilitating the reduction to Cr(III) in the presence of a reducing reagent; on the other hand, basic conditions help the stabilization of Cr(VI), but will de-stabilize Cr(III) by favoring precipitation. Cr(VI) and Cr(III) also affect physiochemical processes differently. Indeed,

Cr(III) is an essential micro-nutrient for biological activities, while Cr(VI) is believed to be toxic and carcinogenic [3]. Speciation analysis (i.e., the determination of the quantity of each individual species) must thus be carried out for toxicological risk assessment of food and drinking water.

3.1.1 IEC as separation technique for chromium speciation analysis

Various types of liquid chromatography, which is one of the most versatile separation techniques in analytical chemistry, have been used to separate this redox pair, including thin layer chromatography [4], reversed phase chromatography [5-9] and ion-exchange chromatography (IEC)[10-16]. The latter is the most widely used approach due to the ionic nature of the chromium species. As the redox pair possesses opposite charges, complexing agents are often used to switch over the charge state of one of the species, usually Cr(III), so as to retain both species onto the stationary phase. A complexing agent can also facilitate desorption of Cr(III), necessitating the use of a less concentrated electrolyte as mobile phase. With this methodology, reasonably good results were reported when the analyte concentration was at the 1-10 $\mu\text{g/L}$ level. Bednar *et al.* used EDTA as complexing agent to convert the charge state of Cr(III) and separated it from Cr(VI) with an anionic ion exchange column set (IonPac®AG-11/AS-11). The same methodology was adopted by researchers using Varian [16] and PerkinElmer [8] ICP-MS instruments. However, an addition of complexing agent may be problematic for analysis at trace levels where contamination control is usually the key to a reliable analysis.

Hence, keeping the sample in its original state is preferred for trace speciation analysis.

This can be achieved using tandem columns to selectively retain analytes of different charge states (cationic, anionic and neutral), which are then separated through sequential elution. Motomizu and coworkers used dual mini-columns or disks that were made of different resins with opposite ion exchange capability to selectively collect Cr(III) and Cr(VI), followed by their sequential elution [17, 18]. In fact, some ion-exchange columns with dual exchange capability are commercially available and were successfully used for speciation studies [13, 19-21]. Beauchemin and coworkers demonstrated the dual exchange capability of IonPac®AG-7 and AS 7 during the speciation analysis of As and the stability constant determination of metal-EDTA complexes [19-21]. Séby *et al.* reported a chromium speciation analysis procedure with a tandem column set IonPac®CG5A-CS5A using nitric acid of varied concentrations as the mobile phases to elute Cr(VI) and Cr(III) in sequence [13]. As will be demonstrated in this work, a simple guard column of such material with both cation and anion exchange capabilities can be used to achieve a quick quantitative separation of Cr(III) and Cr(VI).

3.1.2 ICP-MS as IEC detector

Inductively coupled plasma mass spectrometry (ICP-MS) is the most preferred detection technique in elemental speciation analysis due to its great sensitivity, selectivity, and multi-elemental detection capability, which affords an additional dimension for IEC separation, as, unlike with common ion detectors, separation of the species from different elements is not required, [22, 23]. However, ICP-MS suffers from spectroscopic interferences, which can arise from either isobaric or polyatomic ions. Indeed, although Cr has three stable isotopes, ^{52}Cr , ^{53}Cr , ^{54}Cr , with ^{52}Cr (83.789%) being the most abundant one,

there may be isobaric interference from $^{54}\text{Fe}^+$ on $^{54}\text{Cr}^+$, and polyatomic interferences from $^{40}\text{Ar}^{12}\text{C}^+$, $^{36}\text{Ar}^{16}\text{O}^+$ and $^{35}\text{Cl}^{16}\text{O}^1\text{H}^+$ on $^{52}\text{Cr}^+$, and from $^{40}\text{Ar}^{13}\text{C}^+$ and $^{37}\text{Cl}^{16}\text{O}^+$ on $^{53}\text{Cr}^+$. Given that Fe, C, O and Cl are often abundant in sample solutions (with dissolved carbon dioxide not being negligible), other approaches have been used to circumvent these interferences, such as mathematical corrections [24], or using either a double-focusing sector field mass spectrometer [25] or a collision/reaction cell [5, 11, 14, 15, 26]

However, each approach has its pros and cons. For example, increasing mass resolution may result in a loss in sensitivity and increased equipment cost [27]. Although mathematical correction may appear cost-effective, every parameter cannot always be accurately defined in the presence of complicated matrices and, in any case, such correction increases uncertainty [24]. Instruments equipped with a collision/reaction cell are not as expensive as double-focusing sector field ones, but they can usually only resolve some interferences through selective reaction of the analyte or interferent ion with the collision gas so that the analyte ion becomes free of interference [5, 11, 14, 15, 26]. Contrary to the common utilization on collision/reaction cell, there is far fewer reports on the collision/reaction interface (CRI), where a collision/reaction gas is introduced through the tip of the sampler or skimmer, to remove polyatomic interferences [16, 28]. Although the CRI approach requires a relative larger consumption of collision/reaction gas than typically used in collision/reaction cells, much less stabilization time is needed between CRI and no CRI operation modes.

This work aimed to develop a simple method for chromium speciation analysis in potable water by IEC-ICP-MS, which would be suitable as a quick risk assessment method. To

this end, several conditions must be satisfied. The direct analysis of water samples, without any pretreatment, should be done so as to preserve the original Cr speciation. The mobile phase(s) should be selected so as to avoid inter-conversion of the redox species during separation as well as salt and soot deposition on the ICP-MS interface cones. The stationary phase should retain both Cr species. Any polyatomic interference should be efficiently removed using the CRI so as to improve limits of detection of Cr species.

3.2 Experimental

3.2.1 Instrumentation

3.2.1.1 IEC. A Dionex 600/BioLC liquid chromatography system equipped with a GS 50 gradient pump, a Rheodyne 9750E injector and a 50- μ L sample loop was used. All connections and fittings were made of PEEK. IonPac®AG-7 guard column (10 μ m, 50 \times 4 mm i.d.) was used to separate Cr (III) and Cr (VI). This column has both cation and anion exchange capabilities due to the presence of sulfonic and alkyl quaternary ammonium functionary groups [29]. Gradient elution program was used with 0.1 M ammonium nitrate and 0.8 M nitric acid as mobile phases to remove Cr(VI) and Cr(III) respectively. The operation conditions are summarized in Table 3.1.

The column was cleaned daily by pumping mobile phase B for 10 minutes, and then stabilized with mobile phase A for 30 minutes at a flow rate of 1.5 mL/min. The column was cleaned more rigorously when appreciable broadening or deformation of peak shape was observed. In such a case, mobile phase B was pumped through the column for an hour that has been installed reversely opposite to the normal flow direction for one hour, then the column was reinstalled in the normal flow direction and equilibrated with mobile phase A for 1 hour, at 1.5 mL/min.

The sample solution was manually loaded into a 50- μ L sample loop with a syringe and injected automatically when the elution program was executed. The syringe was rinsed with sample solution thoroughly before injecting any sample for analysis. The outlet of

the column was connected to the liquid inlet of the ICP-MS nebulizer using a 50 cm long, 0.25 mm inner diameter PEEK tubing.

Table 3.1. IEC separation conditions

Parameter	Setting
Column	IonPac® AG-7 4.0 mm ID × 50 mm, 10 μm
Column temperature	Ambient
Mobile phase	A: 0.1 M ammonium nitrate, pH = 4.0 B: 0.8 M nitric acid
Elution program	0-2.5 min: mobile phase A 2.5-4.5 min: mobile phase B 4.5-7.5 min: mobile phase A
Flow rate (mL/min)	1.5
Sample injection volume (μL)	50

3.2.1.2 ICP-MS.

3.2.1.2.1 Varian 820-MS ICP-MS. A quadrupole ICP-MS instrument, model Varian 820-MS, was used and an IEC detector. The ICP-MS was equipped with a Micromist™ nebulizer, a Peltier-cooled Scott-type double-pass spray chamber (see Figure 3.1) and a three-channel peristaltic pump. The unique features of this instrument include a CRI system that can reduce polyatomic ion interferences; a 90-degree ion mirror and low noise

double off-axis quadrupole leading to high sensitivity and low background; and Turner interlaced RF coils that break down sample matrix material more efficiently and thus reduce possible matrix effects, and minimize ion a potential energy spread. The spatial arrangement of these features is shown in Figure 3.2.

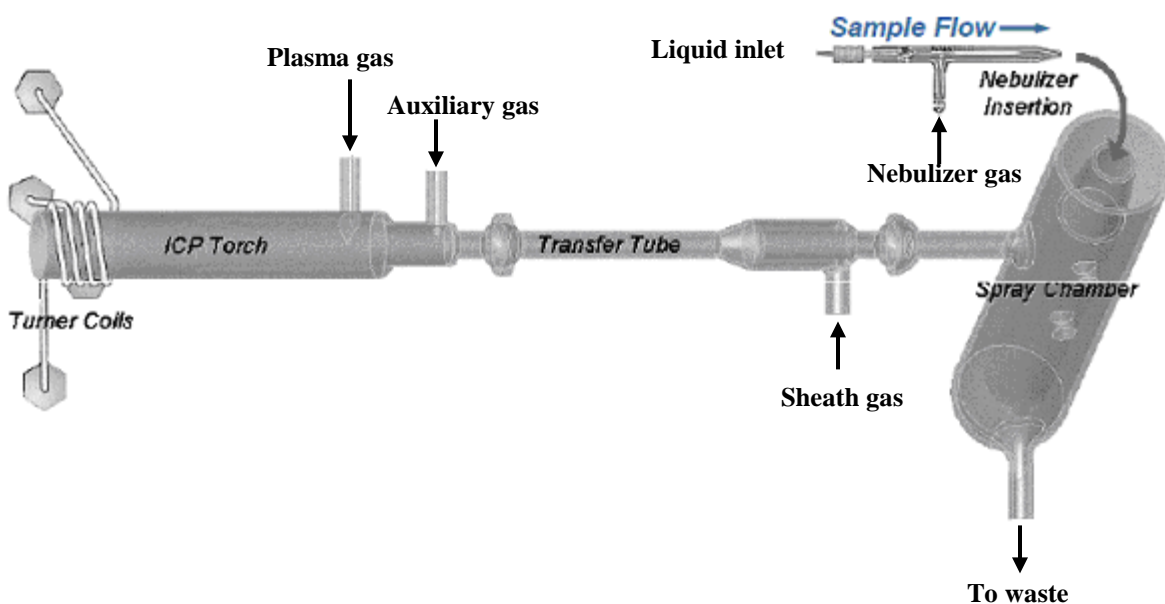


Figure 3.1. Diagram of Varian 820-MS sample introduction system [30].

The CRI feature is very useful to eliminate polyatomic interferences that conventionally plague chromium detection by low resolution ICP-MS. The CRI is spatially located within the sampling interface, i.e., the sampler and skimmer cones (see Figure 3.3). The CRI gas can be introduced through a groove inside the cones and collides/reacts with plasma species as it cuts in the plasma path. The CRI gas causes all the ions passing through the cone(s) to slow down. Because polyatomic ions are physically larger than analyte ions, they have a better chance to collide with the CRI gas and lose more velocity. If they lose

enough energy, they will not be able to pass through the ion optics and into the mass analyzer, and thus become eliminated. Introducing gas through the skimmer cone allows more efficient collision/reaction than through the sampler cone. He and H₂ are frequently used CRI gases, with H₂ being more effective as a reaction gas due to its higher reactivity. However, the CRI gas will also decrease the number of analyte ions and polyatomic interferences at the same time, therefore, it is necessary to optimize the flow rate so that the influence from the interferences is minimized without losing too much sensitivity for the analyte [30].

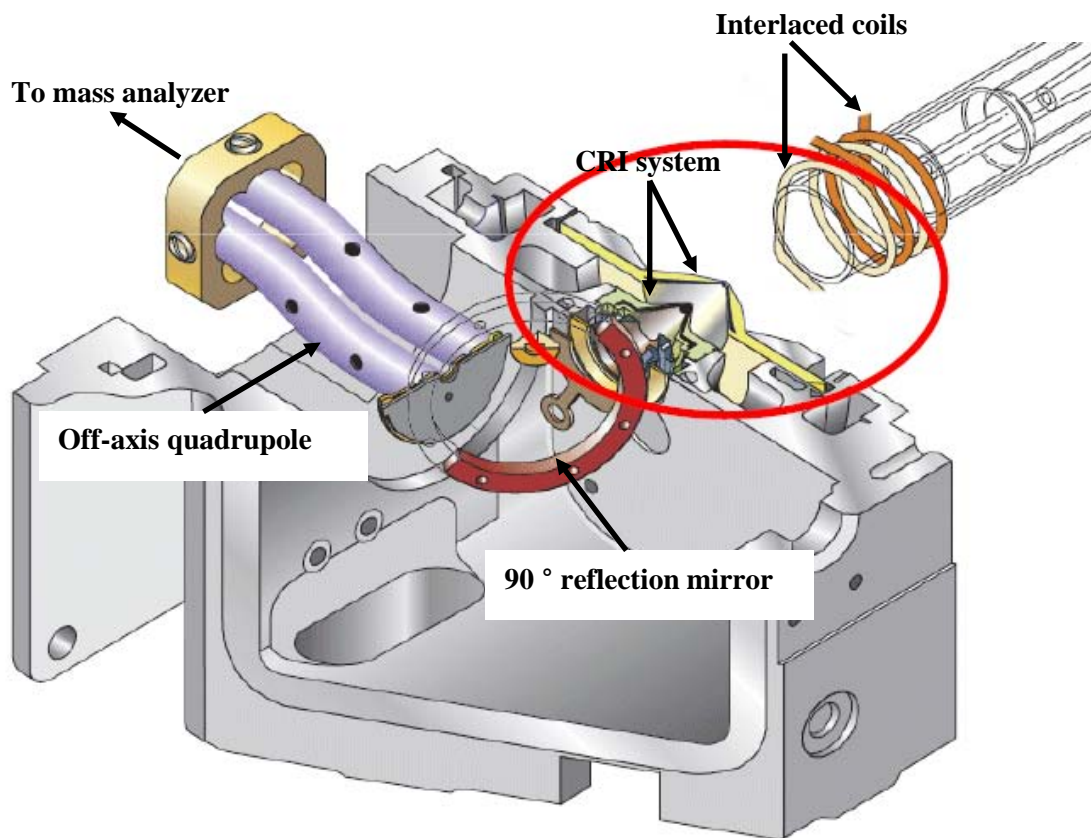


Figure 3.2. Spatial arrangement of the interlaced coils, the CRI system, the 90-degree reflection mirror and the off-axis quadrupole (adapted from reference [31]).

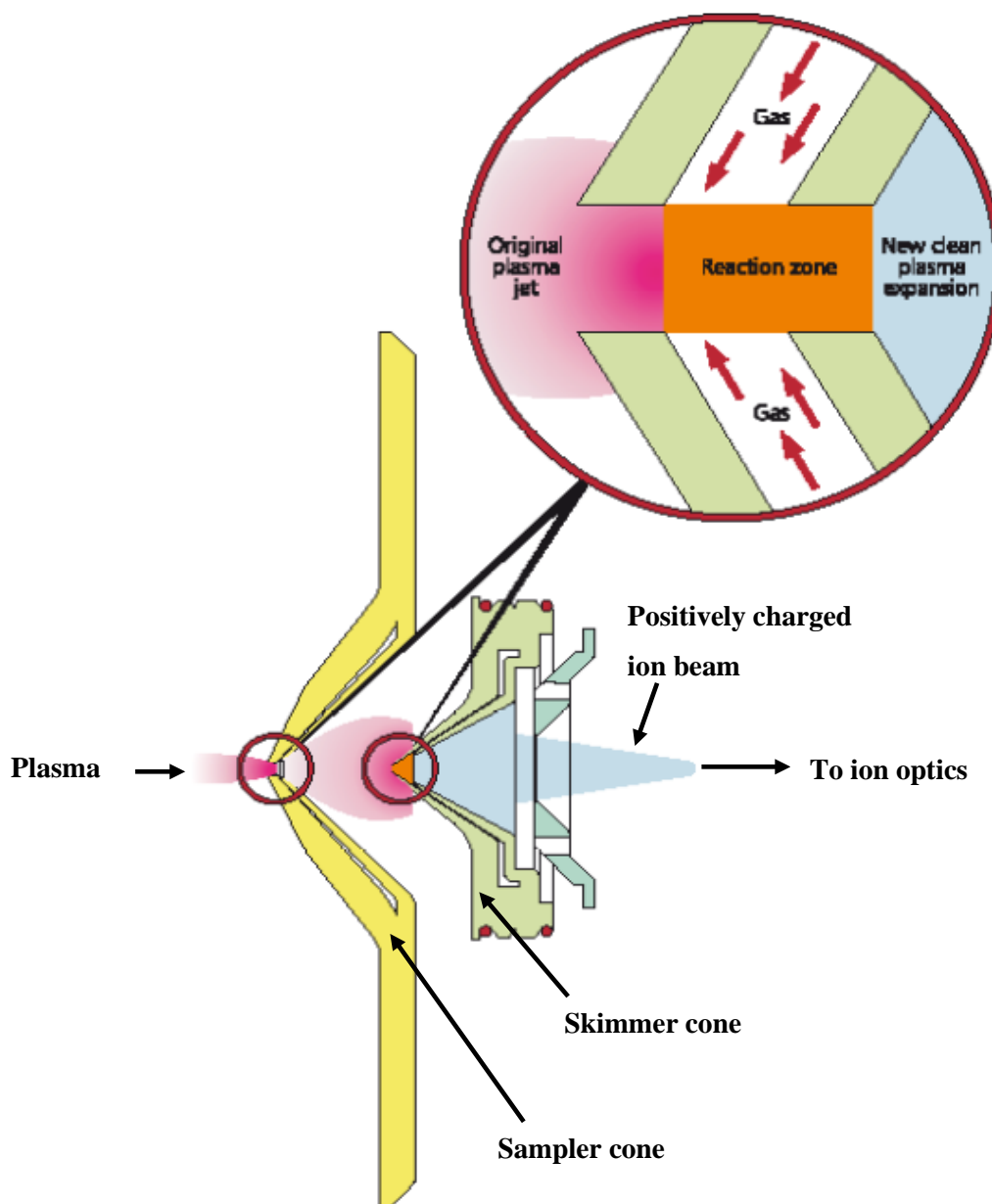


Figure 3.3 Diagrammatic illustration of the CRI system. A collision/reaction gas is introduced through the cone(s). At that point, the plasma still possesses a high temperature and ion density, which facilitate chemical reactions and collisions, leading to efficient removal of interfering polyatomic ions (adapted from reference [32]).

3.2.1.2.2 Optimization for chromium speciation analysis. Torch alignment was performed daily using a tuning solution containing 5 µg/L of Be, Mg, Co, In, Ce, Pb and Ba in 1% nitric acid DDW solution that was prepared by dilution from a 10 µg/mL Varian tuning solution (Spectropure™, St Louis, Missouri, USA).

To optimize the CRI gas flow rate, a 1% isopropanol solution (HPLC grade, Fisher Scientific) in DDW containing 10 µg/L Mn was used, where ⁵⁵Mn acted as a surrogate element for Cr because of the large ⁴⁰Ar¹²C⁺ background generated at m/z 52 by isopropanol. Hence, since the m/z 52 was reserved for monitoring the ⁴⁰Ar¹²C⁺ spectroscopic interference, analyte sensitivity was, in effect, monitored through Mn. The signal ratio of m/z 55 over m/z 52 was monitored while increasing the CRI gas flow rate. As CRI gas was introduced, the sensitivities at both m/z 52 and m/z 55 were reduced, but that at m/z 52 decreased more than that at m/z 55, resulting in an improved signal-to-background ratio. As the CRI gas flow rate was increased, the ratio reached a maximum and then decreased. The flow rate corresponding to the maximum was thus adopted.

At this optimal CRI gas flow rate, a preliminary optimization of the ion optic was carried out using the auto-optimization function with 1% nitric acid containing 20 µg/L of Sc, As and Y. Fine tuning of the ion optic was then done with 1% nitric acid containing 5 µg/L of Cr [30]. For trace analysis, the nebulizer, torch, sampler and skimmer cones were cleaned and a full optimization procedure was performed, including plasma alignment, mass calibration, mass resolution and trim, detector

setup, CRI gas flow rate and ion optic settings.

The conditions given in Table 3.2 were used for the quantitation of Cr species in real samples. During developmental work, $^{53}\text{Cr}^+$ was also monitored to help identify peaks due to Cr through a comparison of the $^{52}\text{Cr}^+ / ^{53}\text{Cr}^+$ peak area ratio to that expected from natural abundances.

Table 3.2. ICP-MS operating conditions

	Parameter	Setting
ICP	Ar plasma gas flow rate (L/min)	18.0
	Ar auxiliary gas flow rate (L/min)	1.80
	Ar nebulizer gas flow rate (L/min)	0.93
	Ar sheath gas flow rate (L/min)	0.23
	Plasma RF power (kW)	1.40
	Monitored m/z	52
	Dwell time (s)	0.5
Sampling interface	Sampler cone; tip i.d.	Ni; 0.9 mm
	Skimmer cone; tip i.d.	Ni; 0.4 mm
CRI	Skimmer gas	H ₂
	Skimmer gas flow rate (mL/min)	70
	Sampler gas	OFF
Spray chamber	Temperature (°C)	3
	Draining pump rate (mL/min)	2.0
Ion optics	First Extraction Lens (V)	-42

Parameter	Setting
Second Extraction Lens (V)	-165
Third Extraction Lens (V)	-210
Corner Lens (V)	-212
Mirror Lens Left (V)	32
Mirror Lens Right (V)	24
Mirror Lens Bottom (V)	28
Entrance Lens (V)	1
Fringe Bias (V)	-3.2
Entrance Plate (V)	-35
Pole bias (V)	0.0

3.2.2 Reagents and solution preparation

3.2.2.1 Reagents. Doubly deionized water (DDW) (18.2 Ω M/cm, Milli-Q Plus System, Millipore, Mississauga, Ontario, Canada), ultrapure nitric acid (ULTREX® II, 70%, J.T. Baker, Phillipsburg, NJ 08865, USA), ultrapure ammonium hydroxide (TraceMetal Grade, Fisher Scientific, Canada) and stock Cr(III) solutions (1000 μ g/ml, 4% HNO₃) from SCP Science (Baie D'Urfé, Québec, Canada) were used. In the case of Cr(VI), a stock solution (1000 μ g/ml, pH = 8.0) was prepared by dissolving potassium dichromate (J.T.Baker, Phillipsburg, NJ 08865, USA) in DDW. All standard solutions were prepared daily by dilution of the stock solutions with DDW.

To optimize the CRI conditions, varying concentrations of sodium chloride (certified ACS reagent, Sigma-Aldrich Laborchemikalien, GmbH, Germany) or sodium bicarbonate (Certified ACS reagent, Fisher Scientific, NJ 07410, USA) were spiked into blank solutions or solutions containing 20 µg/L of both Cr(VI) and Cr(III). These aqueous solutions were prepared immediately before speciation analysis. The accuracy of the method was verified using riverine water SLRS-2 (National Research Council of Canada, Ottawa, ON, Canada) with a certified total chromium concentration. Tap water was collected from the fountain in this laboratory right before analysis and analyzed directly.

3.2.2.2 Sample solution preparation. High-density polyethylene (HDPE) bottles were used as sample containers. They were soaked in 15% nitric acid, rinsed, soaked in DDW for 24 hours, and air-dried. The riverine water SLRS-2 was stored in HDPE bottle at 4 °C and used directly without further treatment. For speciation analysis of SLRS-2 by the method of standard addition, an aliquot of the original riverine water was spiked with 10 µg/L each of Cr(VI) and Cr(III), and left at room temperature for 24 hours. Aliquots of this conditioned spike solution were then diluted with SLRS-2 so as to obtain Cr concentrations ranging from 0.2 to 4 µg/L. For speciation analysis by external calibration, a series of standard solutions with concentrations ranging from 0.1 to 100 µg/L of each species were prepared in 0.1 M ammonium nitrate. The HDPE bottle used for the tap water sample was rinsed with tap water 3 times prior to sample collection, which was done immediately before analysis. Enough tap water was collected to allow analysis by both the method of standard additions and external calibration.

3.2.3 Recovery test

Recovery tests were performed to check the elution efficiency of the injected metal species. Six replicate 50- μ L injections of a standard solution containing 0.5 mg/L each of Cr(III) and Cr(VI) prepared in 1% nitric acid were made onto the AG-7 column using the chromatographic conditions in Table 3.1. The eluates from the different replicates were collected in separate flasks of known weights. The flasks loaded with the elutate were reweighed, and the eluates weights were converted into volumes using the measured density of the mobile phases. External standardization was used to quantify the total metal concentration in the eluate, using standard solutions over the concentration range 1-100 μ g/L prepared in a 27%/73% mixture of mobile phases B and A.

3.2.4 Data processing

An in-house QBASIC® program was used to treat the raw data for smoothing (with a 7-point polynomial Savitzky- Golay moving window) and integration of peak areas. The latter were used for all subsequent calculations, which were done using a Microsoft Excel® (Microsoft Office 2003, Microsoft, USA) spreadsheets.

3.3 Results and discussion

3.3.1 Optimization of CRI conditions to reduce ArC⁺ interference

As described in section 3.2.1.2.2, optimization of the CRI gas flow rate was carried out by maximizing the ratio of the signal of a surrogate element, ⁵⁵Mn, which is close in m/z to Cr, over the signal of the interferent at m/z 52, while aspirating a 1% isopropanol solution containing 10 µg/L Mn. The optimal gas flow rate was 70 mL/min for H₂ and 50 mL/min for He. The ion optics were then re-optimized with the optimal CRI gas. The signal intensities at m/z 52 and m/z 55 and their relative standard deviation (RSD) for a 10 µg/L Mn solution, with and without CRI gas, are summarized in Table 3.3. They show that either He or H₂ significantly reduced the background signal, but that H₂ was most efficient. On the other hand, analyte sensitivity was also concurrently sacrificed. Nonetheless, the best detection limit was obtained with H₂ in the CRI, which was thus used for the remainder of this work. Also, the mass bias at this flow rate was not significantly different than that without CRI tuning.

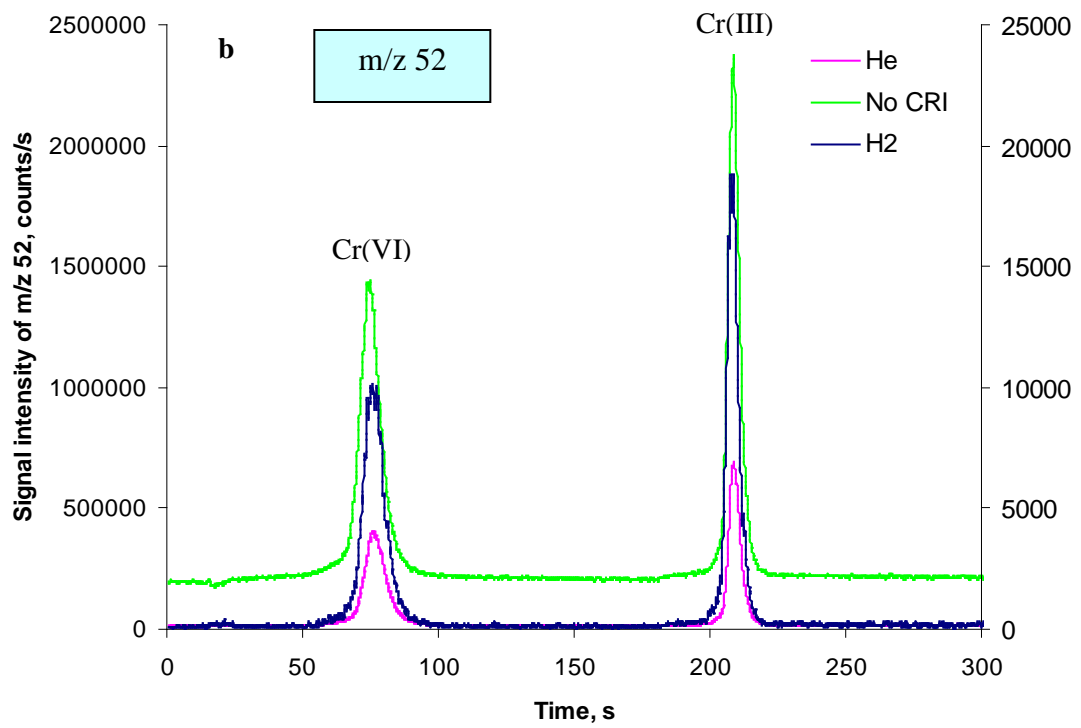
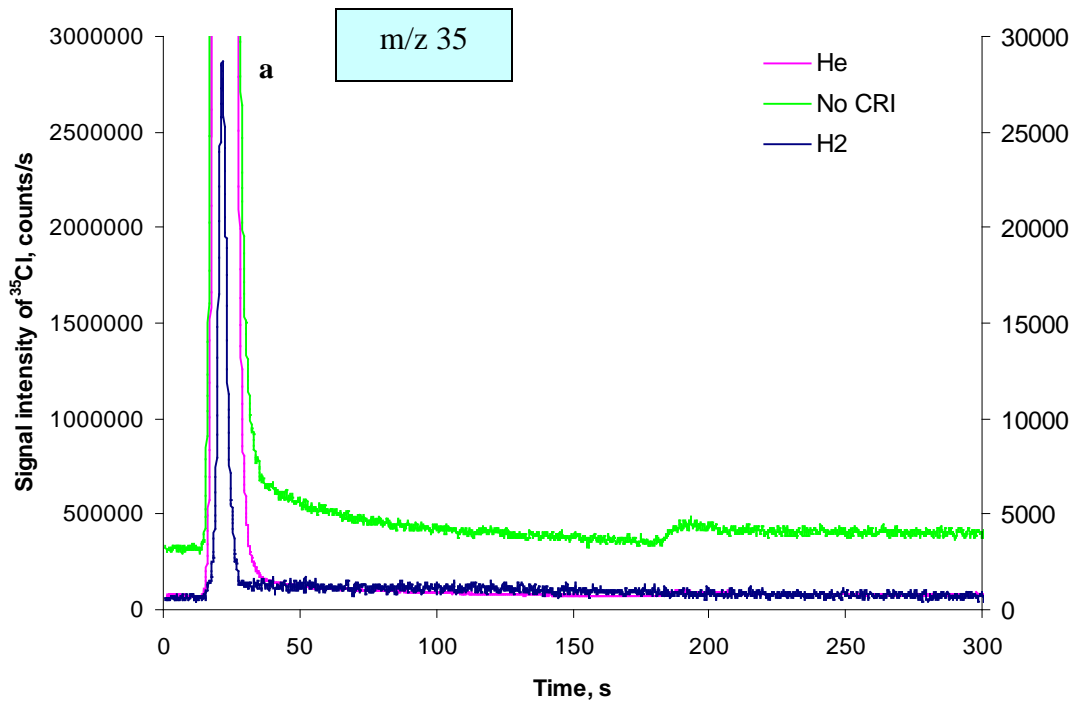
Table 3.3. Signal intensity at m/z 52 and m/z 55 for DDW spiked with 10 µg/L Mn using different CRI modes.

	m/z 52 intensity, counts/s	%RSD (n = 5)	m/z 55 intensity, counts/s	%RSD (n = 5)	m/z 55 /m/z 52	Relative m/z 52 intensity, %	Relative m/z 55 intensity, %	Detection limit for m/z 52, µg/L
No CRI gas	164,300	0.77	5,737,600	0.50	35	100	100	0.1
He, 50 mL/min	24,370	1.1	2,084,000	0.98	86	15	36	0.008
H ₂ , 70 mL/min	5,450	4.0	633,500	0.93	116	0.3	11	0.005

3.3.2 Optimization of Cr speciation analysis method

3.3.2.1 Chromatographic separation. An IonPac® AG-7 guard column was chosen to do the separation due to its dual ion exchange capability [19]. As the chromium redox pair exhibits a very different retention behavior on the stationary phase, a gradient elution program of varying ionic strength was adopted to perform the separation, as shown in Table 3.1. In a typical chromatographic separation, Cr(VI) was eluted with mobile phase A followed by Cr(III) eluted with mobile phase B (see Figure 3.4b). The two major problems with chromium speciation, i.e., precipitation of Cr(III) and reduction of Cr(VI) to Cr(III) in presence of a reducing reagent, were not observed at all with this chromatographic method. The average Cr recovery from the column was $101.5 \pm 2.0\%$ ($n = 6$). Although this result was established using standard solutions, the good agreement obtained for SLRS-2 (see section 3.3.6 *Speciation analysis of chromium in certified riverine water SLRS-2*) indicates that quantitative recovery was also obtained for real samples.

3.3.2.2 Elimination of chlorine-based spectroscopic interferences. Chlorine is commonly present in environmental, food and biological samples. The polyatomic ions $^{35}\text{Cl}^{16}\text{O}^{16}\text{H}^+$ and $^{37}\text{Cl}^{16}\text{O}^+$ may interfere with $^{52}\text{Cr}^+$ and $^{53}\text{Cr}^+$, respectively. However, under the separation conditions summarized in Table 3.1 and as shown in Figure 3.4a, Cl^- elutes completely before Cr(III) and Cr(VI) and will thus not interfere with the detection of either Cr species. Even if no separation was performed, Figure 3.4b demonstrates that this interference would be negligible on $^{52}\text{Cr}^+$, even without H_2 CRI gas, but $^{37}\text{Cl}^{16}\text{O}^+$ would preclude the determination of Cr using $^{53}\text{Cr}^+$ if no separation was done (see Figure 3.4c).



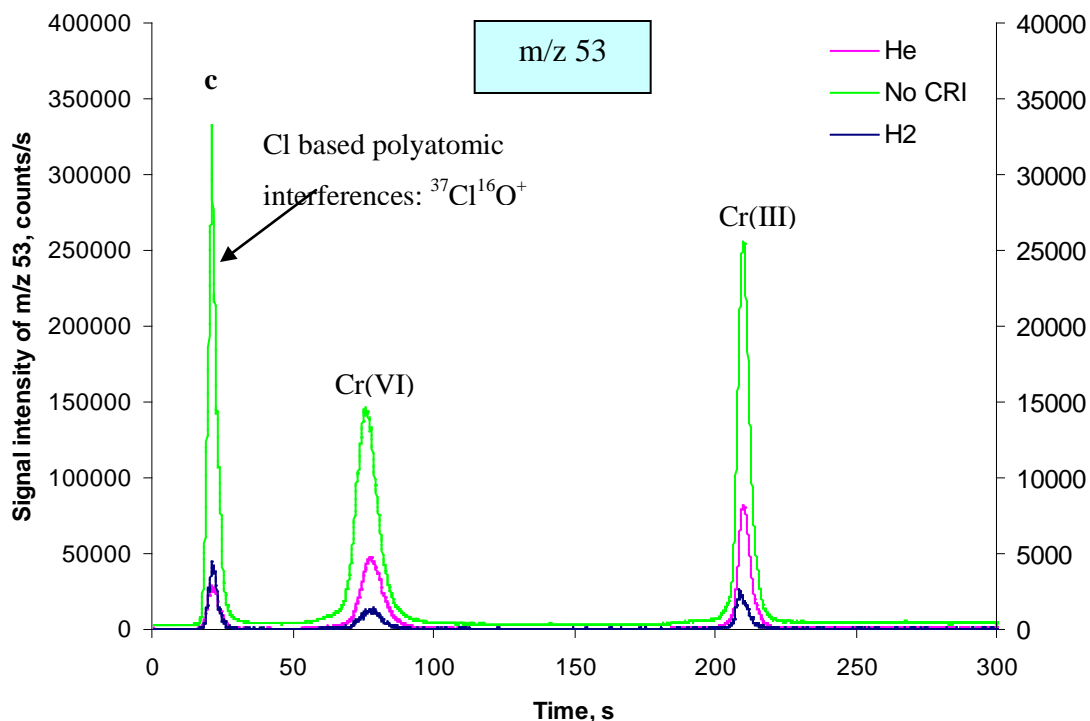


Figure 3.4. Chromatograms obtained for 1000 mg/L of Cl and 20 $\mu\text{g/L}$ each of Cr(VI) and Cr(III) under three different modes: without CRI gas, with 50 mL/min He and with 70 mL/min H_2 . a) m/z 35, b) m/z 52 and c) m/z 53 were monitored. A secondary y-axis (right side) was used for the H_2 CRI mode for better visualization.

3.3.2.3 Elimination of carbon-based spectroscopic interferences. The polyatomic ion $^{40}\text{Ar}^{12}\text{C}^+$ usually is a major contributor to the high background signal intensity at m/z 52, and arises from the ubiquitous presence of carbon dioxide in the air and dissolved in solution as well as organic material in sample matrix. Figure 3.5 shows the chromatograms obtained for a series of Cr-free sodium bicarbonate solutions while monitoring m/z 52 without CRI gas. The blank (DDW) was also included to show that the baseline was higher with mobile phase B (0.8 M HNO_3), i.e., from 180 to 300 s, than with mobile

phase A (0.1 M NH_4NO_3). The peak from 200 to 220 s is caused by the elution of accu-

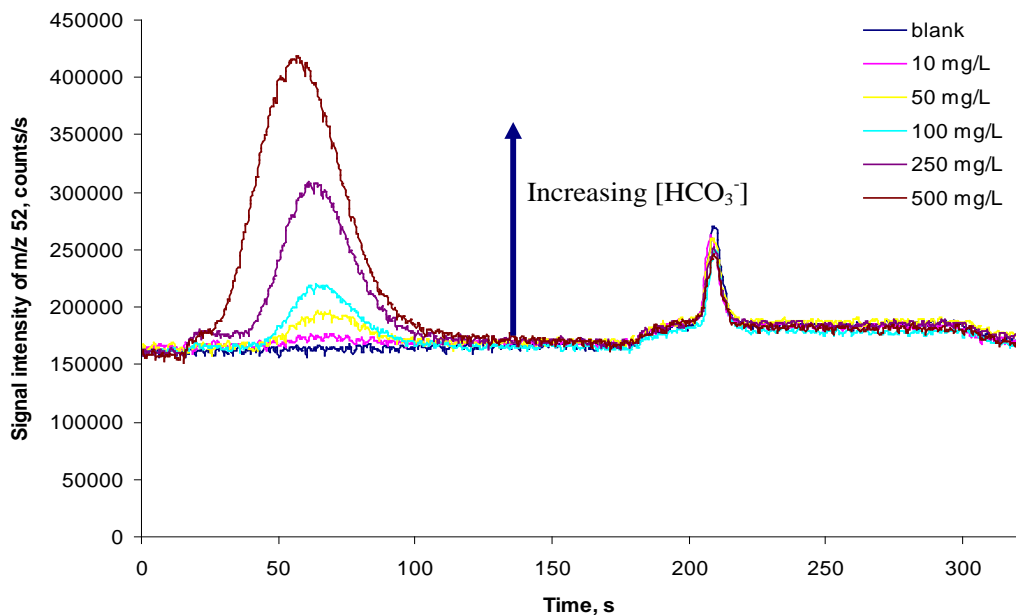
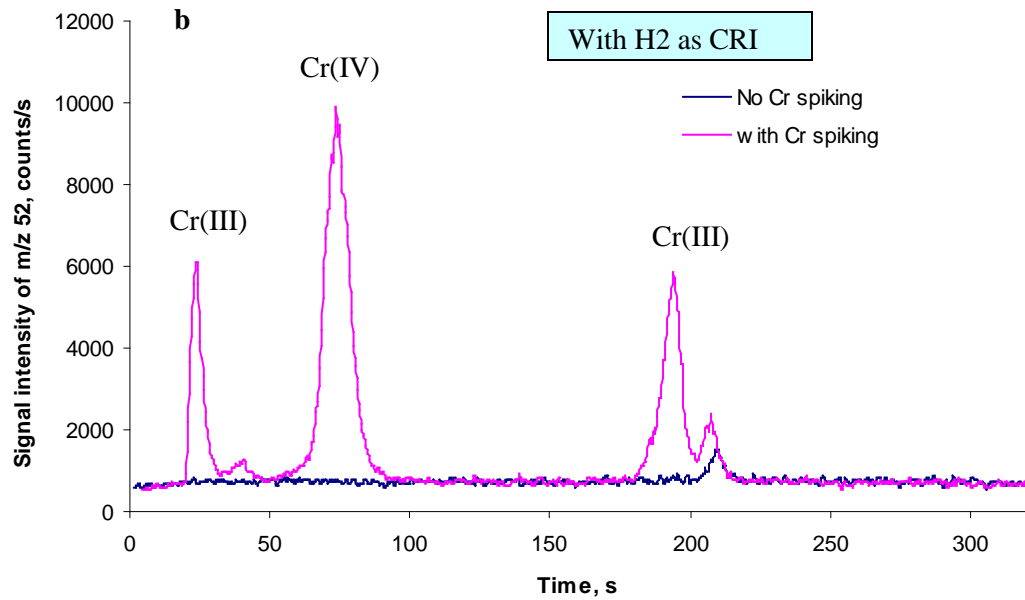
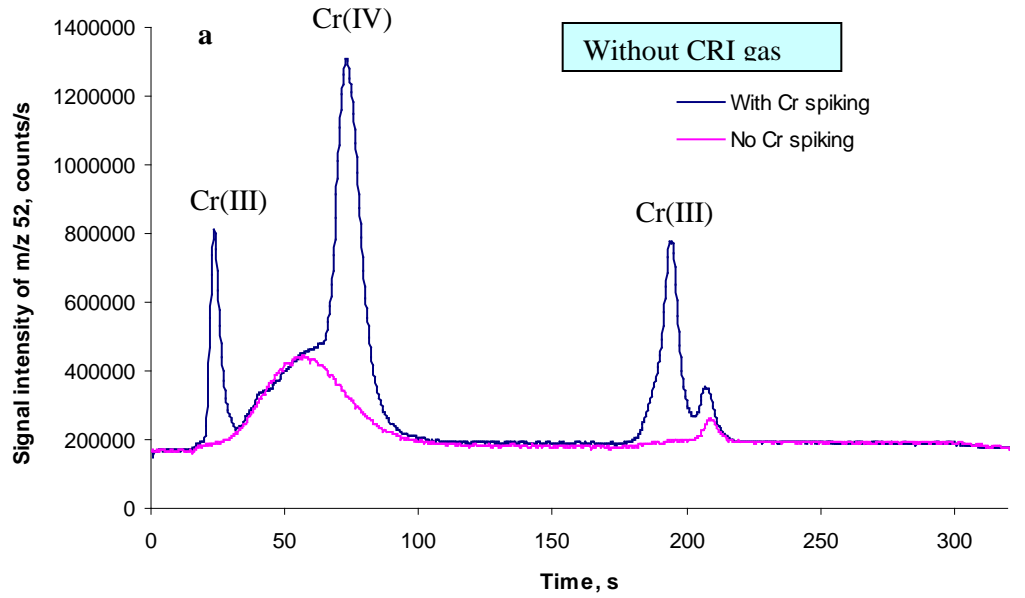


Figure 3.5. Stacked chromatograms observed without CRI gas for a series of sodium bicarbonate solutions with concentrations ranging from 10 to 500 mg/L.

ulated chromium from mobile phase A (see section 3.3.3 *Background correction* for a more detailed discussion). Figure 3.5 also shows that there is an extra peak from 16 to 120 s for all sodium bicarbonate solutions, whose size and intensity increase with sodium bicarbonate concentration. As this extra peak overlaps with the retention time of Cr(VI), it would complicate the speciation analysis of samples containing carbonate ions, which is frequently the case with environmental and biological samples.

Figure 3.6a compares the chromatograms of 500 mg/L bicarbonate solution spiked or unspiked with 20 $\mu\text{g/L}$ each of Cr(VI) and Cr(III). The peaks were assigned by spiking the

bicarbonate solution with Cr(VI) and Cr(III) separately as shown in Figure 3.6c. The splitting of Cr (III) into three peaks was speculated to arise from different charge states of



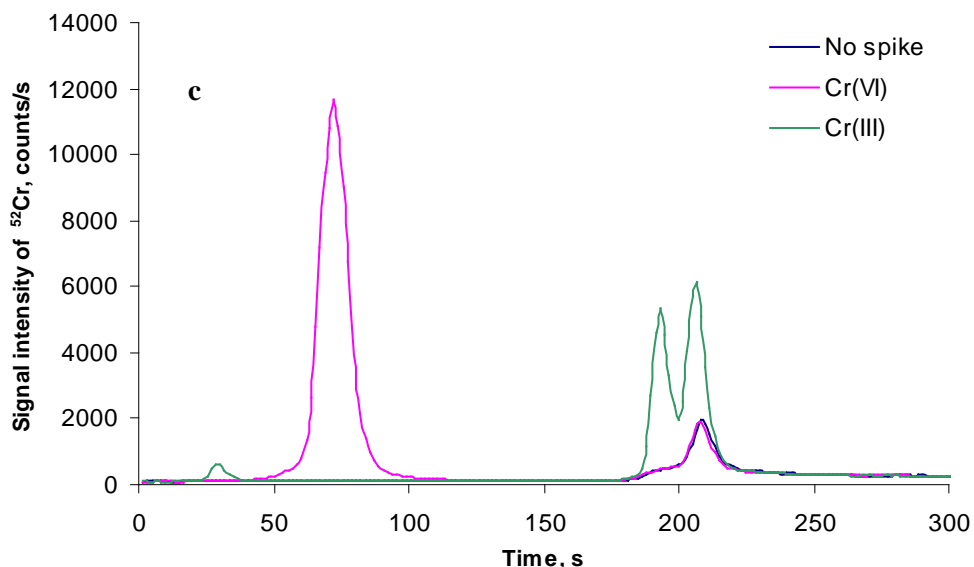


Figure 3.6. Chromatograms obtained a) without CRI gas, b) with 70 mL/min H₂ CRI gas for solutions containing 500 mg/L sodium bicarbonate, with and without 20 µg/L each of Cr(VI) and Cr(III), and c) with 70 mL/min H₂ CRI gas for 250 mg/L sodium bicarbonate solution without Cr (blue), spiked with 10 µg/L of Cr(VI) (pink) and spiked with 10 µg/L of Cr(III) (green).

$[\text{Cr}(\text{OH})_x]^{3-x}$ complexes [13] or from Cr(III)-carbonate complexes, which have multiprotic nature. The sum of the areas of these peaks corresponded to that of Cr(III) in bicarbonate-free solution. Although the peak due to bicarbonate might be eliminated through background subtraction, the preparation of a suitable blank for real sample analysis, where the amount and identity of carbon-containing species varies widely, would not be an easy task. By using the CRI with H₂, the spectroscopic interference from bicarbonate was completely eliminated, as shown in Figure 3.6b. Hence, using H₂ as CRI gas effectively eliminates the polyatomic interferences arising from chlorine and carbon and is thus highly recommended for the chromium speciation analysis of real samples.

3.3.3 Background correction

Chromium contamination of the mobile phases cannot be ignored when performing trace and ultra-trace speciation analysis. A typical chromatogram of the blank is shown in Figure 3.7, where similar elution profiles result for m/z 52 and m/z 53.

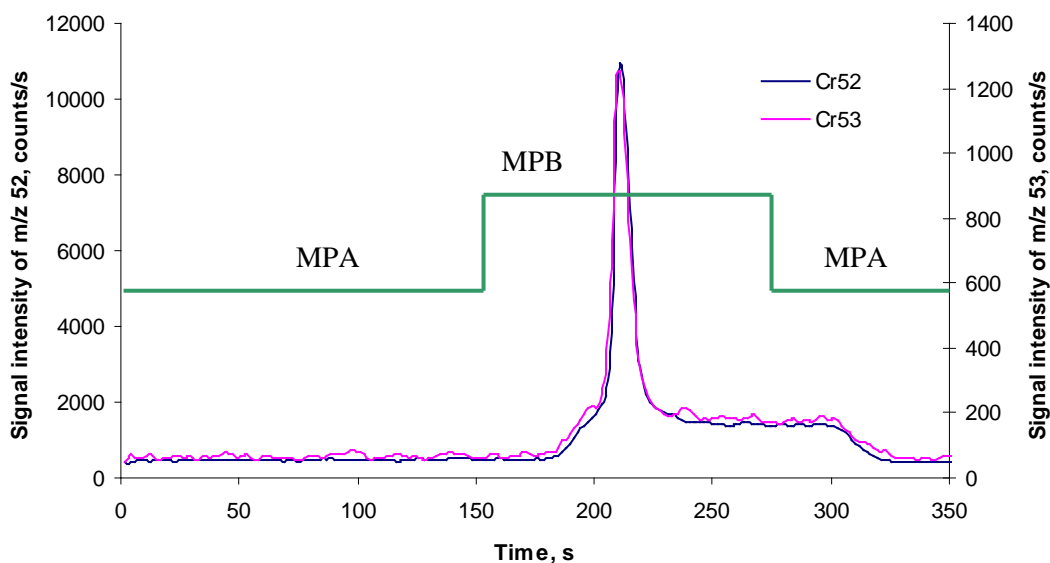


Figure 3.7. Blank chromatogram obtained by injection of DDW with CRI gas on. A secondary y-axis was used for m/z 53 to better visualize the resemblance of these two isotopes as to elution profiles. The green line illustrates the elution gradient.

The ratio of peak areas of m/z 52 vs. m/z 53 is 8.57 ± 0.36 ($n = 5$), which is comparable to that obtained by direct nebulization of a standard Cr solution (8.34 ± 0.01 , $n = 5$). The increase in baseline between 180 and 300 s clearly arises from Cr contamination of mo-

bile phase B, whereas the superimposed peak at around 205 s is due to elution of Cr accumulated from mobile phase A. Indeed, although Cr(VI) is eluted by mobile phase A, Cr(III) can only be eluted by mobile phase B, and can thus accumulate on the column, in addition to Cr(III) from the injected sample, while mobile phase A is pumped through the column.

Even though ultrapure nitric acid and ammonium hydroxide were used to prepare the mobile phases, the latter nonetheless contained around 4 ng/L Cr, which was determined with a pre-concentration procedure (see section 3.3.4 *Determination of limit of detection (LOD)*). Attempts to purify the mobile phases by, for instance, pumping them through a cationic ion exchange column, did not significantly lower this concentration. Because the total volume of mobile phase A passing through the stationary phase is 8.25 mL (1.5 mL/min multiplied by 5.5 min) per chromatographic separation, essentially any trace of Cr can result in a detectable peak at the retention time for Cr(III). This is further supported by the fact that the size of the peak was directly proportional to the length of time during which mobile phase A was pumped through the column prior to switching to mobile phase B. Hence, blank subtraction was required to eliminate the Cr(III) contribution from mobile phase A.

3.3.4 Determination of limit of detection (LOD)

A series of samples containing 0.1-100 µg/L each of Cr(VI) and Cr(III) in 0.1 M ammonium nitrate were analyzed using the conditions shown in Table 3.1 and 3.2. Figure 3.8 illustrates the elution profiles of the standard samples, exemplifying good repeatability as

to retention time and peak shape. The peak area of the blank was calculated over the same retention time range as the spiked samples. Eight blanks were used to calculate the limit of detection.

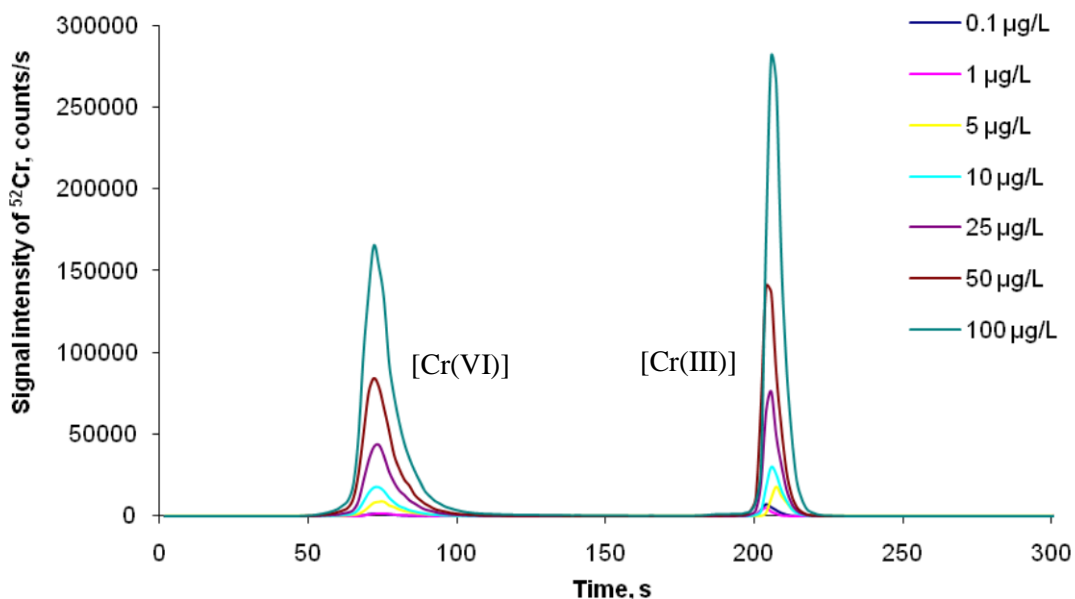


Figure 3.8. Blank-subtracted chromatograms of 0.1-100 µg/L Cr standard solutions.

The calibration curves for Cr(VI) and Cr(III) in Figures 3.9 and 3.10 show good linearity, with correlation coefficients of 0.999 or higher. The resulting LOD was 0.02 and 0.04 µg/L for Cr(VI) and Cr(III) respectively. The residual Cr(III) in the mobile phase is a major cause of the relatively higher LOD for Cr(III).

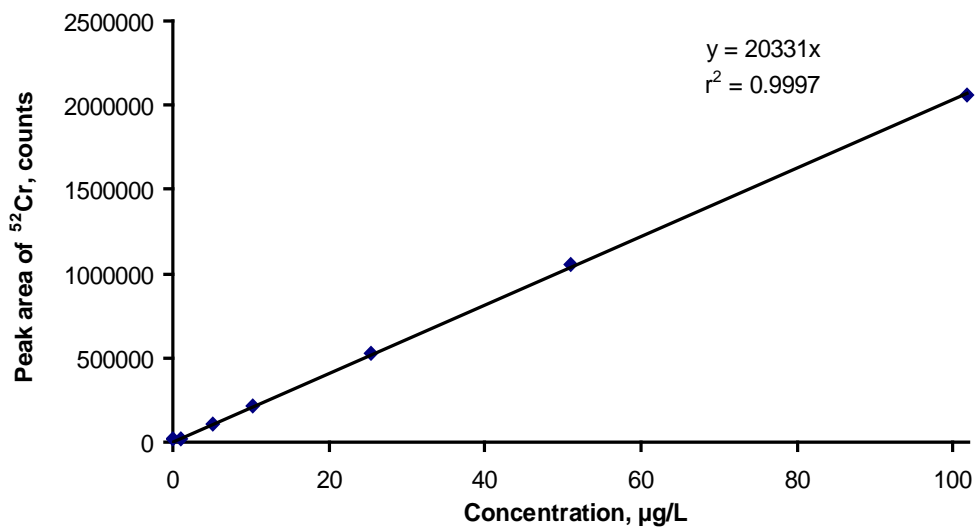


Figure 3.9. Calibration curve for Cr(VI) using standards ranging from 0.1 to 100 µg/L.

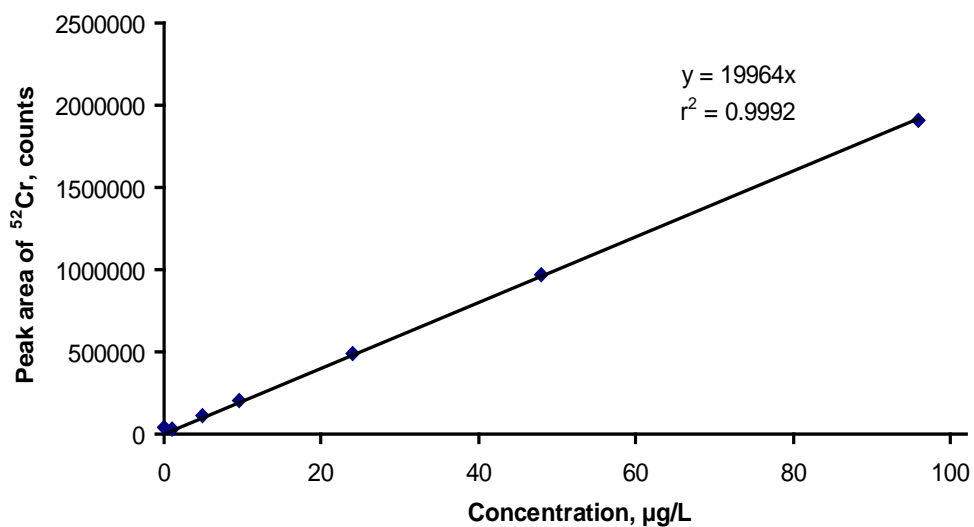


Figure 3.10. Calibration curve for Cr(III) using standards ranging from 0.1 to 100 µg/L.

Note: Because good linearity was observed, only one standard solution was analyzed for each concentration level.

3.3.5 Determination of the Cr content of the mobile phase

The Cr(III) peak of the blank was treated as a real sample in speciation analysis to estimate the Cr content of the mobile phase. The peak area translated to $0.714 \pm 0.053 \mu\text{g/L}$ according to the calibration curve in Figure 3.10. This would correspond to $35.8 \pm 2.7 \text{ pg}$ injected using the $50\text{-}\mu\text{L}$ sample loop. Divided by 8.25 mL , the total volume of 0.1 M ammonium nitrate consumed during one chromatographic separation, the concentration of Cr in the mobile phase is estimated to be $(4.2 \pm 0.8) \times 10^{-3} \mu\text{g/L}$. The purity of the mobile phase and the quality of the water used to prepare the standards affect the actual LOD with this speciation procedure.

Factors affecting the accuracy of sub-ppb to ppb speciation analysis of chromium include (1) measurement precision, (2) possible contamination during sample preparation and transfer, (3) sample loss to the container and injecting syringe and (4) conversion between the redox species inside the container and/or on the stationary phase. Extreme care has to be taken to minimize possible cross-contamination and loss of innate analyte. In our view, the results so far obtained are satisfactory for regular laboratory working conditions.

3.3.6 Speciation analysis of chromium in certified riverine water SLRS-2

The method we developed was applied to analyze a standard reference sample of riverine water, SLRS-2, which has a certified total chromium concentration. Riverine water is usually rich in potential Cr complexing agents, either organic or inorganic. For instance,

fulvic and humic acids can be major components of streams, lakes and seawater. As carboxylic acids, fulvic and humic acids should be good chelators for positively charged multivalent ions, including Cr(III) [33, 34]. Humic acid may also be involved in the reduction of Cr(VI) to Cr(III) by such ion as Fe^{2+} [35]. SLRS-2 was acidified to pH 1.3 with nitric acid for preservation purposes, which likely affected the original Cr speciation.

Figure 3.11 shows the chromatograms of riverine water SLRS-2 and a blank (DDW). The chromatogram of the riverine water after blank subtraction is shown in Figure 3.12. For SLRS-2, there is no peak detected at the retention time corresponding to Cr(VI), but there is one near the void time. Spiking this riverine water with 200 $\mu\text{g/L}$ of Cr(VI) followed by analysis one day later revealed that the Cr(VI) peak disappeared and a peak of commensurate size appeared at near void time. Evidently, this peak evolved from Cr(VI) and may be a complex of Cr(VI). It may also arise from reduction of the 'original' Cr(VI) species under the rather acidic condition of this water sample [36]. Attempts to analyze the eluate of this fraction by electrospray ionization mass spectrometry (ESI-MS) (in positive ion mode) were not conclusive. The mass spectrum (Figure 3.13) included several Cr-containing peaks in the mass range of 300-600 Da, which may have originated from some fulvic acids [37], as can be seen from the tentative assignment made in Table 3.4. However, the masses measured did not match the exact masses of these compounds very well. In any case, the formation of Cr-containing complexes is not surprising in view of the abundant organic compounds present in riverine water [37]. As this early eluting peak remained when the chromatographic separation was carried out on an analytical

column (IonPac® AS-7) instead of just a guard column (not shown), it was thus labeled as ‘Cr-complex’ in the chromatograms and Table 3.5.

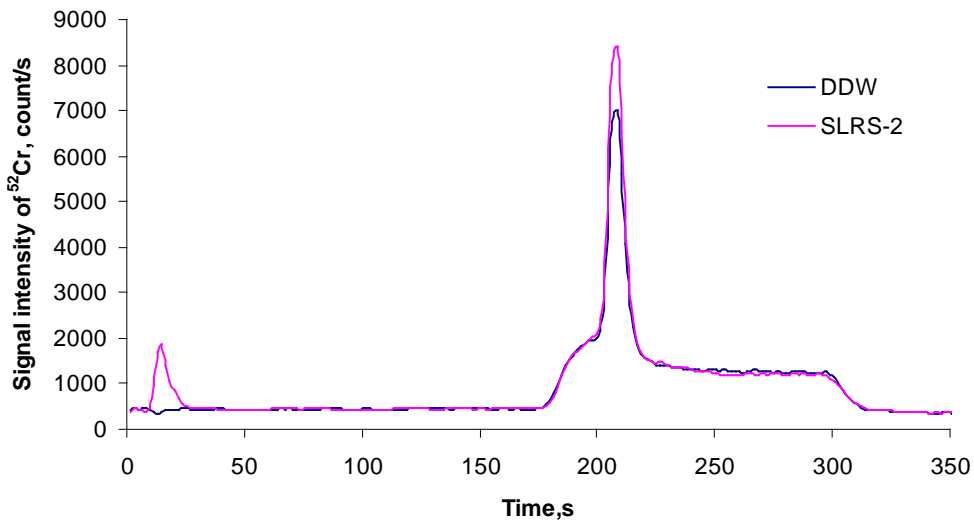


Figure 3.11. Stacked chromatograms of riverine water SLRS-2 and DDW.

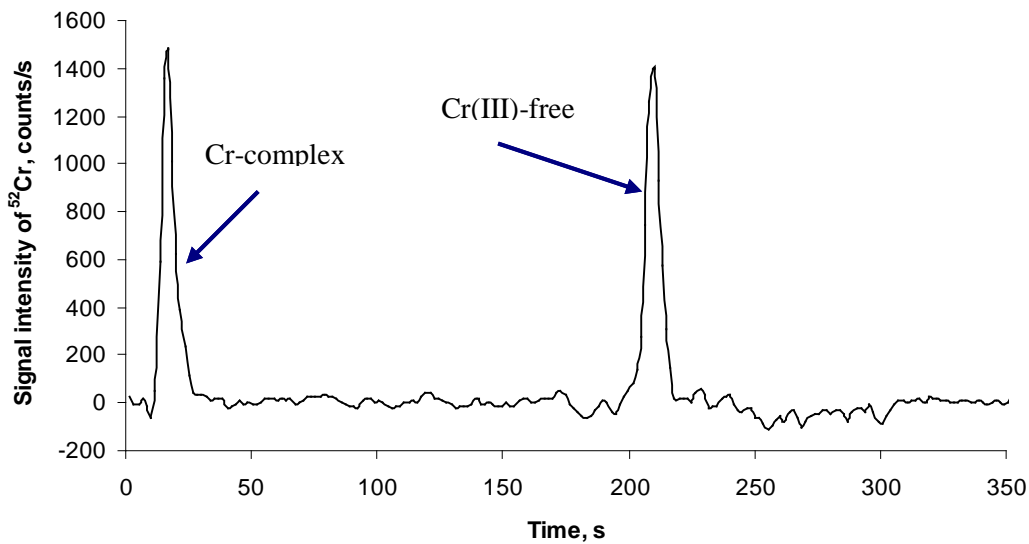


Figure 3.12. Typical blank-subtracted chromatogram for chromium speciation of riverine water SLRS-2.

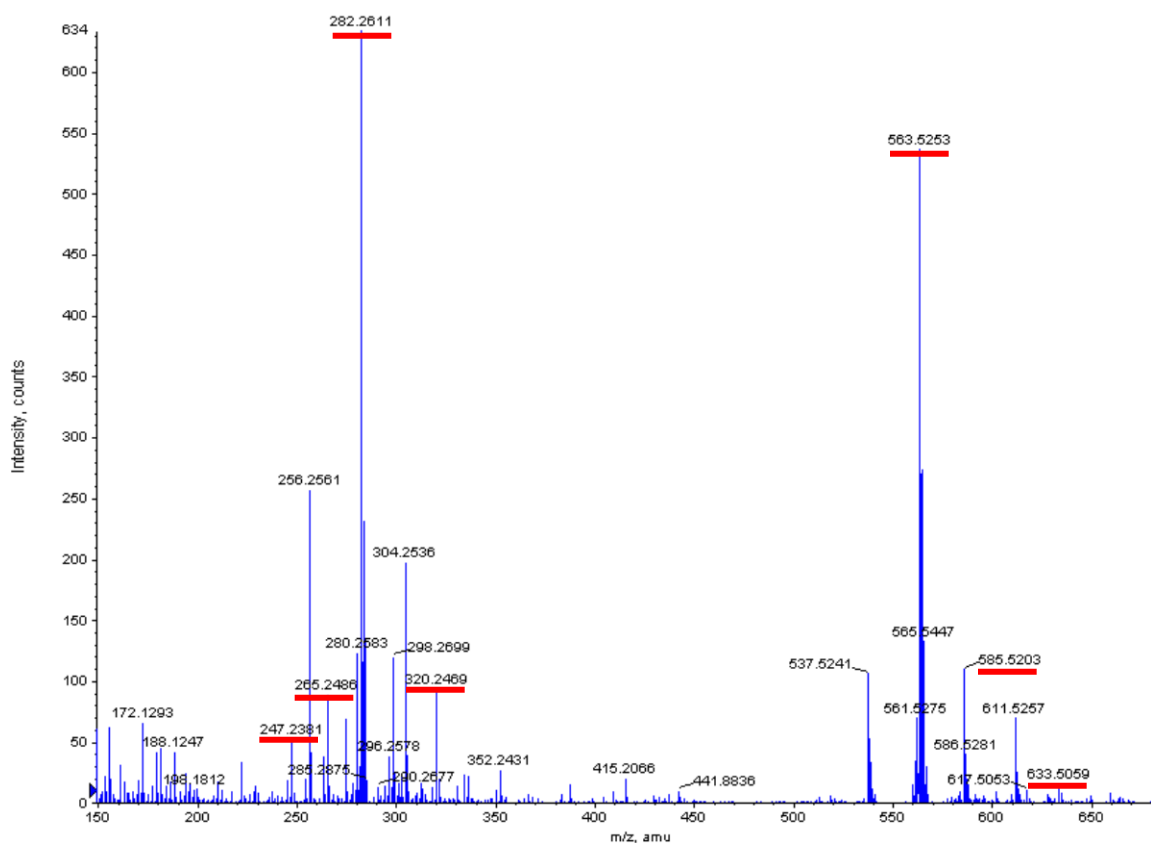
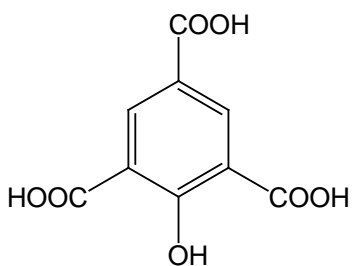


Figure 3.13. Electrospray mass spectrum of the fraction eluted at void time. The peaks that are underlined in red were tentatively assigned in Table 3.4.

Table 3.4. Tentative assignment of the peaks (m/z) on the mass spectrum in Figure 3.13*.

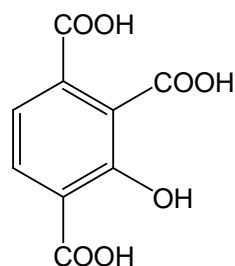
m/z observed	Assignment	
	Source Molecular structure	Molecular ions and adducts
247.2	A	$[A+K-H_2O]^+$
265.3	A	$[A+K]^+$
282.3	A	$[A+Fe]^+$
320.3	A	$[A+Fe+Cr]^+$
563.5	B	$[2B+Na]^+$
585.5	B+C	$[B+C+H]^+$
633.5	B+C	$[B+C+H+Cr]^+$

* The molecules that have the same formula weight were designated with one letter only.
The corresponding molecular structures are shown below.



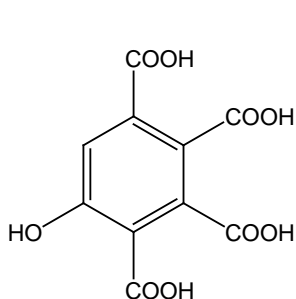
$C_9H_6O_7$
Exact Mass: 226.01
Mol. Wt.: 226.14
C, 47.80; H, 2.67; O, 49.53

A₁



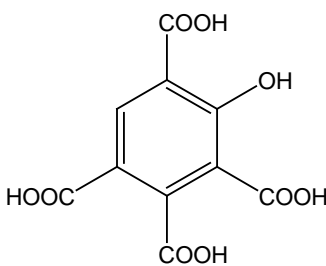
$C_9H_6O_7$
Exact Mass: 226.01
Mol. Wt.: 226.14
C, 47.80; H, 2.67; O, 49.53

A₂



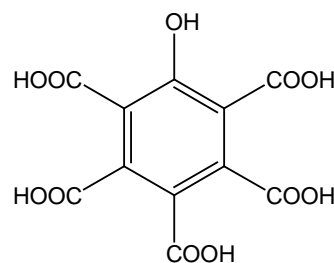
$C_{10}H_6O_9$
Exact Mass: 270.00
Mol. Wt.: 270.15
C, 44.46; H, 2.24; O, 53.30

B₁



$C_{10}H_6O_9$
Exact Mass: 270.00
Mol. Wt.: 270.15
C, 44.46; H, 2.24; O, 53.30

B₂



$C_{11}H_6O_{11}$
Exact Mass: 313.99
Mol. Wt.: 314.16
C, 42.05; H, 1.93; O, 56.02

C

Table 3.5. Concentrations ($\mu\text{g/L}$) of chromium species in SLRS-2 ($n = 3$).

	Cr-complex	Cr(III)	Cr total
Standard addition	0.28 ± 0.01	0.21 ± 0.03	0.49 ± 0.04
External calibration	0.14 ± 0.01	0.26 ± 0.01	0.41 ± 0.01
Batch analysis	---	---	0.46 ± 0.02
Reference value	NA	NA	0.45 ± 0.07

Two calibration procedures were used for chromium speciation analysis of SLRS-2: external calibration and standard addition. The total chromium concentration was determined using the same sample solutions employed for the standard addition procedure. Good linearity with correlation coefficient of over 0.999 was obtained for all the calibration curves. The results are summarized in Table 3.4. The sum of species concentrations obtained by standard addition and batch analysis are in agreement with the certified value at the 95% confidence level, while concentrations measured by external calibration were different at the 95% confidence level. Also, the difference is significant at the 95% confidence level for the concentrations measured for Cr-complex species with these two speciation methods. The data obtained for Cr-complex with standard addition are likely more accurate because the signal response of this chromium complex species may be affected (suppressed) by matrix effects caused by the many unretained components that elute at the void volume. Furthermore, the peak originating from Cr(VI) did not elute at the same time with SLRS-2 as with standard solutions. However, because both peaks were in the same mobile phase and close in retention time, the external calibration curve obtained with Cr(VI) standard solutions was used to quantify it in SLRS-2. Nonetheless, external calibration would be suitable for screening large numbers of samples.

3.3.7 Speciation analysis of chromium in tap water

Municipal water is the major drinking water source for people, so the quality of tap water can be closely related to people's health. In the case of chromium, usually only the total concentration is monitored to meet the regulations. For example, the U.S. Environmental Protection Agency (EPA) regulates the maximum concentration of total Cr in drinking

water to 50 µg/L [38]. As we stated before, due to the different physiological functions played by Cr(VI) and Cr(III), it may be necessary to determine the concentration of each species to evaluate the quality of tap water.

A typical chromatogram of an unspiked tap water sample for chromium speciation is shown in Figure 3.14. Upon spiking, the peak near the void time increased with addition of Cr(III), which was accompanied by the appearance of shoulders around the free Cr(III) peak, as was observed for carbonate-spiked DDW sample (Figure 3.6). In fact, many chromium complexes, whether inorganic, with carbonate and phosphate ions, or organic, with amino acid in biological samples or humic acid in soil or natural water samples, may elute near the void time with this anionic exchange column. For the tested tap water, which came from the municipal water system, carbonate is a likely binder for Cr(III).

Whatever the nature of the complex, it was calculated in combination with the third peak at about 205s, as the contribution from Cr(III). The matrix effect possibly arising from different mobile phases as carrier was neglected for simplification. The concentrations of each chromium species measured by the method of standard addition and by external calibration are summarized in Table 3.6. The values for Cr(III) are in agreement, while those for Cr(VI) only agree at the 99% confidence level. As in the case of SLRS-2, some matrix effect is likely the cause of the difference. A standard solution that is matrix-matched to tap water in terms of concentrations of the major ions, e.g. Na^+ , Ca^{+2} , Mg^{+2} , Cl^- , CO_3^{2-} , would likely be required to increase the accuracy of the external calibration method.

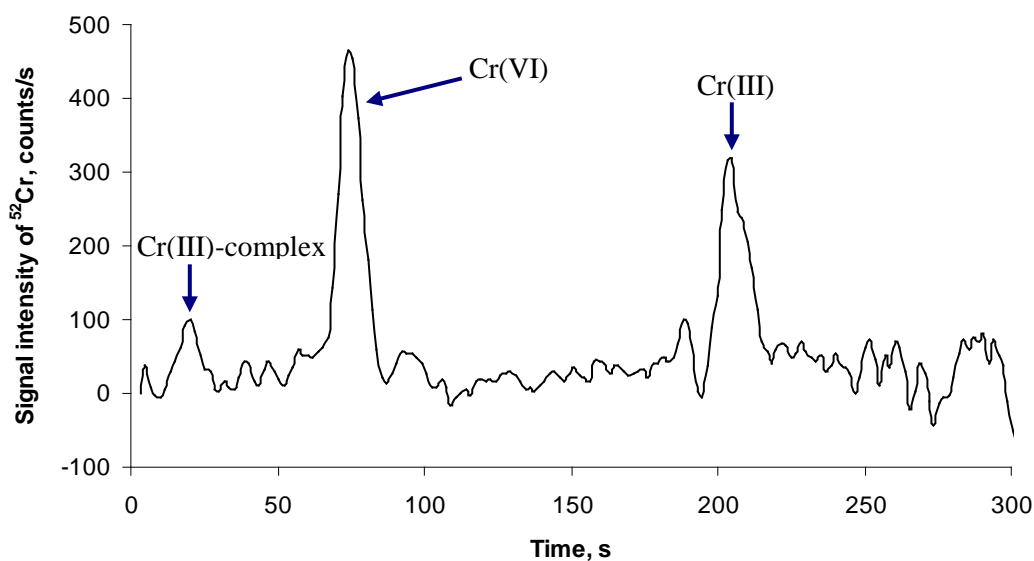


Figure 3.14. Typical blank-subtracted chromatogram for chromium speciation in an unspiked tap water sample.

Table 3.6. Measured concentrations ($\mu\text{g/L}$) of chromium species in tap water ($n = 3$).

Method	Cr(VI)	Cr(III)
External calibration	0.160 ± 0.007	0.080 ± 0.015
Standard addition	0.135 ± 0.009	0.080 ± 0.024

3.4 Summary

This work presents a facile procedure for chromium speciation at a sub $\mu\text{g/L}$ level by coupled IEC and ICP-MS. A guard column with dual ion exchange capability was used to

separate the oppositely charged chromium species with a gradient elution program that employed 0.1 M ammonium nitrate (MPA, pH = 4.0) and 0.8 M nitric acid (MPB) as mobile phases. They were separated directly, without adding complexing or charge switching agent, which is important for contamination control in trace analysis. The common problems with chromium speciation, e.g., precipitation of Cr(III) and reduction of Cr(VI) to Cr(III) were not observed with this chromatographic method. A full separation was achieved within 7.5 min, including a 3-min stabilization, which was shorter than comparable separation procedures [13, 15-17]. Using a micro-bore column would likely further reduce the analysis time. The performance of CRI on reducing the polyatomic interferences based on carbon and chlorine along with argon for Cr analysis was evaluated. The H₂ based CRI was shown to be capable of eliminating this type of interferences effectively. The accuracy of this analytical procedure was validated by speciation analysis of a riverine water SLRS-2 with certified total chromium concentration. It was finally applied successfully to the chromium speciation analysis of municipal water. Speciation analysis of Cr(VI) and Cr(III) is a challenging task for analytical chemists due to the potential interconversion of this redox pair during sample preparation and chromatographic separation. In this method development, the water samples are simple as to matrix composition and used directly without pretreatment. When applying this method to a more complex matrix that requires pretreatment to extract the species prior to HPLC separation, the stability of the Cr species should be evaluated. A species specific double spike isotope dilution (SSDID) approach can be used to account for redox species transformation [39-44]. Further application of the speciation procedure to kinetic studies will be described in the following chapter.

References

1. G. Darrie, *The importance of chromium in occupational health*, in *Trace element speciation for environment, food and health*, L. Ebdon, L. Pitts, R. Cornelis, H. Crews, O.F.X. Donard, and P. Quevauviller, Editors. 2001, The Royal Society of Chemistry: Cambridge, p315-330.
2. J. Kotas and Z. Stasicka, *Chromium occurrence in the environment and methods of its speciation*. *Environmental Pollution*, 107 (2000) 263-283.
3. E.J. Underwood, *Trace elements in human and animal nutrition*. 3rd edition ed. 1971, New York: Academic press.
4. J.P. Lafleur and E.D. Salin, *Speciation of Chromium by High-Performance Thin-Layer Chromatography with Direct Determination by Laser Ablation Inductively Coupled Plasma Mass Spectrometry*. *Analytical Chemistry*, 80 (2008) 6821-6823.
5. R.E. Wolf, J.M. Morrison and M.B. Goldhaber, *Simultaneous determination of Cr(iii) and Cr(vi) using reversed-phased ion-pairing liquid chromatography with dynamic reaction cell inductively coupled plasma mass spectrometry*. *Journal of analytical atomic spectrometry*, 22 (2007) 1051-1060.
6. Y.L. Chang and S.J. Jiang, *Determination of chromium in water and urine by reaction cell inductively coupled plasma mass spectrometry*. *Journal of analytical atomic spectrometry*, 16 (2001) 1434-1438.
7. Y.L. Chang and S.J. Jiang, *Determination of chromium species in water samples by liquid chromatography-inductively coupled plasma-dynamic reaction cell-mass spectrometry*. *Journal of analytical atomic spectrometry*, 16 (2001) 858-862.

8. K.R. Neubauer and W. Renter, *Perkin elmer application note #606780: chromium speciation in water by HPLC/ ICP-MS*. 2003.
9. H. Hagendorfer and W. Goessler, *Separation of chromium(III) and chromium(VI) by ion chromatography and an inductively coupled plasma mass spectrometer as element-selective detector*. *Talanta*, 76 (2008) 656-661.
10. C. Barnowski, N. Jakubowski, D. Stuewer, and J.A.C. Broekaert, *Speciation of chromium by direct coupling of ion exchange chromatography with inductively coupled plasma mass spectrometry*. *Journal of analytical atomic spectrometry*, 12 (1997) 1155-1161.
11. A.J. Bednar, R.A. Kirgan and W.T. Jones, *Comparison of standard and reaction cell inductively coupled plasma mass spectrometry in the determination of chromium and selenium species by HPLC-ICP-MS*. *Analytica Chimica Acta*, 632 (2009) 27-34.
12. F.A. Byrde, L.K. Olson, N.P. Vela, and J.A. Caruso, *Chromium Speciation by Anion-Exchange High-Performance Liquid-Chromatography with Both Inductively-Coupled Plasma-Atomic Emission Spectroscopic and Inductively-Coupled Plasma-Mass Spectrometric Detection*. *Journal of Chromatography A*, 712 (1995) 311-320.
13. F. Seby, S. Charles, M. Gagean, H. Garraud, and O.F.X. Donard, *Chromium speciation by hyphenation of high-performance liquid chromatography to inductively coupled plasma-mass spectrometry - study of the influence of interfering ions*. *Journal of analytical atomic spectrometry*, 18 (2003) 1386-1390.
14. A.P. Vonderheide, J. Meija, K. Tepperman, A. Puga, A.R. Pinhas, J.C. States, and

- J.A. Caruso, *Retention of Cr(III) by high-performance chelation ion chromatography interfaced to inductively-coupled plasma mass spectrometric detection with collision cell*. Journal of Chromatography A, 1024 (2004) 129-137.
15. Z. Chen, M. Megharaj and R. Naidu, *Removal of interferences in the speciation of chromium using an octopole reaction system in ion chromatography with inductively coupled plasma mass spectrometry*. Talanta, 73 (2007) 948-952.
 16. M. Leist, R. Leiser and A. Toms, *Low-level speciation of chromium in drinking waters using LC-ICP-MS*. Spectroscopy, (2006) 29-31.
 17. Y. Furusho, A. Sabarudin, L. Hakim, K. Oshita, M. Oshima, and S. Motomizu, *Automated Pretreatment System for the Speciation of Cr(III) and Cr(VI) Using Dual Mini-Columns Packed with Newly Synthesized Chitosan Resin and ME-03 Resin*. Analytical Sciences, 25 (2009) 51-56.
 18. S. Motomizu, K. Jitmanee and M. Oshima, *On-line collection/concentration of trace metals for spectroscopic detection via use of small-sized thin solid phase (STSP) column resin reactors. Application to speciation of Cr(III) and Cr(VI)*. Analytica Chimica Acta, 499 (2003) 149-155.
 19. C. Huang, *Determination of conditional stability constants using ion chromatography coupled with inductively coupled plasma mass spectrometry*, PhD thesis (2006), Queen's university.
 20. C. Huang and D. Beauchemin, *Simultaneous determination of two conditional stability constants by IC-ICP-MS*. Journal of analytical atomic spectrometry, 21 (2006) 1419-1422.
 21. C. Huang and D. Beauchemin, *A simple method based on IC-ICP-MS to deter-*

- mine conditional stability constants*. Journal of analytical atomic spectrometry, 21 (2006) 317-320.
22. H.G. Infante, K.V. Campenhout, R. Blust, and F.C. Adames, *Inductively coupled plasma time-of-flight mass spectrometry coupled to high-performance liquid chromatography for multi-elemental speciation analysis of metalloproteins in carp cytosols*. Journal of Analytical Atomic Spectrometry, (2002) 79-87.
 23. K. Neubauer, *Innovations in speciation analysis using HPLC with ICP-MS detection*. Spectroscopy, 23 (2008) 22-30.
 24. F. Laborda, M.P. Gorriz, E. Bolea, and J.R. Castillo, *Mathematical correction for polyatomic interferences in the speciation of chromium by liquid chromatography-inductively coupled plasma quadrupole mass spectrometry*. Spectrochimica Acta Part B-Atomic Spectroscopy, 61 (2006) 433-437.
 25. F. Vanhaecke, S. Saverwyns, G. De Wannemacker, L. Moens, and R. Dams, *Comparison of the application of higher mass resolution and cool plasma conditions to avoid spectral interferences in Cr(III)/Cr(VI) speciation by means of high-performance liquid chromatography - inductively coupled plasma mass spectrometry*. Analytical Chimica Acta, 419 (2000) 55-64.
 26. Z. Chen, M. Megharaj and R. Naidu, *Speciation of chromium in waste water using ion chromatography inductively coupled plasma mass spectrometry*. Talanta, 72 (2007) 394-400.
 27. N. Jakubowski, L. Moens and F. Vanhaecke, *Sector field mass spectrometers in ICP-MS*. Spectrochimica Acta Part B-Atomic Spectroscopy, 53 (1998) 1739-1763.

28. I. Kalinitchenko, X. Wang and B. Sturman, *Simple and effective control of spectral overlap interferences in ICP-MS*. Spectroscopy, (2008) 38-46.
29. <http://www.dionex.com/en-us/products/columns/ic-rfic/specialty/ionpac-as7/lp-73274.html>.
30. Varian 810/820MS customer training manual. 2009.
31. <http://www.varianinc.com/image/vimage/docs/products/spectr/icpms/brochure/si-0231.pdf>.
32. http://www.varianinc.com/image/vimage/docs/applications/apps/icpms_an1.pdf.
33. M. Fukushima, K. Nakayasu, S. Tanaka, and H. Nakamura, *Chromium(III) binding abilities of humic acids*. Analytica Chimica Acta, 317 (1995) 195-206.
34. M. Fukushima, K. Nakayasu, S. Tanaka, and H. Nakamura, *Speciation analysis of chromium after reduction of chromium(VI) by humic acid*. Toxicological & Environmental Chemistry, 62 (1997) 207-215.
35. E. Nakayama, H. Tokoro, T. Kuwamoto, and T. Fujinaga, *Dissolved State of Chromium in Seawater*. Nature, 290 (1981) 768-770.
36. J.M. Eckert, J.J. Stewart, T.D. Waite, R. Szymczak, and K.L. Williams, *Reduction of chromium(VI) at sub- μ g levels by fulvic-acid*. Analytica Chimica Acta, 236 (1990) 357-362.
37. J.A. Leenheer, C.E. Rostad, P.M. Gates, E.T. Furlong, and I. Ferrer, *Molecular resolution and fragmentation of fulvic acid by electrospray ionization/multistage tandem mass spectrometry*. Analytical Chemistry, 73 (2001) 1461-1471.
38. EPA, <http://www.epa.gov/safewater/contaminants/index.html#inorganic>, (2010).
39. D. Huo and H.M. Kingston, *Correction of Species Transformations in the Analy-*

- sis of Cr(VI) in Solid Environmental Samples Using Speciated Isotope Dilution Mass Spectrometry. Analytical Chemistry, 72 (2000) 5047-5054.*
40. D. Huo, Y. Lu, and H.M. Kingston, *Determination and Correction of Analytical Biases and Study on Chemical Mechanisms in the Analysis of Cr(VI) in Soil Samples Using EPA Protocols. Environmental Science and Technology, 32 (1998) 3418-3423.*
 41. H.M. Kingston, R. Cain, D. Huo, and G.M.M. Rahman, *Determination and evaluation of hexavalent chromium in power plant coal combustion by-products and cost-effective environmental remediation solutions using acid mine drainage. Journal of Environmental Monitoring, 7 (2005) 899-905.*
 42. H.M. Kingston, D. Huo, Y. Lu, and S. Chalk, *Accuracy in species analysis: speciated isotope dilution mass spectrometry (SIDMS) exemplified by the evaluation of chromium species. Spectrochimica Acta, Part B: Atomic Spectroscopy, 53B (1998) 299-309.*
 43. L. Yang, E. Ciceri, Z. Mester, and R.E. Sturgeon, *Application of double-spike isotope dilution for the accurate determination of Cr(III), Cr(VI) and total Cr in yeast. Analytical and Bioanalytical Chemistry, 386 (2006) 1673-1680.*
 44. L. Yang, S. Willie, and R.E. Sturgeon, *Determination of total chromium in seawater with isotope dilution sector field ICP-MS following on-line matrix separation. Journal of Analytical Atomic Spectrometry, 24 (2009) 958-963.*

Chapter 4

Kinetics study of the reduction of Cr(VI) in natural water with IEC-ICP-MS

4.1 Introduction

In Chapter 3, a simple method for chromium speciation analysis at trace level was described, whose accuracy was verified through the speciation analysis of riverine water SLRS-2 with a certified total chromium concentration. The chromatogram of this water sample showed a peak at the void time instead of at the expected elution time of the Cr(VI) peak. This water CRM was acidified to pH 1.3 for the stabilization of metal species. This relatively acidic condition increases the reduction potential of Cr(VI) and thus its ability to be reduced in presence of natural reducing agents. To test this hypothesis, the riverine water was spiked either with Cr(VI) or with Cr(VI)/Cr(III) and the evolution of each chromium species was monitored temporally by speciation analysis. The peak corresponding to Cr(VI) decreased in size with time, as the peak at the void time increased proportionately. This observation prompted the idea to study the reduction kinetics of Cr(VI) in natural water assisted with online speciation analysis.

As described in the introduction of Chapter 3, the major oxidation states of chromium, Cr(VI) and Cr(III) possess very different physical, chemical properties and toxicological properties. The redox system of Cr(VI) and Cr(III) has been extensively studied to assess the fate of either Cr form in the environment, i.e., the mobility, transformation and bio-

availability, and humic substances (humics) are generally recognized to be involved in the reduction of Cr(VI) [1-12]. Humics are complex mixtures of biogenic aromatic molecules that are extensively substituted with carboxyl and phenolate groups, which are further classified into three sub-groups, i.e., humic acid (HA), fulvic acid (FA) and humin [11]. Humics can bind to multiple metal ions as well as possess a reducing capability due to the numerous oxygen-containing functions. The reduction mechanism, however, is not fully understood. The concentration of humics in natural waters is in the range of 0.1-200 mg/L [13]. A transient species of Cr(V) was found by electron paramagnetic resonance (EPR) by Goodgame *et al* [4] during a study of the interaction of humic acid and Cr(VI), which eventually decayed to Cr(III). The amount of this Cr(V) species increased as the pH was lowered, suggesting a higher reaction rate under more acidic conditions. The reaction was proposed to start with the complexation of Cr(VI) to un-defined binding sites of HA (due to the complexity of HA). The acidity affected the protonation state of binding sites and thus the interaction process. Similar results were reported for different types of humic acids [4].

The study of the reduction of Cr(VI) has been mainly focused on the reaction kinetics. Nakayama *et al.* [14] studied the chromium redox process (or circulation of chromium as they called it) through selective co-precipitation of Cr(VI) with bismuth hydroxide to separate Cr(VI) from Cr(III). The precipitate was collected and re-dissolved in nitric acid prior to flameless atomic absorption analysis [14]. A revised co-precipitation technique was adopted by Eckert *et al.* [2] to study the reduction of Cr(VI) at a sub- $\mu\text{g/L}$ level by fulvic acid and in natural river water. In their work, ^{51}Cr -labelled Cr(VI) was precipitated

by a cobalt tetramethylenedithiocarbamate carrier complex (Co-PDC), the precipitate was collected, re-dissolved in nitric acid, and then submitted for γ analysis [2]. The colorimetric reaction of Cr(VI) with diphenylcarbazide (DPC) [15] was used by Wittbroadt and Palmer to determine the concentration of Cr(VI) during the reduction process by fulvic acids [10] and humic acids [11]. In their procedure, 0.5-mL aliquots of sample, intermittently taken from the reaction reservoir, were mixed with 0.1 mL of DPC and 2.0 mL of 0.1 N H₂SO₄. The solutions were then filtered through 0.1- μ m polysulfonate filter. The absorbance of the solutions at 540 nm was measured 10 minutes after the addition of DPC. The evolution of Cr(III) species was addressed by Fukushima *et al.* [3] through the speciation analysis of chromium after reduction of Cr(VI) by humic acid. In their studies, the concentration of Cr(VI) in a test solution (containing 50 μ M and 40 mg/L of HA) was measured by the colorimetric method with DPC. The solution was then passed through a cationic column (C-25) to separate Cr(III), which was retained on the column, from Cr(VI) and Cr(III)-HA, which passed through. The total concentrations of Cr(VI) and Cr(III) in the C-25 eluent were then determined by atomic absorption spectrometry [3]. The concentration of Cr(III)-HA was then calculated by subtracting the Cr(VI) concentration (as determined by colorimetric reaction) from the total Cr concentration in the C-25 eluent.

The above procedures generally involve offline separations, which are tedious, time consuming and prone to contaminations, in turn lowering sample frequency by taking hours to days. The reduction of Cr(VI) has been shown to involve a nonlinear decline featuring a rapid drop at the beginning of the reaction. However, the behaviour of the initial reac-

tion has rarely been investigated, likely because of limitations of the available speciation methods. This may also account for the lack of reaction kinetics study under very acidic conditions, where the reaction proceeds faster.

In this work, the speciation method developed in Chapter 3, which combines IEC separation with online ICP-MS detection was adopted to study the reaction kinetics of Cr(VI) in a natural water sample. This method features the advantages of small sample consumption, minimal sample manipulation, and easy data interpretation.

4.2 Experimental

4.2.1 Instrumentation and procedure

The same Cr speciation analysis conditions as described in Chapter 3 (see *section 3.2 Experimental*) were used for this kinetic study and will not be repeated here.

Both IEC and ICP-MS systems were optimized and stabilized. The column was cleaned thoroughly with the procedure described in Chapter 3 (see *section 3.2.1.1 IEC*). Chromatograms with good repeatability as to retention time, peak width and peak height were obtained for a standard solution containing 20 µg/L of Cr(VI) and Cr(III). The sample loop was cleaned first with 1% nitric acid then with DDW. The chromatograms of repeated DDW injections were monitored to make sure there was no carry-over Cr species. Then the chromatogram of the unspiked riverine water sample was acquired. The riverine water sample was spiked with Cr(VI) or with Cr(VI)/Cr(III), 20 µg/L of each species, using the stock metal standard solution(s). Acidity of the riverine water was adjusted

with ultrapure nitric acid and ammonium hydroxide. Time counting started upon spiking with Cr species. The time-dependent reaction was monitored over 2 hours. A separate speciation analysis was done after four days.

4.2.2 Data analysis

Peak integration was performed with QBASIC. Peak areas from the original riverine water were subtracted from those of the spiked riverine water. An Excel spreadsheet was used to generate 2-D chromatograms and regression lines. The 3-D chromatograms and non-linear fitting curves were generated with OriginPro8.0®.

4.4 Results and discussion

4.4.1 Evolution of Cr(VI) spike in SLRS-2

Chromatograms displaying the evolution of the Cr(VI), Cr(III) and Cr(III)-complex species (referred as Cr(III)-com hereafter) are shown in Figure 4.1. The original riverine water without chromium spiking was also included. As time went by, the size of the Cr(VI) peak decreased, which was accompanied by the growth of Cr(III)-com and Cr(III) peaks. In fact, the total Cr peak area kept relatively constant over time following the spiking.

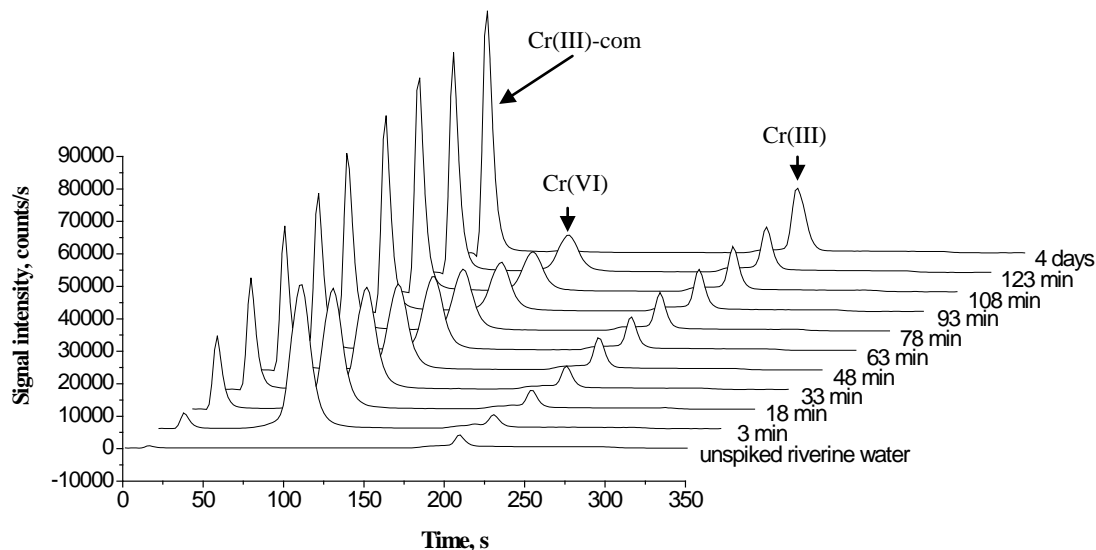


Figure 4.1. IEC-ICP-MS chromatograms showing the time-dependent reduction of Cr(VI) in riverine water sample SLRS-2 (pH = 1.3; ambient temperature = 20 °C, monitored isotope m/z 52). The peaks in the elution sequence are Cr(III)-com, Cr(VI) and Cr(III). The time interval of each speciation analysis is indicated next to each chromatogram.

The change in Cr(VI) level was abrupt at the beginning, following the spiking, and slowed down afterwards. By the fourth day, the Cr(VI) peak disappeared completely. The growth of Cr(III)-com peak followed a similar trend, but in the opposite direction. The growth in Cr(III) peak was much smaller than for the other species.

Figure 4.2 shows plots of peak areas versus time for each chromium species. The level of each species changed as a function of time in a non-linear fashion, that of Cr(VI) and Cr(III)-com changing faster than that of Cr(III). This indicates that both Cr(III)-com and Cr(III) originated from Cr(VI), as there was no external source of these species during this experiment.

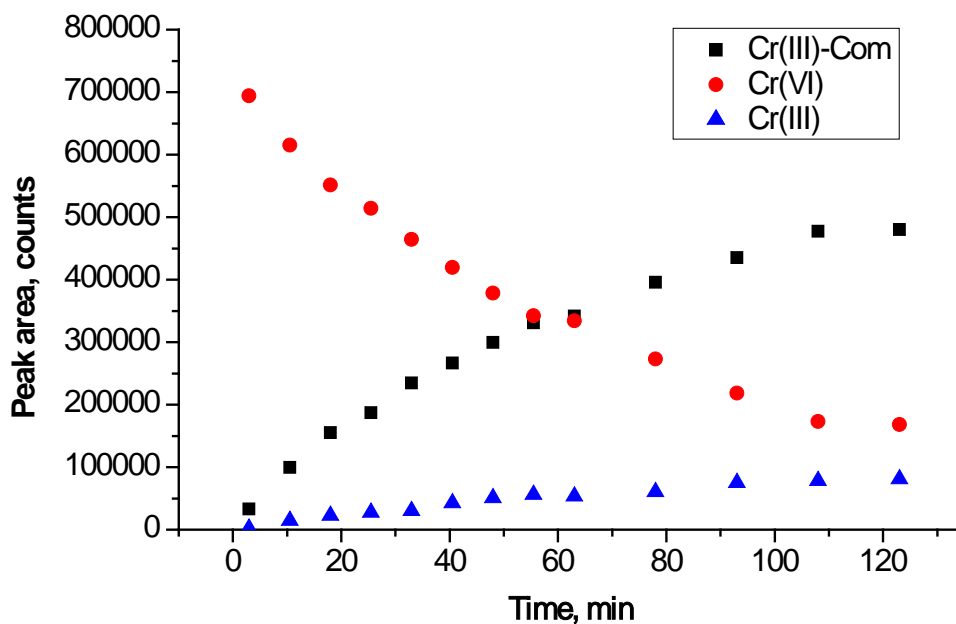
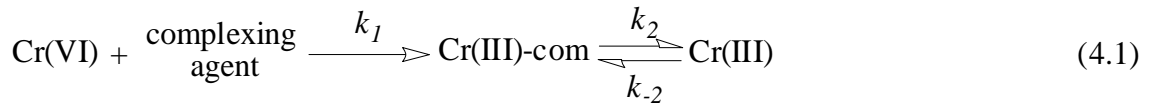


Figure 4.2. Plot of peak area vs. time illustrating the time-dependent evolution of chromium species in riverine water.

As the reduction of Cr(VI) in humic acid [11], fulvic acid [10] and a natural water [2] was reported to be pseudo first order, the reduction of Cr(VI) was assumed to be a pseudo first order reaction in view of the fact that reducing reagents, e.g. humics, would be in large excess relative to the spiked chromium amount. Taking into account that the equilibrium between Cr(III)-HA and Cr(III) has been shown to be a slow process [16], the postulated overall reaction can be expressed as:



As the reduction product may actually be an intermediate that partially dissociates into Cr(III), derivation of the rate constant was based on the concentration change of the starting analyte, Cr(VI). Suppose the concentration of Cr(VI) is c_0 at the beginning of the reaction ($t = 0$) and x after time t , then the rate of the change is $d(c_0-x)/dt$. Thus, for a first order reaction:

$$\frac{d(c_0 - x)}{dt} = k_1 x \quad (4.2)$$

Integration following separation of the variables yields:

$$-\ln x = k_1 t + C \quad (4.3)$$

where C is a constant of the integration. The value of C can be obtained by taking into account the boundary condition, i.e. when $t = 0$, $x = c_0$; therefore

$$-\ln c_0 = C \quad (4.4)$$

Substituting Equation (4.4) into Equation (4.3) yields:

$$\ln \frac{x}{c_0} = -k_1 t \quad (4.5)$$

Figure 4.3 shows the plot of $\ln(x/c_0)$ vs time, from which a linear regression curve with r^2 of 0.995 is obtained. Therefore, the assumption of pseudo first order reduction of Cr(VI) in SLRS-2 was justified. The rate constant k was extracted from the regression equation to be $(1.313 \pm 0.015) \times 10^{-2} \text{ min}^{-1}$ or $(2.189 \pm 0.025) \times 10^{-4} \text{ s}^{-1}$.

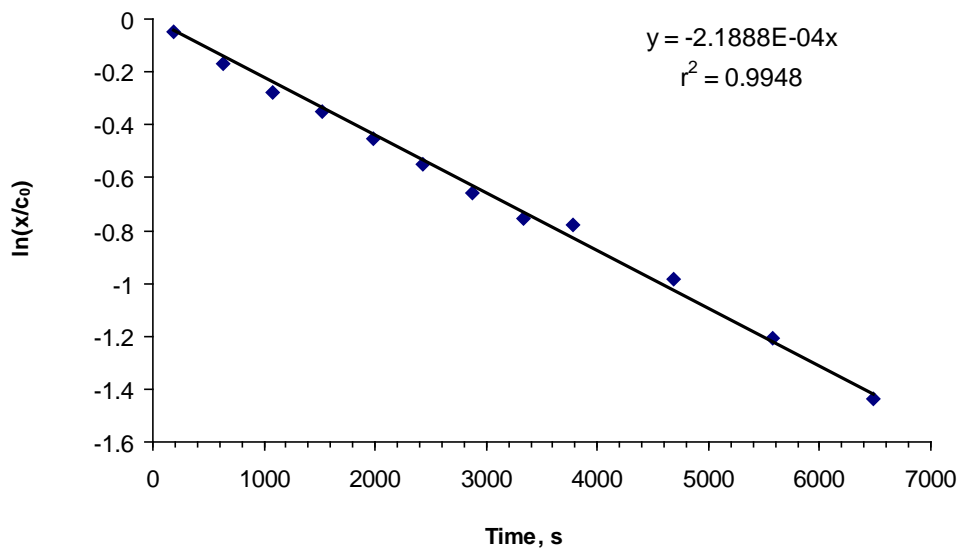


Figure 4.3. Plots of $\ln(x/c_0)$ versus time to determine reaction rate constant k in s^{-1} with linear regression.

Values of reaction rate constant in the literature are not always consistent, largely due to the various working conditions adopted by different researchers, such as the nature and concentration of the reducing reagent(s), the amount of Cr species spiked, the pH and the temperature. Table 4.1 compares previous selected results from the literature with the one determined in this work. Evidently, the latter is most similar to the results obtained with lake water, likely because this matrix resembles that of river water.

Table 4.1. Comparison of rate constants obtained for the reduction of Cr(VI)

No.	Reaction media	Concentration of Cr(VI) spike	Temperature, °C	pH	Reaction rate constant, s ⁻¹	Reference
1	Fulvic acid, 8 µM	0.5 µg/L	20	2.0	3.33×10^{-5}	[2]
2	Fulvic acid, 8 µM	0.5 µg/L	25	2.0	5.28×10^{-5}	[2]
3	Lake water	0.5 µg/L	25	2.0	1.61×10^{-4}	[2]
4	Lake water	0.5 µg/L	25	3.9	1.11×10^{-4}	[2]
5	Humic acid, 40 mg/L	50 µM	25	3.2	7.53×10^{-7}	[3]
6	Humic acid, 40 mg/L	50 µM	25	4.0	5.92×10^{-7}	[3]
7	Riverine water	20 µg/L	20	1.3	2.19×10^{-4}	This work

In contrast to Cr(VI), the overall reaction kinetics of Cr(III)-com and Cr(III) do not follow a definite order. A semi-empirical approach was thus used in an attempt to describe the reaction kinetics. Specifically, curves were fitted to the available data points for all three Cr species, and reaction rate constants of Cr(III)-com and Cr(III) were estimated by comparison to that of Cr(VI) with known values. The fitting curves and the parameters

for the fitting equation ($x = x_0 + A \cdot \exp(-t/b)$) are shown in Figure 4.4 and Table 4.2 respectively. For Cr(VI), x_0 is close to c_0 , and the reciprocal of b , which is $(2.37 \pm 0.18) \times 10^{-4}$ agrees with the rate constant obtained by assuming a pseudo first order reaction. The A value of Cr(III)-com is of the same order of magnitude as that of Cr(VI), so the reaction rate constant can be estimated as the reciprocal of $1/b$, which is $(2.43 \pm 0.03) \times 10^{-4}$. As the A value of Cr(III)-com is smaller than that of Cr(VI), the actual rate constant should be larger. The rate constant of Cr(III) is difficult to estimate from this fitting curve approach as its A value differs substantially from that of Cr(VI).

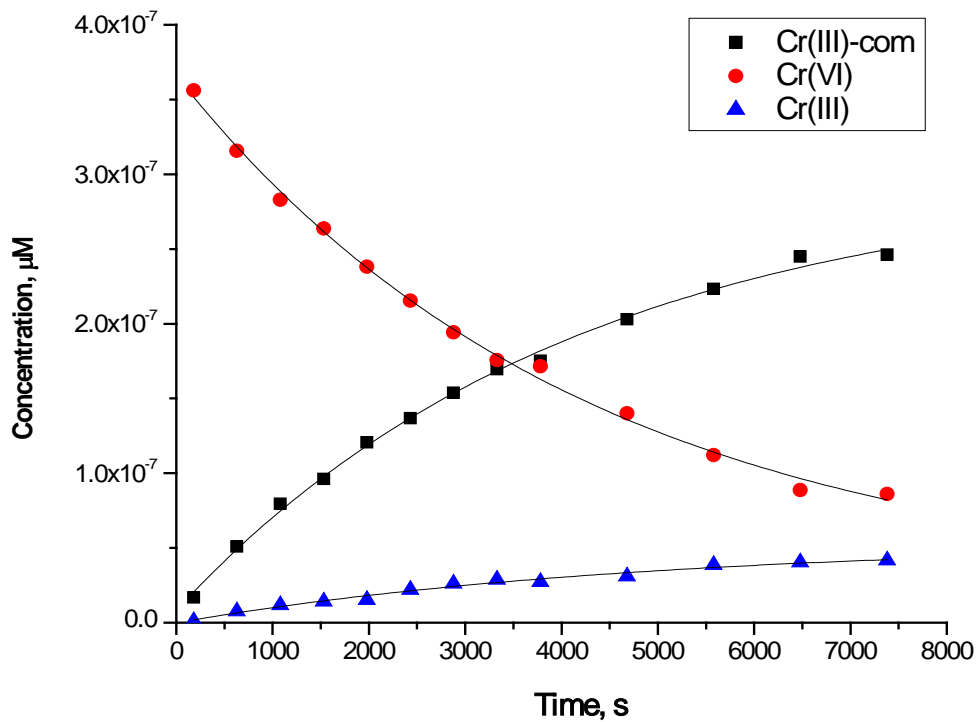


Figure 4.4. The best fitting curves showing the time dependent behaviour of each Cr species during the process of Cr(VI) reduction in riverine water.

Table 4.2. Parameters extracted from the fitting curve expressions for Cr species

Cr species	Parameters	Value	Standard error	Adjusted r^2
Cr(VI)	x_0	2.2E-8	1.2E-8	0.997
	A	3.44E-7	1.1E-8	
	b	4240	320	
Cr(III)-com	x_0	2.988E-7	9.6E-9	0.997
	A	-2.905E-7	8.1E-9	
	b	4150	290	
Cr(III)	x_0	5.37E-8	5.5E-9	0.982
	A	-5.38E-8	4.7E-9	
	b	4790	950	

4.4.2 Reduction of Cr(VI) in presence of Cr(III)

4.4.2.1 Evolution of Cr(VI) spike in presence of a similar Cr(III) concentration

In section 4.4.1, the amount of Cr(III) that was present in the riverine water was very small compared to the 20 $\mu\text{g/L}$ Cr(VI) that was added. As Cr(III) is one of the reduction products, the effect of Cr(III) on the reduction rate of Cr(VI) was also studied. Figure 4.5 are the offset positioned chromatograms displaying the time dependent decay of 20 $\mu\text{g/L}$ Cr(VI) in riverine water in the presence of 20 $\mu\text{g/L}$ Cr(III). All chromium species behaved similarly to when only Cr(VI) was spiked (see Figure 4.1). The change of Cr(III) was less obvious than that without external Cr(III) spike because the amount of Cr(III) was much larger than that *in situ* generated.

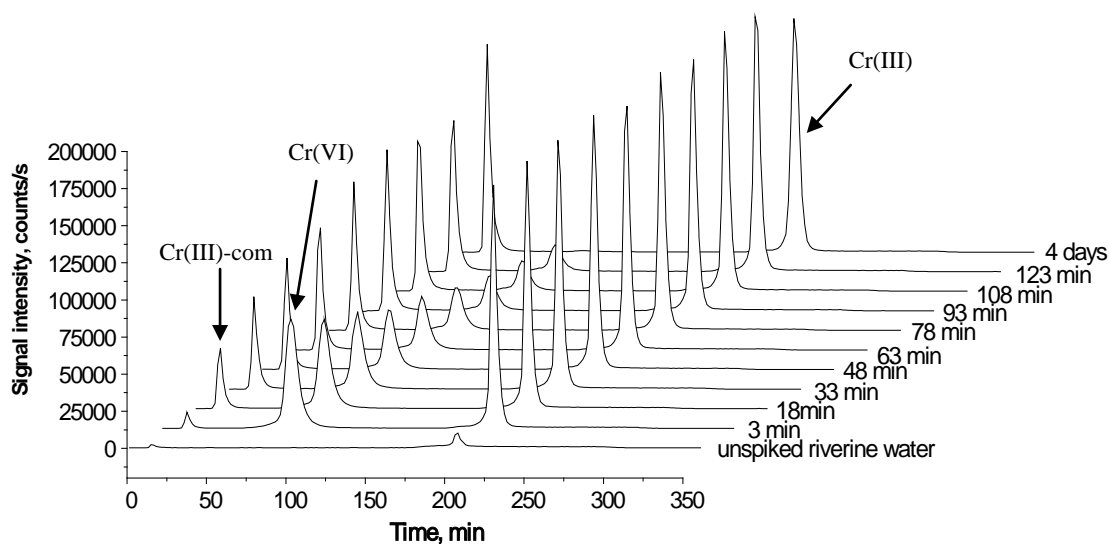


Figure 4.5. IEC-ICP-MS chromatograms showing the time dependent reduction of Cr(VI) in riverine water SLRS-2 (pH = 1.3; ambient temperature = 20 °C) in presence of Cr(III, monitored isotope m/z 52). The peaks in the elution sequence are Cr(III)-com, Cr(VI) and Cr(III). The time interval of each speciation analysis is indicated next to each chromatogram.

With the same treatment as that for Cr(VI) reduction without Cr(III), the reduction rate constant is calculated to be $(1.254 \pm 0.010) \times 10^{-2} \text{ min}^{-1}$ or $(2.090 \pm 0.017) \times 10^{-4} \text{ s}^{-1}$. A Student's t-test showed that it differed significantly at the 95% confidence level from the rate constant obtained without Cr(III), which is not surprising as Cr(III) being on the product side of the reaction would tend to shift the equilibrium towards the reactant side, following Le Châtelier's principle. Nonetheless, the difference is relatively small (less than 10%), indicating that Cr(III) does not have a significant involvement in the reduction of Cr(VI), in agreement with observations made in the literature during a study of the reaction of Cr(VI) with phenol compounds to simulate natural organic and humic matter [17]. Furthermore, this observation in turn indicates that Cr(III), as a reduction product,

results mainly, if not completely, from the dissociation of Cr-com instead of from the direct reduction of Cr(VI) in this case.

4.4.2.2 Effect of pH and temperature

To assess the effect of pH, the pH of the riverine water sample was adjusted to 2.3 with concentrated ammonium hydroxide and spiked with 20 $\mu\text{g/L}$ each of both Cr(VI) and Cr(III) prior to time-dependent speciation analysis. Figure 4.6 compares the linear regression curves obtained under these two pH conditions.

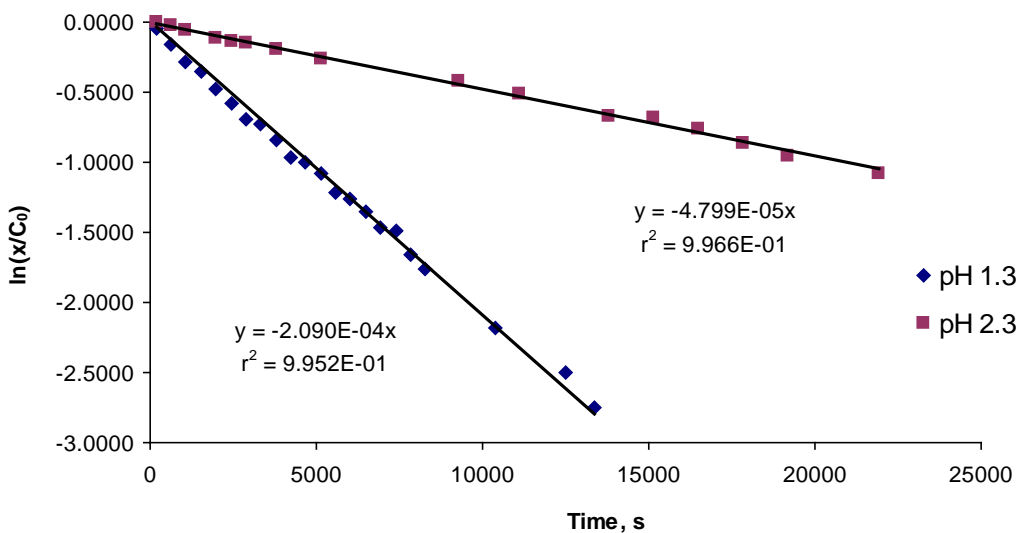


Figure 4.6. Plots of $\ln(x/c_0)$ vs. time in second and linear regression curves under pH 1.3 and pH 2.3 as labelled.

The effect of temperature on the reduction of Cr(VI) was tested with time-dependent speciation analysis at 20 °C, 25 °C and 30 °C, with pH constant at 1.3. The rate constants obtained are summarised in Table 4.3.

Apparently, both the acidity and temperature of the reaction medium exert a significant influence on the reaction rate of Cr(VI) in riverine water. The rate of reduction of Cr(VI) increased with a decrease in pH and with an increase in temperature. An Arrhenius plot of the data at pH 1.3 yields an activation energy of (139.1 ± 7.0) kJ/mol (Figure 4.7). This value is much larger than that reported for the reduction of Cr(VI) with fulvic acid, which is 31 ± 6 kJ/mol. This is not surprising since the reduction conditions (i.e. Cr(VI) concentration, pH, temperature, etc.) and the amount and nature of reducing agents were different.

Table 4.3. Rate constants under different reaction conditions for the reduction of Cr(VI) in riverine water SLRS-2. The initial spiking concentration of Cr(VI)/Cr(III) is 20 μ g/L (or 0.385 μ M) each.

	20 °C		25 °C		30 °C	
	k, $\times 10^4$ s ⁻¹	r ²	k, s ⁻¹	r ²	k, s ⁻¹	r ²
pH = 1.3	2.090 \pm 0.017	0.995	5.010 \pm 0.037	0.996	13.75 \pm 0.20	0.994
pH = 2.3	0.480 \pm 0.005	0.997	n/a		n/a	

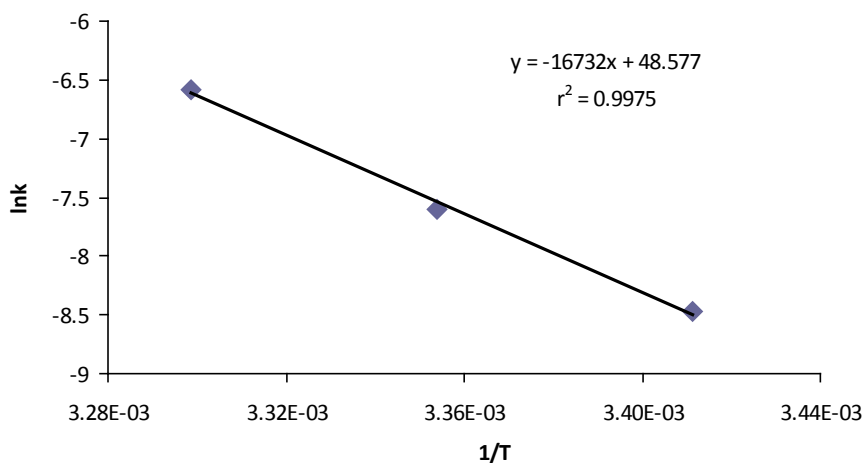


Figure 4.7. Plot of $\ln k$ vs. $1/T$ (in Kelvin) and linear regression treatment to calculate the activation energy.

4.5 Summary

In this work, the chromium speciation method using hyphenated IEC and ICP-MS was used to characterize the reduction kinetics of Cr(VI) in riverine water SLRS-2. The reduction of Cr(VI) behaved as a pseudo first order reaction. The rate constant was extracted as the slope by linear regression treatment of the logarithm of the ratio of the instant concentration of Cr(VI) to its original concentration as the function of time. The rate constant increased with increasing temperature and decreasing pH, in agreement with the literature. The presence of Cr(III) in the reaction medium did not affect the reduction rate constant of Cr(VI) significantly, indicating that the Cr(III) observed arises mainly from the dissociation of Cr(III)-com, instead of being generated directly from Cr(VI). Overall, no specific reaction order could be assigned for Cr(III)-com and Cr(III). Nonetheless, this work presents a simple online procedure to study reaction kinetics (within the time

scale of IEC), which features minimal sample manipulation as well as easy data interpretation. One drawback may be a relatively higher instrument cost compared to previously used approaches.

References

1. S.L. Boyko and D.M.L. Goodgame, *The interaction of soil fulvic acid and chromium(VI) produces relatively long-lived, water soluble chromium(V) species*. Inorganica Chimica Acta, 123 (1986) 189-191.
2. J.M. Eckert, J.J. Stewart, T.D. Waite, R. Szymczak, and K.L. Williams, *Reduction of chromium(VI) at sub-micro g/L levels by fulvic acid*. Analytica Chimica Acta, 236 (1990) 357-362.
3. M. Fukushima, K. Nakayasu, S. Tanaka, and H. Nakamura, *Speciation analysis of chromium after reduction of chromium(VI) by humic acid*. Toxicological & Environmental Chemistry, 62 (1997) 207-215.
4. D.M.L. Goodgame, P.B. Hayman and D.E. Hathway, *Formation of water-soluble chromium(V) by the interaction of humic acid and the carcinogen chromium(VI)*. Inorganica Chimica Acta, 91 (1984) 113-115.
5. S.E. Kaczynski and R.J. Kieber, *Hydrophobic C18 Bound Organic Complexes of Chromium and Their Potential Impact on the Geochemistry of Cr in Natural Waters*. Environmental Science & Technology, 28 (1994) 799-804.
6. R.J. Kieber and G.R. Helz, *Indirect photoreduction of aqueous chromium(VI)*.

Environmental Science & Technology, 26 (1992) 307-312.

7. T. Liu, P. Rao and I.M.C. Lo, *Influences of humic acid, bicarbonate and calcium on Cr(VI) reductive removal by zero-valent iron*. Science of the Total Environment, 407 (2009) 3407-3414.
8. T. Liu, D.C.W. Tsang and I.M.C. Lo, *Chromium(VI) Reduction Kinetics by Zero-Valent Iron in Moderately Hard Water with Humic Acid: Iron Dissolution and Humic Acid Adsorption*. Environmental Science & Technology, 42 (2008) 2092-2098.
9. C.D. Palmer and P.R. Wittbrodt, *Processes affecting the remediation of chromium contaminated sites*. Environmental Health Perspectives, 92 (1991) 25-40.
10. P.R. Wittbrodt and C.D. Palmer, *Reduction of Cr(VI) in the Presence of Excess Soil Fulvic Acid*. Environmental Science & Technology, 29 (1995) 255-263.
11. P.R. Wittbrodt and C.D. Palmer, *Reduction of Cr(VI) by soil humic acids*. European Journal of Soil Science, 48 (1997) 151-162.
12. D.M. Zhilin, P. Schmitt-Kopplin and I.V. Perminova, *Reduction of Cr(VI) by peat and coal humic substances*. Environmental Chemistry Letters, 2 (2004) 141-145.
13. D.G. Kinniburgh, C.J. Milne, M.F. Benedetti, J.P. Pinheiro, J. Filius, L.K. Koopal, and W.H. Van Riemsdijk, *Metal Ion Binding by Humic Acid: Application of the NICA-Donnan Model*. Environmental Science & Technology, 30 (1996) 1687-1698.
14. E. Nakayama, H. Tokoro, T. Kuwamoto, and T. Fujinaga, *Dissolved state of chromium in seawater*. Nature (London), 290 (1981) 768-770.

15. R.T. Pflaum and L.C. Howick, *The chromium-diphenylcarbazide reaction*. Journal of the American Chemical Society, 78 (1956) 4862-4866.
16. M. Fukushima, K. Nakayasu, S. Tanaka, and H. Nakamura, *Chromium(III) binding abilities of humic acids*. Analytica Chimica Acta, 317 (1995) 195-206.
17. M.S. Elovitz and W. Fish, *Redox Interactions of Cr(VI) and Substituted Phenols: Kinetic Investigation*. Environmental Science & Technology, 28 (1994) 2161-2169.

Chapter 5

General discussion

Hyphenated HPLC-ICP-MS has been established as the leading instrumental technique in speciation analysis, in which HPLC and ICP-MS act as the sample introduction system and the element-specific detector respectively. ICP-MS offers the advantages of multi-element and isotope measurement capabilities, high sensitivity, low detection limits and large linear dynamic range, making it practically the default detector for speciation analysis. HPLC offers great versatility in separating chemical mixtures through a careful selection of stationary and mobile phases, temperature and pH [1]. IEC is most common in combination with ICP-MS due to the naturally ionic character of most elemental species as well as the better compatibility of column eluents with ICP-MS detection.

The physical hyphenation of HPLC and ICP-MS is straightforward, by connecting the outlet of the HPLC system to the liquid inlet of the ICP-MS nebulizer, without the need for a specially designed interface as required when hyphenating GC and CE to ICP-MS. However, there are two major factors of concern for an adequate hyphenation: (1) match up of the eluent flow rate with the sample uptake rate of the nebulizer, and (2) selection of an ICP-MS compatible eluent. The mobile phase flow rate of 0.2-1.5 mL/min, for typical HPLC separations, corresponds to the sample uptake rate of the conventional sample introduction system of ICP-MS. Low flow rate HPLC requires the use of a micro-nebulizer with small-volume spray chamber or of some DIN to minimize the dead vol-

ume. The mobile phase for HPLC separations often contains a relatively high concentration of dissolved salts and/or volatile organic solvents, which may be problematic for ICP-MS detection. Indeed, the matrix may affect ICP-MS performance by introducing spectroscopic and non-spectroscopic interferences as well as causing analyte signal drift and loss of sensitivity from soot and salt deposition on the interface cones and ion optics. A few approaches have been adopted to tackle these matrix effects, which fall into two groups: (1) reducing the total amount of eluent uptake, such as by using a flow splitter or a low flow rate HPLC, and (2) alleviating the detrimental effect of organic matter, such as by titrating oxygen to assist the complete combustion of organic solvent or selecting electrolytes that form volatile compounds or decompose into gaseous components in the plasma.

5.1 Selection of mobile phases

In this work, ammonium nitrate and nitric acid were chosen as the mobile phases for IEC separations. The distinct advantages of these compounds include (1) complete dissociation into gaseous species in the plasma, so as to avoid the problem of salt deposition on the interface cone and/or ion optics and (2) introduction of no other elements into ICP-MS than those originally present in water and air. For ammonium nitrate, a solution of high purity can easily be prepared by mixing high purity nitric acid and ammonium hydroxide in DDW, with pH being readily adjusted with these acid and base. Also, the eluent strength of ammonium nitrate solution was found to be independent of pH, which was an advantage during the separation of As species with a pH gradient of ammonium nitrate

solution according to the protonation states of the species to improve selectivity [2].

In the experiments to determine the stability constant of Co-EDTA and Zn-EDTA with IonPac®AG-7, 0.1 M ammonium nitrate was used to separate the complexed and free metal species. With IonPac®AG-7A, while the same mobile phase was used to elute the complexed species, a second mobile phase involving spiking 0.1 M ammonium nitrate with 3×10^{-5} M EDTA was used to facilitate the elution of the free metal species, resulting in shortened elution time and sharper peak shape for the free metal species. For the examined concentration range, the matrix effect of EDTA on ICP-MS analyte signal was negligible [3].

In experiments on chromium speciation, a gradient program with 0.1 M ammonium nitrate (MPA) and 0.8 M nitric acid (MPB) was adopted to separate Cr(VI) and Cr(III). As a rule, with IonPac®AG-7 as the separation column, Cr(VI) was eluted with MPA, followed by Cr(III) with MPB. The solution pH of MPA was adjusted to 4 to avoid reduction of Cr(VI) that possessed higher reduction potential in acidic conditions. After the elution of Cr(VI), MPB of higher ionic strength was applied to elute Cr(III) that was retained stronger by the stationary phase. With this combination of mobile phases, the two major problems with chromium speciation, precipitation of Cr(III) and reduction of Cr(VI) to Cr(III) in presence of a reducing reagent, were circumvented.

5.2 Selection of columns

Conventionally, there are two types of ion exchange columns: anionic exchange column

(AEC) and cationic exchange column (CEC), defined by the functional groups grafted on the surface of the polymer base material. Each type of column is further divided into strong and weak ion-exchange columns. In addition to this general classification, there are ion exchange columns that possess dual exchange capability, such as IonPac®AG-7 and CG-5A that were used for speciation analysis in this work (see *section 2.2.1.1 IEC* for details). The dual ion exchange capability is a useful feature when separating chemical species with different charge states, e.g. Cr(III) and Cr(VI). The usual practice is to use complexing agent to switch over the charge state of one of the species so as to retain both species onto the stationary phase [4-6]. However, with an addition of complexing agent, this procedure maybe problematic for analysis at trace levels where contamination control is usually the key to a reliable analysis.

Another procedure is to use tandem mini-columns or disks that were made of different resins with opposite ion exchange capability to selectively collect Cr(III) and Cr(VI), followed by their sequential elution [7, 8]. In chemical analysis, 'less is more', i.e., the less manipulation, the more benefits. In fact, some ion-exchange columns with dual exchange capability are commercially available and were successfully used for speciation studies [9-11]. IonPac®AG-7 is designed as the guard column to be placed before the analytical column. It has, however, the same packing material as the analytical counterpart and sufficient resolving power to perform the separations as reported in this thesis. As the resolving power of a column is inversely proportional to the square of the column diameter [1], microbore column may be considered in future work, which may bring additional benefit of lower mobile phase consumption.

5.3 Alleviating spectroscopic interferences

Although ICP-MS is the most preferred detector for elemental speciation analysis, it suffers from spectroscopic interferences, which can arise from either isobaric or polyatomic ions. Cr is a good example: there is isobaric interference from $^{54}\text{Fe}^+$ on $^{54}\text{Cr}^+$, polyatomic interferences from $^{40}\text{Ar}^{12}\text{C}^+$, $^{36}\text{Ar}^{16}\text{O}^+$ and $^{35}\text{Cl}^{16}\text{O}^1\text{H}^+$ on $^{52}\text{Cr}^+$, and from $^{40}\text{Ar}^{13}\text{C}^+$ and $^{37}\text{Cl}^{16}\text{O}^+$ on $^{53}\text{Cr}^+$. There are a few approaches to reduce/eliminate the interference on, mostly, $^{52}\text{Cr}^+$, the most abundant isotope, which include applying mathematical corrections [12], using a high resolution mass spectrometer [13] or using a collision/reaction cell [5] [6, 14, 15]. The ICP-MS instrument used for chromium speciation in this study is equipped with a unique feature (CRI) to combat polyatomic interferences, which is mechanically incorporated with the sampling interface. Contrary to the common utilization on collision/reaction cell, there are far fewer reports on CRI [4, 16]. It is necessary to optimize its flow rate so that the influence from the interferents is minimized without losing too much sensitivity for the analyte [17]. H_2 and He are the two commonly used CRI gases, and our results have clearly demonstrated that H_2 can be used to eliminate the polyatomic interferences more efficiently.

References

1. M.C. McMaster, *HPLC, a practical user's guide*. 2nd ed. 2007, Hoboken, N.J: Wiley-Interscience.

2. A.A. Ammann, *Arsenic speciation by gradient anion exchange narrow bore ion chromatography and high resolution inductively coupled plasma mass spectrometry detection*. Journal of Chromatography A, 1217 (2010) 2111-2116.
3. C. Huang, *Determination of conditional stability constants using ion chromatography coupled with inductively coupled plasma mass spectrometry*, PhD thesis (2006), Queen's university.
4. M. Leist, R. Leiser and A. Toms, *Low-level speciation of chromium in drinking waters using LC-ICP-MS*. Spectroscopy, (2006) 29-31.
5. Z. Chen, M. Megharaj and R. Naidu, *Removal of interferences in the speciation of chromium using an octopole reaction system in ion chromatography with inductively coupled plasma mass spectrometry*. Talanta, 73 (2007) 948-952.
6. A.J. Bednar, R.A. Kirgan and W.T. Jones, *Comparison of standard and reaction cell inductively coupled plasma mass spectrometry in the determination of chromium and selenium species by HPLC-ICP-MS*. Analytica Chimica Acta, 632 (2009) 27-34.
7. S. Motomizu, K. Jitmanee and M. Oshima, *On-line collection/concentration of trace metals for spectroscopic detection via use of small-sized thin solid phase (STSP) column resin reactors. Application to speciation of Cr(III) and Cr(VI)*. Analytica Chimica Acta, 499 (2003) 149-155.
8. Y. Furusho, A. Sabarudin, L. Hakim, K. Oshita, M. Oshima, and S. Motomizu, *Automated Pretreatment System for the Speciation of Cr(III) and Cr(VI) Using Dual Mini-Columns Packed with Newly Synthesized Chitosan Resin and ME-03 Resin*. Analytical Sciences, 25 (2009) 51-56.

9. C. Huang and D. Beauchemin, *Simultaneous determination of two conditional stability constants by IC-ICP-MS*. Journal of analytical atomic spectrometry, 21 (2006) 1419-1422.
10. C. Huang and D. Beauchemin, *A simple method based on IC-ICP-MS to determine conditional stability constants*. Journal of analytical atomic spectrometry, 21 (2006) 317-320.
11. F. Seby, S. Charles, M. Gagean, H. Garraud, and O.F.X. Donard, *Chromium speciation by hyphenation of high-performance liquid chromatography to inductively coupled plasma-mass spectrometry - study of the influence of interfering ions*. Journal of analytical atomic spectrometry, 18 (2003) 1386-1390.
12. F. Laborda, M.P. Gorriz, E. Bolea, and J.R. Castillo, *Mathematical correction for polyatomic interferences in the speciation of chromium by liquid chromatography-inductively coupled plasma quadrupole mass spectrometry*. Spectrochimica Acta Part B-Atomic Spectroscopy, 61 (2006) 433-437.
13. F. Vanhaecke, S. Saverwyns, G. De Wannemacker, L. Moens, and R. Dams, *Comparison of the application of higher mass resolution and cool plasma conditions to avoid spectral interferences in Cr(III)/Cr(VI) speciation by means of high-performance liquid chromatography - inductively coupled plasma mass spectrometry*. Analytical Chimica Acta, 419 (2000) 55-64.
14. R.E. Wolf, J.M. Morrison and M.B. Goldhaber, *Simultaneous determination of Cr(iii) and Cr(vi) using reversed-phased ion-pairing liquid chromatography with dynamic reaction cell inductively coupled plasma mass spectrometry*. Journal of analytical atomic spectrometry, 22 (2007) 1051-1060.

15. A.P. Vonderheide, J. Meija, K. Tepperman, A. Puga, A.R. Pinhas, J.C. States, and J.A. Caruso, *Retention of Cr(III) by high-performance chelation ion chromatography interfaced to inductively-coupled plasma mass spectrometric detection with collision cell*. *Journal of Chromatography A*, 1024 (2004) 129-137.
16. I. Kalinitchenko, X. Wang and B. Sturman, *Simple and effective control of spectral overlap interferences in ICP-MS*. *Spectroscopy*, (2008) 38-46.
17. Varian 810/820MS customer training manual. 2009.

Chapter 6

Summary and Conclusions

The applications of elemental speciation technique with hyphenated HPLC-ICP-MS to 1) the determination of the stability constant of an equilibrium process; 2) the speciation analysis of chromium species with different oxidation states; and 3) the investigation on the kinetics of reduction of Cr(VI) in natural water were described in this thesis.

Hyphenated IEC and ICP-MS is a useful method for the determination of stability constants of metal complexes at very low concentrations (μM level) with appropriate mathematical treatments, which has been exemplified with model metal complex of Co-EDTA and Zn-EDTA separately. The over simplification of the formation constant expression (H-1) caused the deviation of the chelation number in the previous approach. The primary assumption made when using ion exchange chromatography to separate metal complexes is that there is no shift in equilibrium during the elution process [1-4]. It is preferable that the free metal ions bind to the ion exchanger while the complexes elute freely from the column. As the data fit the equations that were deduced without considering the influence of the ion exchanger, the primary assumption appears to be justified. Both IonPac®AG-7 and CG-5A are suitable columns for this purpose. With AG-7, isocratic elution was sufficient to separate both the metal complex and free metal species of Co and Zn within 5 minutes. With CG-5A, a gradient elution using a complexing agent to elute the free metal species was adopted. The gradient elution procedure resulted

in narrower peak shape and was applicable to metal species that was difficult to elute by isocratic elution. The multielemental detection capability of ICP-MS provides the possibility of extending the method thus developed to a multielemental complexation system. However, because fundamental calculations showed that the ratio of metal complex to free metal is proportional to the formation constant, K_f , it is, in practice, very difficult to perform such measurement for metals that have relatively large differences in K_f values. In view of such limitation, this was not pursued further.

The hyphenated IEC and ICP-MS approach was also used to carry out chromium speciation analysis at trace and ultra trace levels in potable water. A guard column, Ion-Pac®AG-7, with dual ion exchange capability was used to separate the oppositely charged chromium species. The separation was achieved with a gradient elution program using 0.1 M ammonium nitrate (MPA) and 0.8 M nitric acid (MPB) as mobile phases. A full separation was achieved within 7.5 min, including 3-min stabilization, which was shorter than comparable separation procedures [5-8]. The redox pair was separated directly, without adding complexing or charge switching agent, which is important for contamination control in trace analysis. Using a micro-bore column would likely further reduce the analysis time.

The CRI is an efficient way to eliminate polyatomic interferences that conventionally plague chromium determination by ICP-MS. The attenuation of interference signals from carbon- and chlorine-based matrices was evaluated and H_2 proved to be most effective at eliminating these polyatomic interferences. Residual Cr in the mobile phase is detrimental to speciation analysis at trace level, as a substantial amount of mobile phase will pass

through the column during a separation. It is a common phenomenon with liquid chromatography, yet generally ignored in literature. The effect of residual Cr was evaluated and a background correction procedure was adopted.

The accuracy of this speciation method was verified by speciation analysis of riverine water SLRS-2 with certified total chromium concentration. However, in the chromatogram, there was no peak at the retention time corresponding to Cr(VI); instead, a peak appeared at void time, which was speculated to arise from a complexed form of Cr. Both external calibration and standard addition were used for quantification. With external calibration, the calibration curve for Cr(VI) was used to calculate Cr-com. With standard addition, the measured total Cr concentration agreed with the certified value at a 95% confidence level, while, due to matrix effects, a significant difference was observed at the same confidence level by external calibration. Although the standard addition procedure proved to be more accurate, external calibration could still be useful for risk assessment, when screening a large number of samples. The speciation analysis method was also applied to municipal tap water. In this case, the data obtained by external calibration and standard addition agreed at 99% confidence level. With either quantitation method, the concentration of Cr(VI) was greater than that of Cr(III), both of which were, however, below the regulation limit. Future work will focus on applying this method to chromium speciation analysis of more complex sample matrices.

The reduction kinetics of Cr(VI) was studied in riverine water SLRS-2 with the online speciation procedure described above. The riverine water was spiked with Cr(VI) in the presence or absence of Cr(III). In both cases, the reduction of Cr(VI) followed a pseudo

first order reaction. The concentration of reducing reagent in the sample, arguably humics, is in much excess compared to the spiked Cr(VI), so that a concentration change of humics with time would not exert a significant influence on the reaction rate. By plotting the logarithm of the ratio of instant concentration of Cr(VI) over the original spiked concentration versus time, the reduction rate constant was obtained as the slope of the linear regression curve. The presence of Cr(III) did not affect on the reaction rate significantly, indicating that Cr(III) was not significantly involved in the reduction of Cr(VI). This observation in turn indicates that Cr(III), as a reduction product, mainly resulted from the dissociation of Cr(III)-com instead of Cr(VI). This supports the mechanism that Cr(VI) reduction starts following complexation of Cr(VI) with reducible organic substances. Both pH and temperature affected the reaction rate, i.e. the reaction rate increased as pH decreased and temperature increased. The activation energy of the reduction of Cr(VI) in the tested media was calculated using an Arrhenius plot of the rate constant data versus temperature.

The speciation method proved useful for this type of kinetic studies. It has the advantages of small sample consumption, minimal sample manipulation, ease of execution, real-time process monitoring and simple data interpretation. Further work may involve a more thorough investigation of the effect of pH and temperature. Controlled studies with measured amounts of known reducible organic substances should also be tried to further assess the analytical performance of this method. Finally, the applicability of this method could also be tested on different natural water samples, including those that have been exposed to known chromium-containing contaminants.

Overall, this work demonstrated the versatility and power of HPLC, in particular IEC, in combination with ICP-MS, for trace metal speciation analysis and investigation of the thermodynamics and kinetics of equilibration processes.

References

1. P. Hajos, G. Revesz, C. Sarzanini, G. Sacchero, and E. Mentasti, *Retention model for the separation of anionic metal-EDTA complexes in ion chromatography*. Journal of Chromatography A, 640 (1993) 15-25.
2. P. Janos, *Ion-interaction chromatographic separation of metal cations in the presence of complexing agents*. Fresenius' Journal of Analytical Chemistry, 350 (1994) 646-648.
3. C.Y. Li, J.Z. Gao, G.H. Zhao, J.W. Kang, and H.H. He, *Determination of stability constants of Cu(II), Fe(III), and Pb(II) chelates with N,N,N',N'-ethylenediamine tetrakis(methylenephosphonic acid) by reversed-phase ion-pair chromatography*. Chromatographia, 46 (1997) 489-494.
4. M.R. Pitluck, B.D. Pollard and D.T. Haworth, *Determination of stability constants of a copper/citric acid complex by ion-exchange chromatography and atomic absorption spectrometry*. Analytica Chimica Acta, 197 (1987) 339-342.
5. Z. Chen, M. Megharaj and R. Naidu, *Removal of interferences in the speciation of chromium using an octopole reaction system in ion chromatography with inductively coupled plasma mass spectrometry*. Talanta, 73 (2007) 948-952.
6. Y. Furusho, A. Sabarudin, L. Hakim, K. Oshita, M. Oshima, and S. Motomizu,

Automated Pretreatment System for the Speciation of Cr(III) and Cr(VI) Using Dual Mini-Columns Packed with Newly Synthesized Chitosan Resin and ME-03 Resin. Analytical Sciences, 25 (2009) 51-56.

7. M. Leist, R. Leiser and A. Toms, *Low-level speciation of chromium in drinking waters using LC-ICP-MS.* Spectroscopy, (2006) 29-31.
8. F. Seby, S. Charles, M. Gagean, H. Garraud, and O.F.X. Donard, *Chromium speciation by hyphenation of high-performance liquid chromatography to inductively coupled plasma-mass spectrometry - study of the influence of interfering ions.* Journal of analytical atomic spectrometry, 18 (2003) 1386-1390.